January 2023

Beta-Catenin Nuclear Transport In Wnt Signaling: Kap-Beta2/ transportin Mediates Nuclear Import Of Beta-Catenin Via A Py-Nls Motif In A Ran Gtpase Dependent Manner

Woong Y. Hwang

Abstract

Beta-catenin Nuclear Transport in Wnt Signaling: Kap-beta2/Transportin Mediates Nuclear Import of Beta-catenin via a PY-NLS Motif in a Ran GTPase Dependent Manner

Woong Yul Hwang

2023

Wnt signaling is essential for embryonic development and adult tissue homeostasis; mutations in Wnt pathway components are major drivers of multiple diseases especially cancer. β-catenin is a key effector in this pathway that translocates into the nucleus and activates Wnt responsive genes. However, due to our lack of understanding of β-catenin nuclear transport, therapeutic modulation of Wnt signaling has been challenging. Here, we took an unconventional approach to address this long-standing question by exploiting a heterologous model system, the budding yeast *Saccharomyces cerevisiae,* which contains a conserved nuclear transport machinery. In contrast to prior work, we demonstrate that β-catenin accumulates in the nucleus in a Ran dependent manner, suggesting the use of a nuclear transport receptor (NTR). Indeed, a systematic and conditional inhibition of NTRs revealed that only Kap104, the orthologue of Kap-β2/Transportin-1 (TNPO1), was required for β-catenin nuclear import. We further demonstrate direct binding between TNPO1 and β-catenin that is mediated by a conserved amino acid sequence that resembles a PY NLS. Finally, using *Xenopus* secondary axis and TCF/LEF reporter assays, we demonstrate that our results in yeast can be directly translated to vertebrates.

By elucidating the NLS in β-catenin and its cognate NTR, our study provides new therapeutic targets for a host of human diseases caused by excessive Wnt signaling. Indeed, we demonstrate that a small chimeric peptide designed to target TNPO1 can reduce Wnt signaling as a first step towards therapeutics.

Beta-catenin Nuclear Transport in Wnt Signaling: Kap-beta2/Transportin Mediates Nuclear Import of Beta-catenin via a PY-NLS Motif in a Ran GTPase Dependent Manner

A Dissertation

Presented to the Faculty of the Graduate School

Of

Yale University

In Candidacy for the Degree of

Doctor of Philosophy

By

Woong Yul Hwang

Dissertation Director: Mustafa K. Khokha

Chairperson: Michael Nitabach

May 2023

Table of Contents

List of Tables and Figures

Glossary of Terms and Abbreviations

β-catenin – beta catenin

arm – Armadillo

DVL – Dishevelled

FZD – Frizzled

LRP – Low Density Lipoprotein Receptor-related protein

GSK3β – Glycogen Synthease Kinase 3 beta

APC – Adenomatous Polyposis Coli

NTR – Nuclear Transport Receptor

Kap α – Karyopherin alpha

Kap β1 – Karyopherin beta 1

Kap β2 – Karyopherin beta 2

TNPO1 – Transportin 1

NLS – Nuclear Localization Signals

NES – Nuclear Export Signals

CRISPR – Clustered Regularly Inter-spaced Short Palindrolic Repeats

X. tropicalis – Xenopus tropicalis

X. laevis – Xenopus laevis

Saccharomyces cerevisiae – S. cerevisiae

WISH -Whole mount *in situ* hybridization

IVF – *in vitro* fertilization

WB – Western Blot

PCR – Polymerase Chain Reaction

DNA – Deoxyribonucleic Acid

RNA – Ribonucleic Acid

mRNA – messenger Ribonucleic Acid

sgRNA -single guide Ribonucleic Acid

WT – Wild Type

UIC – Un-injected Controls

bp – base pair

Acknowledgements

First and foremost, Soli Deo Gloria! I would like to thank God, Abba Father, for his guidance and comfort and steadfast love throughout this journey. Indeed, it is my firm belief that "I can do all this through him who gives me strength" (Philippians 4:13), and I will continue to strive to pursue my path with a full trust on You!

To my beloved mom and dad- What a crazy journey we have gone through as immigrant family for the past 17 years. There are no words that can truly encompass my gratitude and love for you. I am deeply indebted to you for all the sacrifices you have made to support me so that I could pursue my own dream. You are my true inspiration and a living example of the "American Dream", the belief that anyone can reach your dream through tenacity and discipline in this land of opportunity. 엄마,아빠 너무 사랑하고 감사합니다!

To my mentor, Mustafa Khokha- You really helped me realize that research is a diligent pursuit of knowledge that discipline and perseverance are key to discovering answers. Thank you for encouraging me and pushing me beyond my limits. You were the best exemplary of physician scientist I just hope to emulate in my future. I have grown a lot both personally and professionally because of your mentorship. Thank you!

To my Thesis Committee, Drs. Patrick Lusk, Michael Caplan, and Michael Nitabach- it is my sincere gratitude for all your valuable feedback, suggestions, and encouragements for the past five years. You helped me to prioritize experiments that really matter to complete my project. In particular, I want to thank Dr. Lusk for your help on yeast experiments. I would never

have thought to use Yeast as a screening model to study nuclear transport of β-catenin without your suggestion.

To members in Khokha lab aka Khokhanuts, you all made my time in lab more meaningful and special. There are so many memories we cherished together- dressing up each other for the Halloween, learning new slang words (special thanks to V$), throwing our own khokhanuts happy hour every Friday, playing Super Smash brothers in the conference room, and so on. I wish you all the best for future endeavors. Thank you!

To Yale MD-PhD program especially Dr. Jamieson, Dr. Kazmierczak, Dr. Reiko Fitzsimonds, Cheryl Defillippo, Sue Sansone, and Alexandra Mauzerall – it was impossible to complete this work without your support for the past seven years. You always care for MD-PhD students and act in our best interests. In particular, I want to thank Cheryl and Alex for their help with NRSA F30 and Paul & Daisy Soros Fellowship application. Thank you all!

This work was supported by the NIH (NHLBI F30 HL143878-03), the Yale School of Medicine Medical Scientist Training Program, and a Paul & Daisy Soros Fellowship.

Chapter 1: Introduction

1.1 A historical perspective of Wnt

Canonical Wnt signaling is a well conserved pathway in multicellular organisms that regulates a multitude of essential developmental and homeostatic processes throughout the lifespan. At the plasma membrane, Wnts are a soluble lipid modified ligand that initiate a signaling cascade ultimately leading to target gene activation. Wnt or *wingless* (*wg*) was initially discovered in *Drosophila melanogaster* as an essential gene for proper segment polarity; Nusslein and Wieschaus performed a large genetic screening and observed that *wg* mutants had severe developmental defects in anterior to posterior axis patterning including wing formation (Nusslein-Volhard & Wieschaus, 1980).

Soon after, Nusse and Varmus independently identified *int-1,* as a proto-oncogene in mice, which would later be identified as the mammalian *wg* homolog. They found that a viral insertion of mouse mammary tumor virus (MMTV) DNA at the *int-1* locus induced breast tumors revealing a potential role of Wnt in cancer (Nusse & Varmus, 1982). Once sequence homology between *wg* and *int-1* was established, a new gene nomenclature (Wnt) was derived to rename homologs and paralogs across different species in metazoans, including zebrafish, *Xenopus,* mouse, and human (Rijsewijk et al., 1987).

Over the years, multidisciplinary research has greatly expanded our understanding of other key components in the Wnt pathway. In particular, for the canonical Wnt pathway, β-catenin (CTNNB1) was found to be the key messenger that relays the signal from a Wnt ligand at the plasma membrane to transcription factors in the nucleus (MacDonald, Tamai, & He, 2009; Niehrs, 2012). Interestingly, β-catenin was not initially identified as a Wnt transcriptional effector but as a part of the cell adhesion complex in which β-catenin and three other proteins (α-

catenin, γ-catenin and plakoglobin) form a complex with E-cadherin to link actin cytoskeletal structures (Ozawa, Baribault, & Kemler, 1989). The role of β-catenin in the Wnt pathway was uncovered soon after from epistatic analysis of Armadillo (arm), a β-catenin orthologue in *Drosophila,* and *wg*. Not only did *arm* mutants phenocopy *wg* null mutants, Arm protein stability and expression pattern was dictated by *wg* suggesting that β-catenin/Armadillo is the downstream target of Wnt/Wg (Riggleman, Schedl, & Wieschaus, 1990; Wieschaus, Nusslein-Volhard, & Jurgens, 1984; Wieschaus & Riggleman, 1987). Subsequent studies showed that β-catenin translocates to the nucleus and activates Wnt-regulated transcription by binding to T-cell factor (TCF)/Lymphoid enhancer-binding factor (LEF) factors (Behrens et al., 1996; Brunner, Peter, Schweizer, & Basler, 1997; O. Huber et al., 1996; Molenaar et al., 1996; van de Wetering et al., 1997).

1.2 Canonical Wnt signaling

As summarized above, the Wnt ligand initiates signaling and β-catenin ultimately delivers the message to the nucleus to activate gene transcription. Given the potency of Wnt signaling on determining cell fate and initiating cancer, there are numerous checkpoints throughout the signaling cascade to tightly control Wnt activation. Here, we will focus on the regulation of cytosolic β-catenin although regulation at the level of the Wnt ligand is also well established and reviewed elsewhere (MacDonald et al., 2009; Nusse & Clevers, 2017). In the absence of Wnt ligands, cytosolic β-catenin is phosphorylated by the destruction complex that comprises Axin, APC, GSK-3, and CK-1 (**Figure A**) (MacDonald et al., 2009; Wodarz & Nusse, 1998). Phosphorylated β-catenin is ubiquitinated by β-TrCP and degraded by the proteosome machinery (Aberle, Bauer, Stappert, Kispert, & Kemler, 1997; Liu et al., 1999; MacDonald et

al., 2009). However, Wnt stimulation inactivates the degradation complex and stabilize β-catenin in the cytosol. Wnt ligand binding to the Frizzled transmembrane receptors (FZD) and LRP5/6 co-receptors on the membrane will recruit cytosolic Dischevelled (Dvl), which in turn sequesters the destruction complex to the membrane, allowing β-catenin to accumulate in the cytosol. Free cytosolic β-catenin then enters the nucleus where it drives the transcription of Wnt-responsive genes (**Figure A**) (MacDonald et al., 2009; Niehrs, 2012).

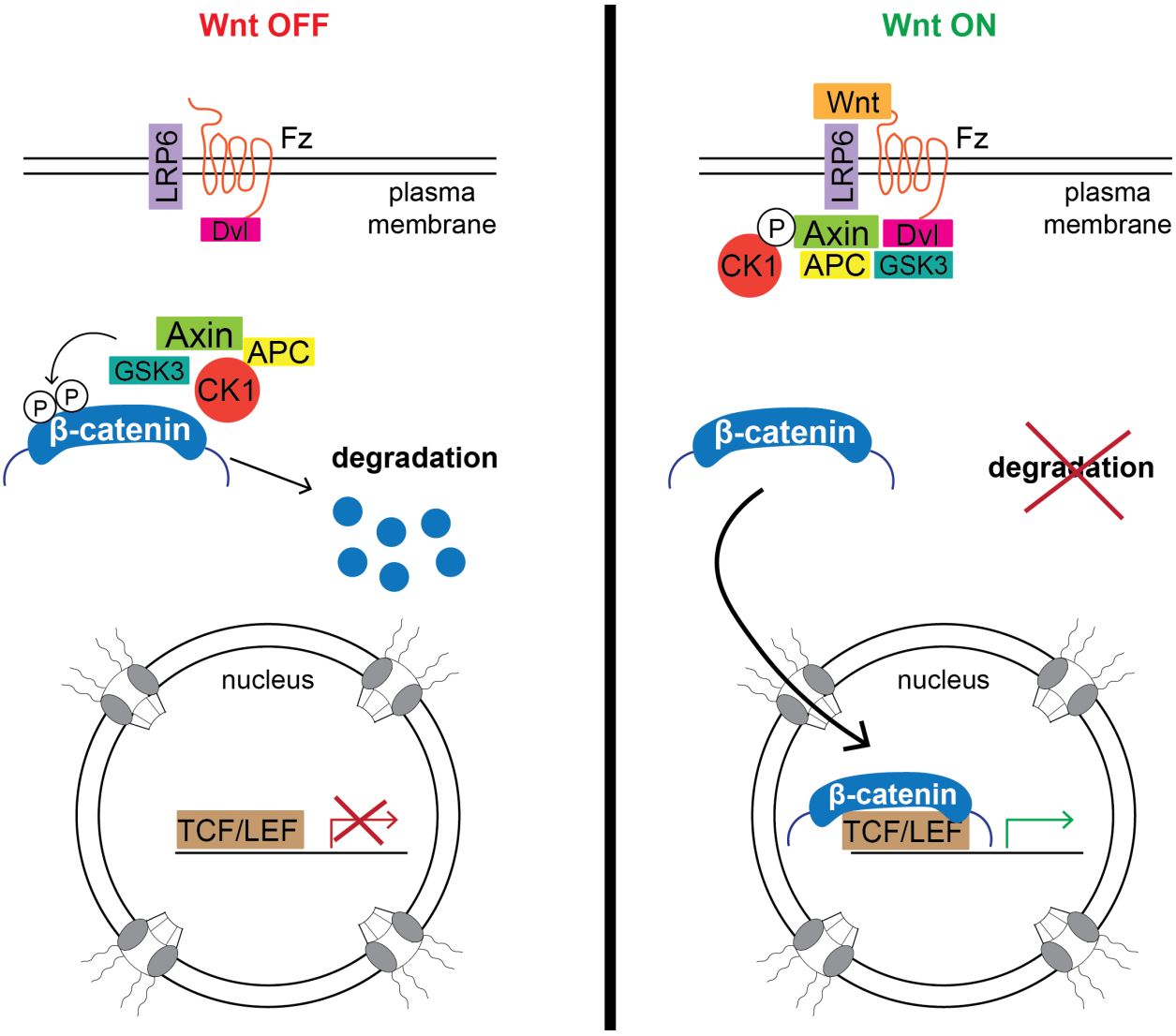

Figure A. Overview of the downstream of canonical Wnt signaling cascade

1.3 Wnt signaling in development

Canonical Wnt signaling is evolutionarily conserved in Metazoans (Ruiz-Trillo, Roger, Burger, Gray, & Lang, 2008; Schierwater et al., 2009). Body axis patterning distinguishes metazoans from unicellular protozoans, and the Wnt pathway is a crucial driving force of these events during early development. For example, in *Xenopus*, fertilization triggers cortical rotation which leads to the dorsal accumulation of nuclear β-catenin (**Figure B**) (Schneider, Steinbeisser, Warga, & Hausen, 1996; Schohl & Fagotto, 2002). Subsequently, high levels of Wnt activity on the dorsal side cue cells to form the Spemann organizer (dorsal blastopore lip in *Xenopus*, the shield in zebrafish, and the node in the mouse), a key organizing center that is responsible for mesoderm and neural induction (**Figure B**) (Harland & Gerhart, 1997; Marlow, 2010; Petersen & Reddien, 2009; Schier & Talbot, 2005). As a test of sufficiency, increased Wnt signaling can lead to a duplication of the dorsal axis and form a two-headed embryo (**Figure C**). Conversely, β-catenin depletion can lead to a radially ventralized embryo by eliminating the induction of the Spemann's Organizer by the signals from the Nieuwkoop center (**Figure C**) (Heasman et al., 1994; Heasman, Kofron, & Wylie, 2000; Khokha, Yeh, Grammer, & Harland, 2005; McMahon & Moon, 1989; Moon, Brown, & Torres, 1997; Nishisho et al., 1991; Smith & Harland, 1991; Sokol, Christian, Moon, & Melton, 1991). Therefore, careful titration of Wnt signaling is essential to properly pattern the embryo. Indeed, axis duplication in *Xenopus* has since become a classic assay to study components of the Wnt pathway in developmental biology.

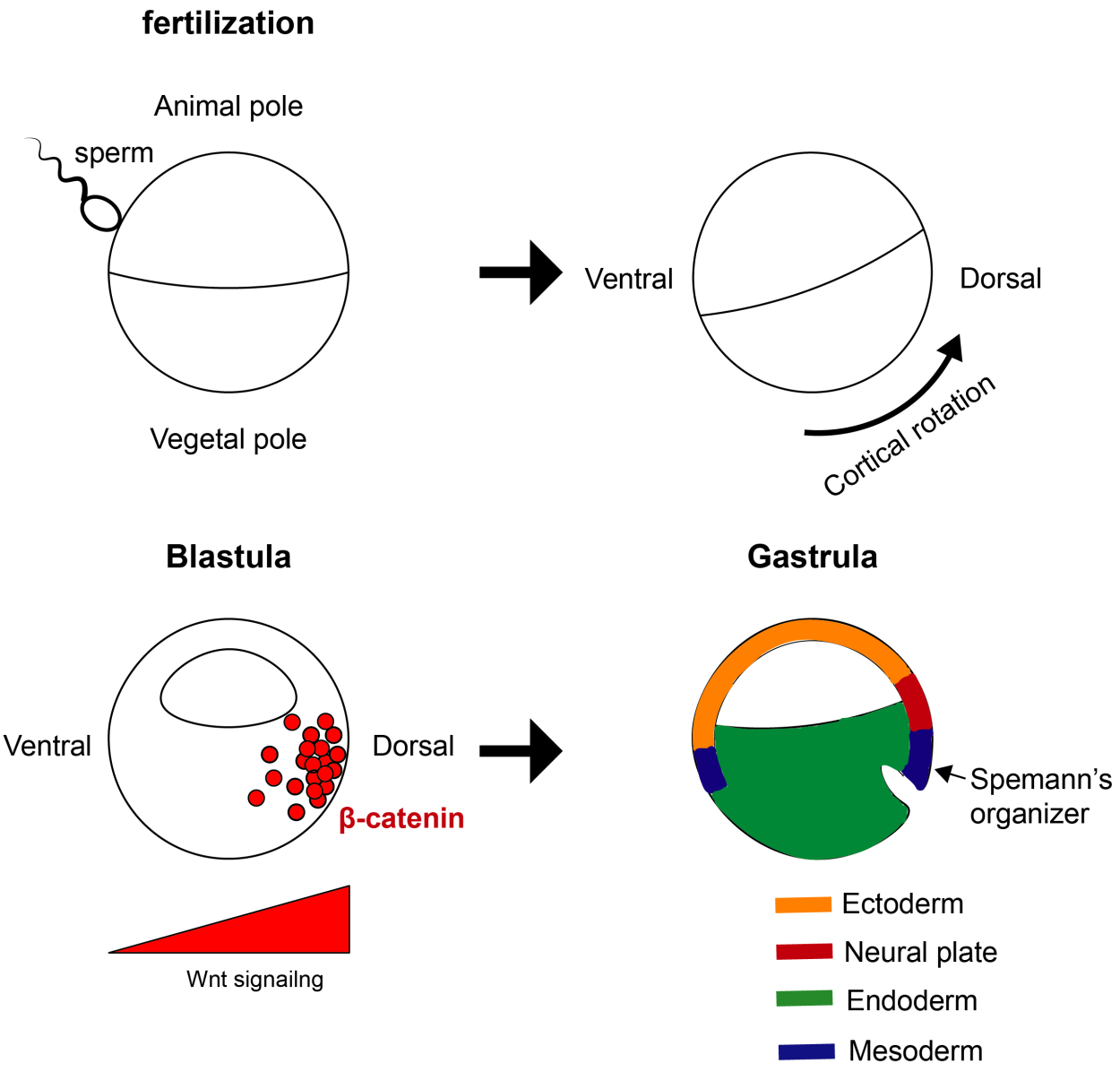

Figure B. Schematic diagram of Wnt pathway in early embryonic development. Sperm entry induces the cortical rotation which in turn establishes the dorsal to ventral axis. Subsequently, β-catenin level gets enriched in dorsal region leading to the formation of Spemann's organizer. Adapted from (De Robertis, Larrain, Oelgeschlager, & Wessely, 2000).

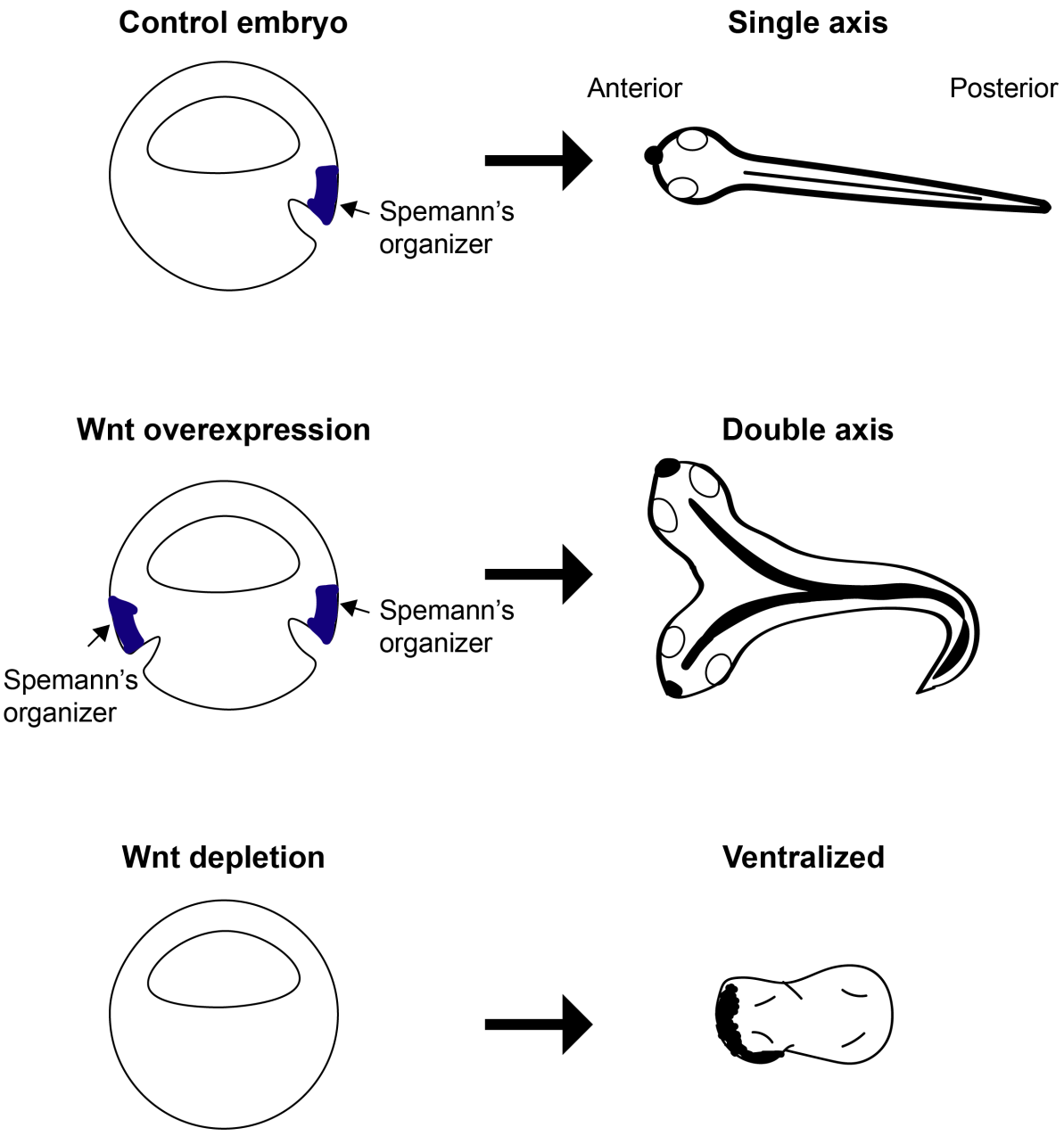

Figure C. Schematic diagram of Wnt signaling in axis patterning. Spemann's organizer functions in anterior to posterior patterning. Overexpression of Wnt can induce extra Spemann's organizer formation on the ventral side, generating a two headed embryo. Conversely, if Wnt is depleted, no Spemann's organizer is assembled, and the embryo becomes "ventralized", losing dorsal structures such as the head.

1.4 Wnt signaling in cancer

While mis-regulation of Wnt signaling has detrimental effects on development, in adult tissue, aberrant activation of the Wnt pathway can lead to excessive cell growth and cancer. Since the discovery of *int1* as a proto-oncogene, more components in the Wnt pathway have been implicated in a variety of human diseases especially cancer (**Table A**) (Clevers & Nusse, 2012; MacDonald et al., 2009; Moon, Kohn, De Ferrari, & Kaykas, 2004; Morin et al., 1997; Nusse & Varmus, 1982; Polakis, 2012; Wood et al., 2007). Indeed, recent efforts to dissect the genetic basis of cancer by comprehensive tumor sequencing have revealed that mutations in the Wnt pathway occur frequently in cancers (Vogelstein et al, 2013; Pleasance et al, 2010). In fact, 90% of colorectal cancers are caused by genetic alterations in Wnt pathway factors (Cancer Genome Atlas, 2012).

Such high prevalence of Wnt associated colorectal cancer cases can be explained by the role of Wnt signaling in the proliferation and self-renewal of intestinal epithelial stem cells. As the intestinal epithelial lining is renewed frequently to maintain barrier integrity upon damage due to toxins and injuries, the intestinal stem cells are particularly sensitive to genetic alterations that induce Wnt hyperactivation (Barker, 2014; Schepers & Clevers, 2012). Among many Wnt components, mutations in the gene encoding APC were the first genetic mutation discovered as a cause of the hereditary colon cancer syndrome, familial adenomatous polyposis (FAP) (Groden et al., 1991; Soravia et al., 1998). FAP patients who inherited a mutated APC allele will develop numerous adenomatous polyps, which will often progress into malignant colorectal cancers if untreated (Croner, Brueckl, Reingruber, Hohenberger, & Guenther, 2005). A small fraction of Axin and β-catenin mutations were also identified as drivers of Wnt dependent tumor growth in colorectal cancer. Essentially, all of these genetic alterations stabilize cytosolic β-catenin leading

to elevated levels of nuclear translocation of β-catenin even in the absence of Wnt ligand (**Figure D**). Currently, nine different chemical inhibitors are being tested in clinical trials of various Wnt dependent cancers with no definitive treatments available in market (**Table B**) (Jung & Park, 2020).

Affected gene	DNA/mRNA alteration	Functional outcome	Cancer type	Reference
CTNNBl (b-catenin)	Missense/in-frame deletion	Enhanced protein stability	Hepatocellular/ Medulloblastoma	Polakis 2007
APC (APC)	Truncation	Reduced regulatory activity	Colorectal/gastric	Clements et al. 2003
Axins (Axin I, Axin II)	Truncation/ missense	Reduced regulatory activity	Hepatocellular/ colorectal	Salahshor and Woodgett 2005
CREBP(CBP)	Truncation/ missense	Inactive acetyltransferase	Lymphoma/ leukemia	Teo and Kahn 2011
GSK3b	Missplicing, in-frame deletion	Inactive kinase	Leukemia	Abrahamsson et al. 2009
LRP5	Missplicing, in-frame deletion	Loss of repression by DKK1	Breast/parathyroid	Bjorklund et al. 2009
TCF7L2 (TCF4)	Missense/deletion/ truncation	Loss of repression	Colorectal	Cuilliere-Dartigues et al. 2006
TCF7L2 (TCF4)	Fusion with VT11A gene	Unclear	Colorectal	Bass 2011
FAB123B (WTX)	Truncation/ deletion	Loss of function	Wilm's tumor	Ruteshouser et al. 2008

Table A. Wnt associated genetic mutations identified in cancer (Polakis, 2012)

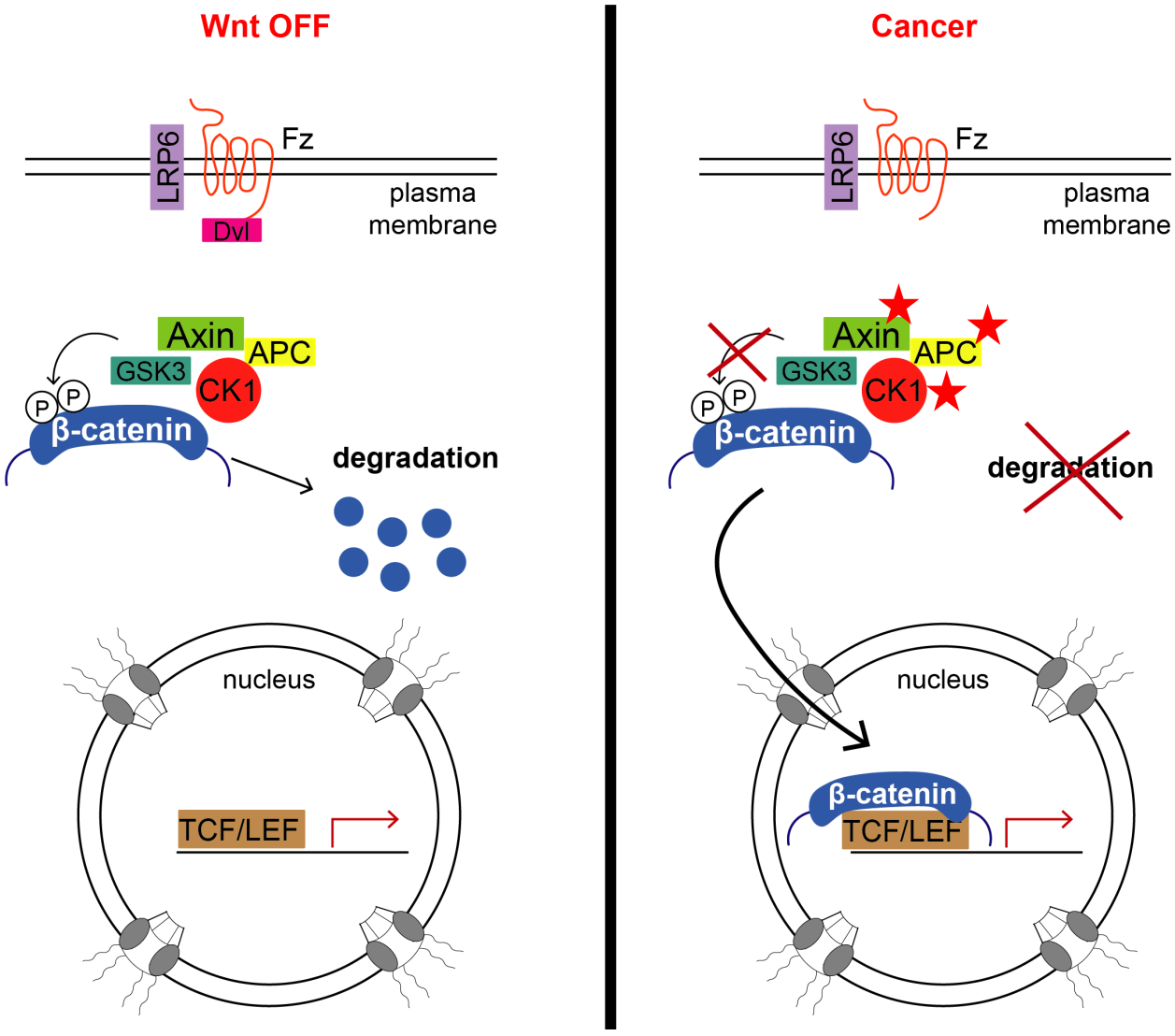

Figure D. Schematic diagram of Wnt pathway in cancer. Loss of function mutations in destruction complex (indicated by red star) that promote β-catenin stabilization are commonly found in cancer.

Chemical Inhibitors	Mechanism of action	Cancer types	Phase	Identifier
WNT974	PORCN inhibitor (Inhibition of Wnt secretion)	Metastatic CRC, Pancreatic cancer, BRAF mutant CRC, Melanoma, Triple negative Breast cancer, Head & Neck cancer, Squamous cell cancer (cervical, esophageal, lung)	Phase 1	NCT02278133 NCT01351103
		Squamouse cell cancer Head&Neck cancer	Phase 2	NCT02649530
ETC-1922159		Solid tumor	Phase 1	NCT02521844
RXC004		Solid tumor	Phase 1	NCT03447470
CGX1321		Colorectal adenocarcinoma Gastric adenocarcinoma Pancreatic adenocarcinoma Bile duct carcinoma Hepatocellular carcinoma Esophageal carcinoma Gastrointestinal cancer	Phase 1	NCT03507998 NCT02675946
OTSA101-DTPA-90Y	FZD10 (Wnt receptor) antagonist	Sarcoma, Synoival	Phase 1	NCT01469975
OMP-18R5	Monoclonal antibody against FZD	Solid tumors Metastatic breast cancer Pancreatic cancer Stage IV pancreatic cancer	Phase 1	NCT01957007 NCT01973309 NCT01345201 NCT02005315
OMP-54F28	FZD8 decoy receptor	Hepatocellular cancer Liver cancer Ovarian cancer Pancreatic cancer Stage IV pancreatic cancer Solid tumors	Phase 1	NCT02069145 NCT02092363 NCT02050178 NCT01608867
PRI-724	CBP/β-catenin antagonist	Advanced pancreatic cancer Metastatic pancreatic cancer Pancreatic adenocarcinoma Advanced solid tumors Acute myeloid leukemia Chronic myeloid leukemia	Phase 1&2	NCT01764477 NCT01302405 NCT01606579 NCT02413853
SM08502	β-catenin controlled gene expression inhibitor	Solid tumor	Phase 1	NCT03355066

Table B. List of Wnt signaling chemical inhibitors in clinical trials. Adapted from (Jung & Park, 2020)

1.5 Nuclear transport mechanism of β-catenin

Spatial separation of stabilized β-catenin in the cytosol and transcription factors in the nucleus provides another check point to ensure that Wnt target genes are expressed only when the Wnt pathway is activated. Importantly, this spatial separation also necessitates a selective nuclear import system to deliver β-catenin from the cytosol to the nucleus. Indeed, β-catenin is a 92 kD macromolecule that cannot pass through the nuclear pore by passive diffusion alone suggesting that a nuclear transport carrier is required for nuclear entry (Stewart, 2007).

From a therapeutic potential, blocking the nuclear transport of β-catenin would be applicable for many of the genetic alterations in the Wnt pathway that lead to cancer. However, most therapeutic strategies have focused on upstream components which may limit their potential. Unfortunately, the proteins that directly bind β-catenin and mediate its nuclear transport have been unknown until recently.

Essentially, the nuclear transport system requires three components: 1) a **cargo** protein containing a nuclear localization signal (NLS) 2) the **import** protein (a nuclear transport receptor - NTR) that binds to the cargo at the nuclear localization signal (NLS) and anchors it to the nuclear pore complexes (NPCs). NPCs create a selective barrier for the exchange of proteins between the nucleus and cytoplasm. and 3) a small soluble **GTPase** that unloads the cargo inside the nucleus. (**Figure E**) (Cautain, Hill, de Pedro, & Link, 2015; Wente & Rout, 2010). To date in humans, there are at least 15 different nuclear transport receptors, and they all share common features and mechanism although each recognizes a different NLS (Harel & Forbes, 2004).

For example, as one of the first and best studied nuclear transport receptors, Importin-α/β recognizes the classical NLS, either monopartite (PKKKRKV) or bipartite (KR[PAATKKAGQA]KKKK, on a cargo protein (Jans, Xiao, & Lam, 2000; Weis, 2003).

Subsequently, importin-β brings this NLS-importin complex to the NPCs by interacting directly with nuclear pore proteins (Fahrenkrog & Aebi, 2003; Suntharalingam & Wente, 2003). To bias shuttling of the NTR-cargo into the nucleus, a Ran-GTP gradient is critical. In the nucleus, Ran-GTP binds to the importin complex to release the cargo. The importin-Ran complex can exit the nucleus, and in the cytoplasm, dephosphorylation of Ran-GTP leads to release of Ran from the importin complex so additional cargo can be bound. The concentration of Ran-GTP is higher in the nucleus than in the cytoplasm by the differential enrichment of the guanine exchange factor (GEF) RCC1 in the nucleus and the GTPase activating protein, RanGAP1 in the cytoplasm (**Figure E**) (Bischoff & Ponstingl, 1991; Gorlich, Pante, Kutay, Aebi, & Bischoff, 1996; Izaurralde, Kutay, von Kobbe, Mattaj, & Gorlich, 1997) .

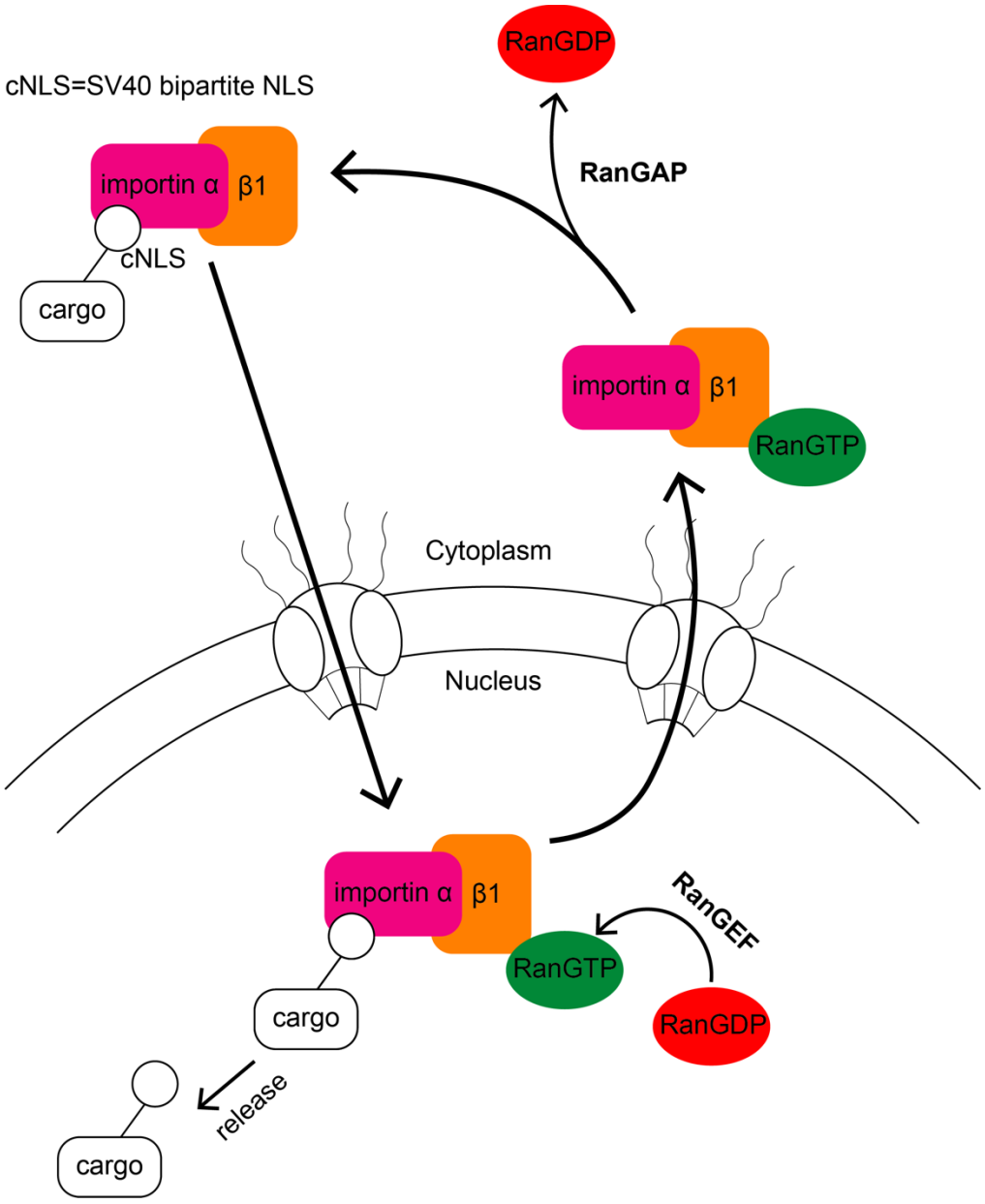

Figure E. Schematic diagram of the classic nuclear transport system. A cargo bearing cNLSs forms an import complex with importin α/β1 in the cytosol. Once the importin complex passed through the NPCs, Ran GTP binding to importin β1 releases the cargo inside the nucleus. High level of nuclear RanGTP is maintained by RanGEF. Importin α/β1-RanGTP then exits the nucleus and RanGTP hydrolysis by RanGAP releases importin α/β1 in the cytosol.

Despite intensive study, the mechanism of β-catenin translocation from the cytosol to the nucleus remains obscure. First, while early studies suggested that β-catenin nuclear import was energy dependent, they excluded a role for the Ran GTPase (Cavazza & Vernos, 2015). Second, additional studies demonstrated that β-catenin nuclear import did not require the Kap-α/Kap-β1 (Importin α/β1) nuclear transport receptor (NTR) complex (Fagotto, Gluck, & Gumbiner, 1998; Yokoya, Imamoto, Tachibana, & Yoneda, 1999), a notion at the time thought to be consistent with Ran independence. Finally, the structural similarity between β-catenin and Kap-α, both made up of armadillo-repeats, suggested that β-catenin might itself act as an NTR by directly interacting with the Phe-Gly (FG) nups responsible for selective passage across the nuclear pore complex (NPC) (Andrade, Petosa, O'Donoghue, Muller, & Bork, 2001; Conti & Kuriyan, 2000; Fagotto et al., 1998; A. H. Huber, Nelson, & Weis, 1997; Sharma, Johnson, Brocardo, Jamieson, & Henderson, 2014; Xu & Massague, 2004; Yano, Oakes, Tabb, & Nomura, 1994). However, Kap-α does not directly bind to FG-nups and the evidence that β-catenin does so is controversial (Sharma, Jamieson, Lui, & Henderson, 2014; Suh & Gumbiner, 2003). Using a CRISPR based screening platform, recent work provides evidence that β-catenin may be imported by the NTR, Imp11; however, this mechanism appears curiously relevant only for a subset of colon cancer cells (Mis et al., 2020). Alternative models for β-catenin nuclear transport have been proposed; however, molecules that directly bind β-catenin to modulate nuclear transport remain undefined (Goto et al., 2013; Griffin et al., 2018; Komiya, Mandrekar, Sato, Dawid, & Habas, 2014).Thus, a complete understanding of β-catenin nuclear transport remains outstanding, leaving open a key gap in our knowledge of Wnt signaling that could otherwise be targeted for therapeutic intervention.

1.6 *Saccharomyces cerevisiae* as a model for studying nuclear transport

A major stumbling block with understanding the β-catenin nuclear import mechanism is the myriad of binding partners that modulate its steady-state distribution and, hence, complicate the direct interrogation of the nuclear transport step (Fagotto, 2013; MacDonald et al., 2009). For example, any manipulation that reduces the nuclear accumulation of β-catenin, must also consider whether the underlying cause is due to enhanced degradation of β-catenin in the cytosol or more binding at the plasma membrane in cell adhesion complexes. Additionally, any change in Wnt signaling might also feedback on the pathway adding another complexity on the regulation of β-catenin levels. Therefore, the diverse roles and regulation of β-catenin complicate the interrogation of the nuclear transport step; a simplified experimental system is needed in which β-catenin can undergo nuclear transport without other complicating steps.

The budding yeast, *S. cerevisiae*, is a heterologous system that may fulfill our criteria for isolating the nuclear transport step. Yeast do not have a Wnt pathway nor a β-catenin ortholog, which presumably emerged in metazoans with the onset of multicellularity and cell fate specialization (Holstein, 2012). Yeast also likely lack β-catenin binding partners and its degradation machinery and thus provide a simplified system to specifically evaluate nuclear import. Most critically, the nuclear transport system including NTRs, NPCs and Ran are well conserved from yeast to human (Malik, Eickbush, & Goldfarb, 1997; Wente & Rout, 2010; Wozniak, Rout, & Aitchison, 1998). Indeed, even NLS and NES sequences are recognized by orthologous NTRs across millions of years of evolution (Conti & Kuriyan, 2000; Fontes, Teh, & Kobe, 2000; Kosugi, Hasebe, Tomita, & Yanagawa, 2008; Lange, Mills, Devine, & Corbett, 2008; Soniat et al., 2013). Therefore, we set out to determine first if yeast would be a suitable model and then identify the molecular members that regulate β-catenin nuclear transport.

Chapter 2: Materials and Methods

2.1 Experimental Model and Subject details

1. *Xenopus laevis & tropicalis*

Xenopus tropicalis and *Xenopus laevis* were maintained and cared for in accordance to the Yale University Institutional Animal Care and Use Committee (IACUC) protocols (protocol number-2021-11035). *In vitro* fertilization was performed as per standard protocols (del Viso & Khokha, 2012; Sive, Grainger, & Harland, 2007). *X. tropicalis* embryos were raised in 1/9X MR + gentamycin at 25-28°C and *X. laevis* embryos were raised in 1/3X MR + gentamycin at 18°C until desired staging.

2. *Saccharomyces cerevisiae* strains

All yeast strains used in this study are listed in **Table S1**. Yeast strains were grown at 30°C, unless indicated otherwise in YPAD medium (1% Bacto yeast extract, 2% bactopeptone, 2% glucose, 0.05% Adenine sulfate). Transformation of yeast was carried out using standard protocols (Amberg, 2005) with minor modifications. The yeast strain to be transformed was inoculated in 5 ml of YPAD medium and incubated on a shaker at 225 rpm at 30°C overnight. Next day, 200 µl of overnight yeast culture was inoculated to 10 ml of YPAD media and incubated on a shaker at 30°C for 3-4 hours or until it reaches the optical density of 0.8-1.0. Cultured cells were transferred to 15-ml falcon tube and centrifuged at 3000 g for 5 minutes. Supernatant was discarded and yeast pellet was resuspended in 1 ml of 100 mM Lithium Acetate (LiAc). Cells were centrifuged again at top speed for 20-30 seconds and the supernatant was discarded. Yeast cell pellet was finally resuspended in 500-600 µl of 100 mM Lithium Acetate and ready for transformation. Transformation mix was prepared in 1.5 ml Eppendorf tube as

follows: 1.2 ml of Polyethylene glycol (PEG) 4000 (sigma) 50% (w/v), 180 µl of 1.0 M LiAc, and 125 µl of single stranded salmon sperm DNA. The transformation mix was vortexed vigorously for 30 seconds. Subsequently, 3 µl of linearized plasmid DNA (1 µg) and 100 µl of yeast cells suspended in 100 mM LiAc were added to 300 µl of transformation mix. The transformants were vortexed vigorously again for 1 minutes and heat shocked in a 42°C water bath for 45 minutes. The transformants were centrifuged at 3000 rpm for 5 minutes to remove the supernatant and re-suspended in 100 µl of 0.9% NaCl. Re-suspended transformants were then plated out the selective plate (eg. -uracil +CSM plate for pRS406ADH1 plasmid). The plate was incubated at 30°C until colonies can be detected. It usually takes about 2 days for colonies to develop. Individual colonies were streaked out onto the new plate using a sterile toothpick and the plate was incubated at 30°C until sufficient growth can be seen.

3.Mammalian cells

HEK293T and HeLa cells were maintained and cultured with DMEM medium + 10% Fetal Bovine Serum (FBS) + 1% Penicillin and Streptomycin (PS) in a T-75 flask. The engineered 3T3 mouse fibroblast cell line that stably expresses the TCF/LEF luciferase transgene was maintained with DMEM medium + Cell Growth Medium Concentrate (Enzo life sciences). Further experimental procedures for the 3T3 cell line can be found under the TCF/LEF luciferase assay section (see below). Upon 70-80% cell confluency, cells were transfected with plasmids (0.5 µg per well in 24-well plate) or siRNAs (25 pmoles per well in 24-well plate) using jetPRIME (Polyplus-transfection) following the manufacturer's instructions. Cells were fixed with 4% paraformaldehyde/PBS and further processed for immunofluorescence 24-48 hours post-

transfection. Antibodies used in this study are listed in **Key Resources Table**. Cells were tested for mycoplasma using MycoAlert Detection Kit (Lonza).

Table S1. Yeast strains

Name	Genotype	Origin	Generation
W303a	MATa, *ade2-1 can1-100 his3-11,15 leu2-3,112 trp1-1 ura3-1*	EUROSCARF	
W303α	MATα, *ade2-1 can1-100 his3-11,15 leu2-3,112 trp1-1 ura3-1*	EUROSCARF	
HHY110	W303, *MAT alpha tor1-1 fpr1*::*natMX6MX6 PMA1-2xFKBP12*::*TRP1*	Euroscarf (Haruki et al., 2008)	
DTCPL1635	HHY110, HEH2-mCherry::*KAN*	This study	Integration through PCR product transformation in HHY110
WHCPL13	DTCPL1635, *Kap95-FRB*:: *HIS3,*	This study	Integration through PCR product transformation in DTCPL1635
WHCPL1	DTCPL1635, *Kap104-FRB*::*HIS3,*	This study	Integration through PCR product transformation in DTCPL1635
WHCPL2	DTCPL1635, *Kap108-FRB*::*HIS3*	This study	Integration through PCR product transformation in DTCPL1635
WHCPL3	DTCPL1635, *Kap111-FRB*::*HIS3*	This study	Integration through PCR product transformation in DTCPL1635
WHCPL7	DTCPL1635, *Kap114-FRB*::*HIS3*	This study	Integration through PCR product transformation in DTCPL1635
WHCPL10	DTCPL1635, *Kap119-FRB*::*HIS3*	This study	Integration through PCR product transformation in DTCPL1635
WHCPL14	DTCPL1635, *Kap120+FRB*::*HIS3*	This study	Integration through PCR product transformation in DTCPL1635
WHCPL15	DTCPL1635, *Kap121+FRB*::*HIS3*	This study	Integration through PCR product transformation in DTCPL1635
WHCPL11	DTCPL1635, *Kap122-FRB*::*HIS3*	This study	Integration through PCR product transformation in DTCPL1635
WHCPL12	DTCPL1635, *Kap123-FRB*::*HIS3*	This study	Integration through PCR product transformation in DTCPL1635
BWCPL1314	W303, HEH2-mCherry::*natMX6*	(Thaller et al., 2019)	
WHCPL16	*mtr1-1*::*TRP1*, HEH2-mCherry::*KAN*	This study	Integration through PCR product transformation in *mtr1-1* strain[39]
WHCPL17	WHCPL16, xβ-catenin (1-782)-GFP::*URA3*	This study	Transformation of linearized xβ-catenin_GFP_pRS406ADH1 in WHCPL1316
WHCPL19	WHCPL16, xβ-catenin (665-745)-GFP::*URA3*	This study	Transformation of linearized xβ-catenin_665-745_GFP_pRS406ADH1 in WHCPL1316
WHCPL21	BWCPL1314, xβ-catenin (1-782)-GFP::*URA3*	This study	Transformation of linearized xβ-catenin_GFP_pRS406ADH1 in BWCPL1314
WHCPL23	BWCPL1314, xβ-catenin (1-664)-GFP::*URA3*	This study	Transformation of linearized xβ-catenin_ΔC-terminus_GFP_pRS406ADH1 in BWCPL1314
WHCPL25	BWCPL1314, xβ-catenin (141-782)-GFP::*URA3*	This study	Transformation of linearized xβ-catenin_ΔN-terminus_GFP_pRS406ADH1 in BWCPL1314

WHCPL27	BWCPL1314, xβ-catenin (Δ141-664)-GFP::*URA3*	This study	Transformation of linearized xβ-catenin_ΔARM_GFP_pRS406ADH1 in BWCPL1314
WHCPL29	BWCPL1314, xβ-catenin (1-140)-GFP::*URA3*	This study	Transformation of linearized xβ-catenin_N-terminus_GFP_pRS406ADH1 in BWCPL1314
WHCPL31	BWCPL1314, xβ-catenin (141-664)-GFP::*URA3*	This study	Transformation of linearized xβ-catenin_ARM_GFP_pRS406ADH1 in BWCPL1314
WHCPL33	BWCPL1314, xβ-catenin (665-782)-GFP::*URA3*	This study	Transformation of linearized xβ-catenin_C-terminus_GFP_pRS406ADH1 in BWCPL1314
WHCPL35	BWCPL1314, xβ-catenin (665-745)-GFP::*URA3*	This study	Transformation of linearized xβ-catenin_665-745_GFP_pRS406ADH1 in BWCPL1314
WHCPL37	BWCPL1314, xβ-catenin (704-782)-GFP::*URA3*	This study	Transformation of linearized xβ-catenin_704-782_GFP_pRS406ADH1 in BWCPL1314
WHCPL39	BWCPL1314, xβ-catenin (746-782)-GFP::*URA3*	This study	Transformation of linearized xβ-catenin_746-782_GFP_pRS406ADH1 in BWCPL1314
WHCPL41	BWCPL1314, MBP(x3)-GFP::*HIS*	This study	Transformation of linearized MBP(x3)_GFP in BWCPL1314
WHCPL43	BWCPL1314, xβ-catenin (665-703)-MBP(x3)-GFP::*HIS*	This study	Transformation of linearized xβ-catenin_(665-703)_MBP(x3)_GFP in BWCPL1314
WHCPL45	BWCPL1314, xβ-catenin (665-703, P687A, M688A)-MBP(x3)-GFP::*HIS*	This study	Transformation of linearized xβ-catenin_(665-703, P687A,M688A)_MBP(x3)_GFP in BWCPL1314

Method details

2.2 Key resources

Key resources and all plasmids used in this study are listed in **Key Resources Table** and **Table S2**, respectively. *Xenopus* β-catenin-GFP (Addgene #16839), *Xenopus* cNLS-β-catenin-GFP (Addgene #16838), GST-human β-catenin (Addgene #24193), and NLS-mCherry (Addgene #49313) plasmids were obtained from Addgene. GST-transportin 1 (TNPO1) and Gal-MBP(x3)-GFP plasmids were generous gifts from Dr. Yuh-min Chook at UTSW and Dr. Liesbeth M. Veenhoff at University of Groningen, respectively. Gibson Assembly (New England Biolabs) was used to generate GFP tagged *Xenopus* β-catenin truncation constructs following the manufacturer's instructions. A detailed Gibson Assembly protocol is available below. Both the human and *Xenopus* β-catenin P687A, M688A variants were generated using Q5 site- directed mutagenesis (New England Biolabs) following the manufacturer's instructions. Subsequently, the β-catenin constructs were sub-cloned into the pRS406 vector containing an ADH1 promotor for yeast studies or a pCS2+ vector for mammalian/*Xenopus* studies. mRNAs were generated using the SP6 mMessage machine kit (Thermo Fisher Scientific) and RNA clean & concentrator kit (Zymo Research) following the manufacturer's instructions. We obtained siRNAs directed against mouse TNPO1 (s108857), mouse TNPO2 (s102754) and a control siRNA (4390843) from Thermo Fisher Scientific. To generate CRISPR sgRNAs, we used the EnGen sgRNA synthesis kit (NEB) following the manufacturer's instructions with the following targeting sequences *tnpo1* sgRNA#1 (5'-GGCATGGGGGCCACCTCTTG-3'), *tnpo1* sgRNA#2 (5'-GGGTTACGTTTGTCCTCAAG-3'), *tnpo2* sgRNA #1 (5'- GGGCGTTTAGCCGCGTTCTA-3'), and *tnpo2* sgRNA #2 (5'- GGCGTCATGGATGAGTCCGA-3') (designed using

CRISPRscan (Moreno-Mateos et al., 2015)). CRISPR experiments in wildtype or transgenic *Xenopus tropicalis* were performed as previously described (Bhattacharya, Marfo, Li, Lane, & Khokha, 2015).CRISPR gene editing efficiency was assessed using Synthego ICE (ice.synthego.com) as previously described (Sempou, Lakhani, Amalraj, & Khokha, 2018). The M9M peptide (GGSYNDFGNYNNQSSNFGPMKGGNFGGRFEPYANPTKR) and the M9M-A peptide (GGSYNDFGNYNNQSSNAAAAKGGNFGGAFEAAANPTKR) were synthesized by LifeTein.

KEY RESOURCES TABLE

Reagent type (species) or resource	**Designation**	**Source or reference**	**Identifiers**	**Additional information**
strain, strain background (*Xenopus tropicalis*)	Tg(pbin7LEF-dGFP)	National Xenopus Resources at MBL	NXR_1094	
strain, strain background (*Xenopus laevis*)	*Xenopus laevis*	NASCO	LM00535 & LM00715	
strain, strain background (*Escherichia coli*)	BL21 Gold (DE3)	Agilent	230132	
strain, strain background (*Escherichia coli*)	XL-10 Gold	Agilent	200314	
strain, strain background (*Escherichia coli*)	DH5-alpha	NEB	C2987	

cell line (*M. musculus*)	Leading Light Wnt Reporter Cell line- TCF/LEF luciferase 3T3 mouse fibroblast	Enzo Life Sciences	ENZ-61001-0001	
cell line (*Homo-sapiens*)	Human embryonic kidney 293 (HEK293T)	ATCC	CRL-3216	
cell line (*Homo-sapiens*)	HeLa	ATCC	CCL-2	
cell line (*Homo-sapiens*)	Human Colorectal Cancer (HCT 116)	ATCC	CCL-247	
cell line (*Homo-sapiens*)	Human Colorectal Cancer (DLD-1)	ATCC	CCL-221	
transfected construct (*M. musculus &* human)	siRNA to TNPO1 & 2	Thermo Fisher		
antibody	anti-β-catenin (mouse monoclonal)	Santa Cruz	sc-7963 HRP, RRID:AB_626807	WB (1:1000)
antibody	anti-β-actin (mouse monoclonal)	Santa Cruz	sc-47778 HRP, RRID:AB_2714189	WB (1:10000)
antibody	anti-GFP (mouse monoclonal)	Santa Cruz	sc-9996 HRP, RRID:AB_627695	WB (1:1000)

antibody	anti-Transportin-1 (mouse monoclonal)	Abcam	ab10303, RRID:AB_2206878	WB (1:1000)
antibody	anti-Transportin-2 (Rabbit polyclonal)	Proteintech	17831-1-AP, RRID:AB_10598481	WB (1:3000)
antibody	anti-LaminB1 (Rabbit polyclonal)	Abcam	Ab16048, RRID:AB_443298	IF (1:500) WB (1:1000)
antibody	Anti-GAPDH (mouse monoclonal)	Santa Cruz	sc-47724 HRP; RRID:AB_627678	WB (1:3000)
sequence-based reagent	tnpo1 CRISPR 1	This paper	Oligonucleotides	ttctaatacgactcactataGGCATGGGGGCCACCTCTTGgtttagagctagaa
sequence-based reagent	tnpo1 CRISPR 2	This paper	Oligonucleotides	ttctaatacgactcactataGGGTTACGTTTGTCCTCAAGgttttagagctagaa
sequence-based reagent	tnpo2 CRISPR 1	This paper	Oligonucleotides	ttctaatacgactcactataGGGCGTTTAGCCGCGTTCTAgttttagagctagaa
sequence-based reagent	tnpo2 CRISPR 2	This paper	Oligonucleotides	ttctaatacgactcactataGGCGTCATGGATGAGTCCGAgttttagagctagaa
sequence-based reagent	siRNA: negative control	Thermo Fisher	4390843	Silencer Select
sequence-based reagent	siRNA: mouse TNPO1	Thermo Fisher	s108857	Silencer Select

sequence-based reagent	siRNA: mouse TNPO2	Thermo Fisher	s102754	Silencer Select
sequence-based reagent	siRNA: human TNPO1	Thermo Fisher	s7934	Silencer Select
sequence-based reagent	siRNA: human TNPO2	Thermo Fisher	s26881	Silencer Select
peptide, recombinant protein	M9M-A	Lifetein	Custom	N-GGSYNDFGNYNNQSSNAAAAKGGNFGGAFEAAANPTKR-C
peptide, recombinant protein	M9M	Lifetein	Custom	N-GGSYNDFGNYNNQSSNFGPMKGGNFGGRFEPYANPTKR-C
commercial assay or kit	Luciferase Assay System	Promega	E1500	
commercial assay or kit	NE-PER Nuclear Cytoplasmic Extraction Reagents	Thermo Scientific	78833	
commercial assay or kit	jetPRIME	Polyplus transfection	114-15	
commercial assay or kit	ProteoJuice Protein Transfection	Millipore Sigma	71281	

commercial assay or kit	MycoAlert Detection Kit	Lonza	LT07-118	
chemical compound, drug	Rapamycin	Fisher scientific	AAJ62473MF	
chemical compound, drug	Glutathione Sepharose 4B	Millipore Sigma	GE17-0756-01	
chemical compound, drug	Protease Inhibitor Cocktail mix	Millipore Sigma	P8340-5ML	
chemical compound, drug	ProTEV Plus	Promega	V6101	
chemical compound, drug	NEBExpress Ni-NTA Magnetic Beads	NEB	S1423S	
chemical compound, drug	Isopropyl β-d-1-thiogalacto pyranoside (IPTG)	Thermo Fisher	15529019	
software, algorithm	Fiji	ImageJ	https://imagej.net/Fiji	
software, algorithm	Prism 9	Graphpad	https://www.graphpad.com/	

Table S2. Plasmids

Plasmids for Yeast Experiments			
Name	Insert	Vector	Cloning Strategy/Source
xβ-catenin_GFP_pRS406ADH1	*Xenopus* β-catenin (1-782)_GFP	pRS406ADH1	Gibson assembly
xβ-catenin_ΔN-terminus_GFP_pRS406ADH1	*Xenopus* β-catenin (141-782)_GFP	pRS406ADH1	Gibson assembly
xβ-catenin_ΔARM_GFP_pRS406ADH1	*Xenopus* β-catenin (Δ141-664)_GFP	pRS406ADH1	Gibson assembly
xβ-catenin_ΔC-terminus_GFP_pRS406ADH1	*Xenopus* β-catenin (1-664)_GFP	pRS406ADH1	Gibson assembly
xβ-catenin_N-terminus_GFP_pRS406ADH1	*Xenopus* β-catenin (1-140)_GFP	pRS406ADH1	Gibson assembly
xβ-catenin_ARM_GFP_pRS406ADH1	*Xenopus* β-catenin (141-664)_GFP	pRS406ADH1	Gibson assembly
xβ-catenin_C-terminus_GFP_pRS406ADH1	*Xenopus* β-catenin (665-782)_GFP	pRS406ADH1	Gibson assembly
xβ-catenin_665-745_GFP_pRS406ADH1	*Xenopus* β-catenin (665-745)_GFP	pRS406ADH1	Gibson assembly
xβ-catenin_704-782_GFP_pRS406ADH1	*Xenopus* β-catenin (704-782)_GFP	pRS406ADH1	Gibson assembly
xβ-catenin_746-782_GFP_pRS406ADH1	*Xenopus* β-catenin (746-782)_GFP	pRS406ADH1	Gibson assembly
MBP(x3)_GFP	no insert	MBP(x3)_GFP	Popken et al., 2015
xβ-catenin_(665-703)_MBP(x3)_GFP	*Xenopus* β-catenin_(665-703)	MBP(x3)_GFP	Gibson assembly
xβ-catenin_(665-703, P687A,M688A)_MBP(x3)_GFP	*Xenopus* β-catenin_(665-703, P687A,M688A)	MBP(x3)_GFP	Site-directed mutagenesis
Plasmids for Vertebrate Experiments			
Name	Insert	Vector	Cloning Strategy
GFP_pCS2+	GFP	pCS2+	Gibson assembly
xβ-catenin_GFP_pCS2+	*Xenopus* β-catenin (1-782)_GFP	pCS2+	Gibson assembly
xβ-catenin_Δ665-745_GFP_pCS2+	*Xenopus* β-catenin (Δ665-745)_GFP	pCS2+	Gibson assembly
cNLS_xβ-catenin_Δ665-745_GFP_pCS2+	cNLS_*Xenopus* β-catenin (Δ665-745)_GFP	pCS2+	Gibson assembly

xβ-catenin_665-745_GFP_pCS2+	*Xenopus* β-catenin (665-745)_GFP	pCS2+	Gibson assembly
hβ-catenin_GFP_pCS2+	full length Human β-catenin_GFP	pCS2+	Gibson assembly
hβ-catenin_Δ665-745_GFP_pCS2+	Human β-catenin (Δ665-745)_GFP	pCS2+	Site-directed mutagenesis
hβ-catenin_665-782_GFP_pCS2+	Human β-catenin (665-782)_GFP	pCS2+	Gibson assembly
hβ-catenin_(665-782, P687A,M688A)_GFP_pCS2+	Human β-catenin (665-782, P687A,M688A)_GFP	pCS2+	Site-directed mutagenesis
cNLS_hβ-catenin_GFP_pCS2+	full length Human β-catenin_GFP	pCS2+	Site-directed mutagenesis

2.3 Gibson Assembly

NEBuilder Assembly Tool was used to design primers for Gibson Assembly reaction (https://nebuilder.neb.com/#!/). When designing primers, an insert should be placed downstream of a promoter in the recipient plasmid (i.e. SP6 for pCS2+ or ADH1 for pRS406ADH1 vector) and in-frame with any tagged coding sequence (i.e. GFP at c-terminus). Insert sequence was flanked by 20 bp long DNA segment from the recipient vector by PCR reaction (flanking sequence was indicated by yellow and green in **Figure D**). Amplified PCR was purified using DNA purification kit (Qiagen) and the eluted PCR concentration was measured using Nanodrop. The recipient plasmid was linearized with restriction enzyme(s) to create a cloning site just downstream of the promoter. 5' phosphate group was removed using Quick Calf Intestinal alkaine Phosphatase (CIP) treatment to prevent self-ligation of linearized plasmid DNA (NEB) (**Figure D**). Dephosphorylated plasmid was purified using DNA purification kit (Qiagen). Gibson assembly reaction was set up following the manufacturer's instructions (NEB) and transform the assembly reaction into DH5-alpha E.coli cells (**Figure E**).

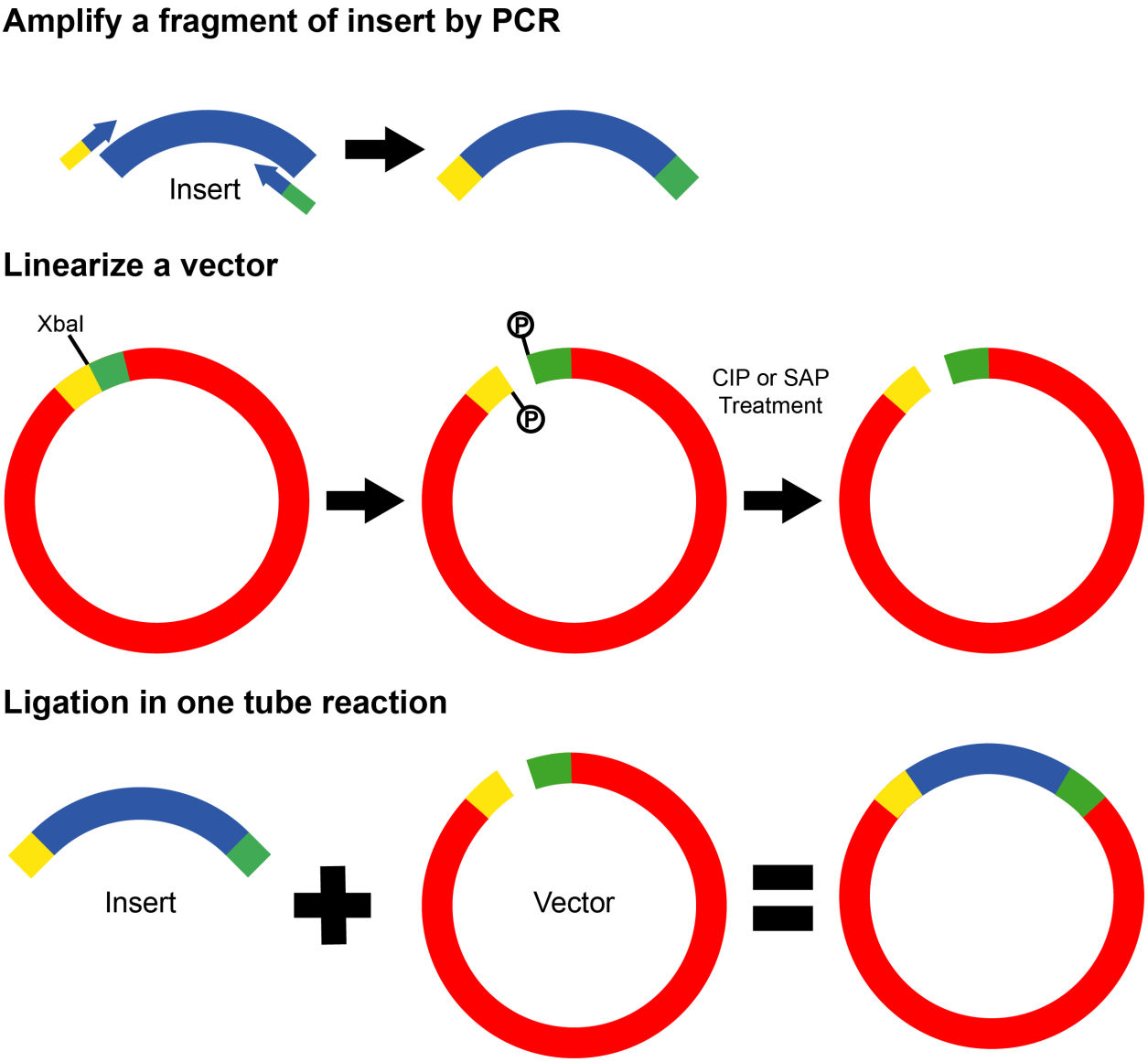

Figure F. Schematic diagram of Gibson assembly cloning strategy.

Gibson assembly in one tube reaction

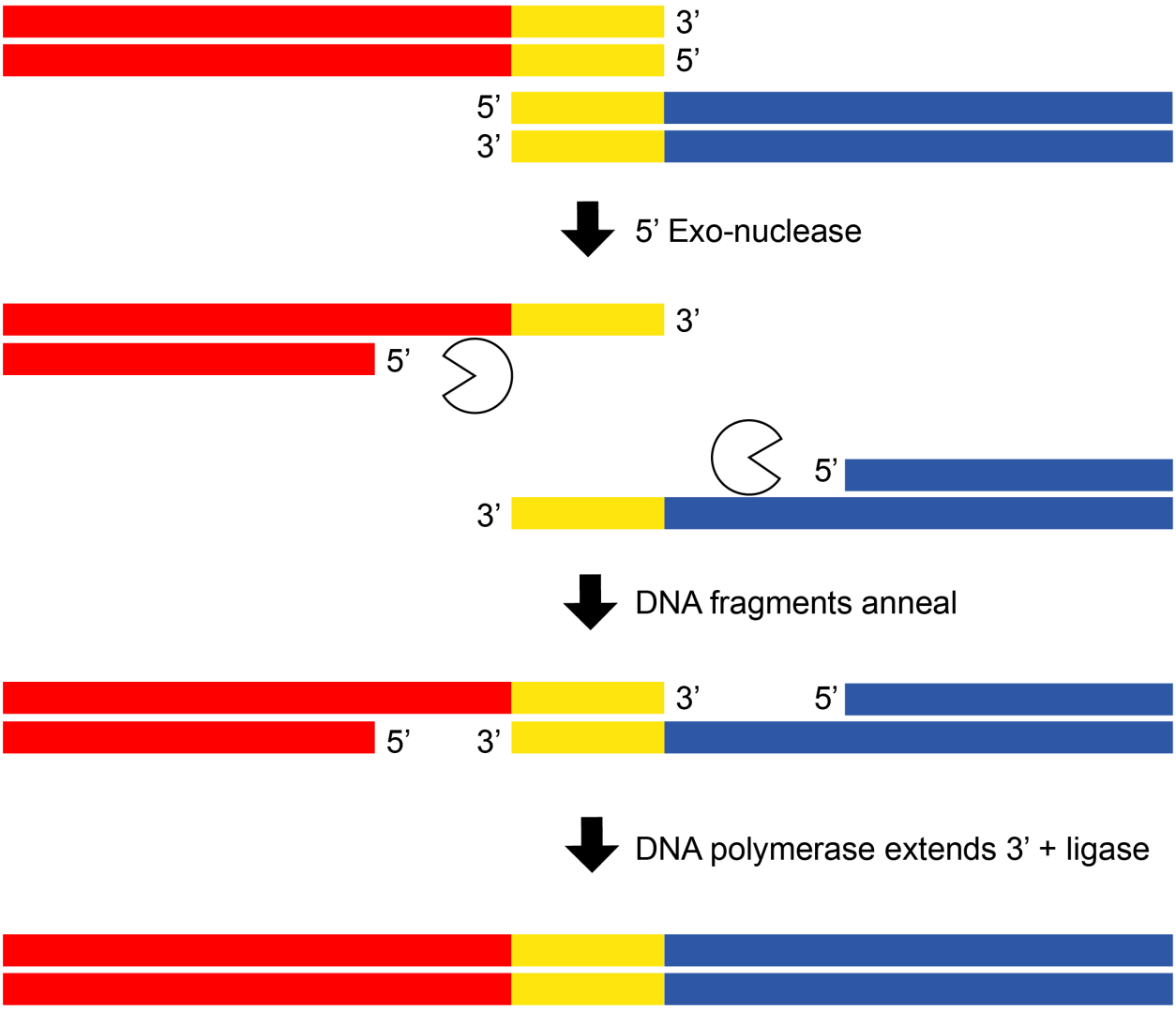

Figure G. Schematic diagram of Gibson assembly reaction. Gibson assembly master mix contains three enzymes (Exo-nuclease, DNA Polymerase and DNA Ligae) that facilitate a DNA segments assembly in one tube reaction. T5 Exo-nuclease will chew back 5’ end to create a single strand 3’ overhangs. Complementary DNA fragments (indicated by yellow region) will then anneal to each other. Subsequently DNA polymerase will add nucleotides to fill in the gaps. DNA Ligase will join the annealed DNA fragments together.

2.4 Yeast and mammalian β-catenin sub-cellular localization by microscopy

Expression plasmids containing full length and fragments of the β-catenin-GFP coding sequence under the control of the *ADH1* promoter were transformed into the W303, Heh2-mCherry::NAT (BWCPL1314) strain. A yeast colony that incorporated the plasmid sequence was cultured in 2 ml YPAD overnight. 200 µl of overnight yeast culture was inoculated to 10 ml of YPAD media and incubated on a shaker at 30°C for 3-4 hours to make sure that yeast undergoes 2 cell division. Subsequently, 0.5 ml-1 ml of yeast culture was transferred to 1.5 ml Eppendorf tube, centrifuged at 2000 rpm for 1 minute to remove the YPAD media and washed in 50 µl CSM + glucose solution. Yeast cells were centrifuged again at 2000 rpm for 1 minute and finally re-suspended in 50 µl CMS + glucose solution. 2-4 µl of resuspended yeast cells were mounted onto a coverslip for live imaging on a DeltaVision wide-field microscope (GE Healthcare) with a CoolSnapHQ^2 CCD camera. Yeast fluorescent images were deconvolved using the iterative algorithm sofWoRx. 6.5.1 (Applied Precision, GE Healthcare). B-catenin-GFP transfected HeLa or HEK293T cells were mounted on Pro-Long Gold coated coverslip for imaging on a Zeiss Axio Observer microscope. All fluorescent images were analyzed with Fiji software. For quantification, the oval selection tool was used to draw a circle in both the nuclear and cytosolic regions on the same image plane to measure florescence intensity.

2.5 Secondary axis assays and β-catenin sub-cellular localization

Xenopus laevis embryos were injected with a mixture of either 200pg of *Xenopus* or human β-catenin-GFP mRNA and cNLS-mCherry mRNA in one of four cells (targeting the ventral side). Embryos were assessed for a secondary axis via stereomicroscopy at stage 17-19. For the β-catenin localization experiments by fluorescence, Stage 10 embryos were fixed in 4%

paraformaldehyde/PBS at 4°C overnight on a nutator. Embryos were washed in 1x PBS + 0.1% TritonX-100, and the dorsal blastopore lips were sectioned with a razor blade and mounted on Pro-Long Gold (Invitrogen) coated coverslip before imaging on a Zeiss 710 confocal microscope.

2.6 The Anchor Away assay

To employ the Anchor Away approach, we used a yeast strain that harbors a FKBP12 fusion of the endogenous plasma membrane H^+-ATPase (*PMA1* gene), a Heh2-mCherry fusion to mark the nuclear envelope, and a mutated *TOR1* gene (HHY110: *HEH2-mCherry::KAN, PMA1-2xFKBP12, fpr1::NAT tor1-1*). In this strain, individual, endogenous NTRs are tagged with the FRB domain at the C-terminus by homologous recombination of a PCR product that contains an FRB sequence, a 3x HA epitope, and a selective marker, *HIS3*, flanked by a 60 bp homology arm of endogenous NTR coding sequence (**Figure H**) (Haruki, Nishikawa, & Laemmli, 2008; Longtine et al., 1998). Primers for PCR were designed in following manner: forward primer (60 bp upstream of endogenous NTR stop codon + F2 sequence (CGGATCCCCGGGTTAATTAA) and reverse primer (60bp downdream of stop codon)* + R1 sequence (GAATTCGAGCTCGTTTAAAC) (**Table S3** for Anchor away primers). In some cases, reverse primer was designed beyond the 3' UTR in order to identify a GC rich genomic site and made sure that the sequence did not overlap with other essential genomic sequence. Integration of an FRB sequence is confirmed by colony PCR using a gene specific forward and a plasmid specific reverse primer and rapamycin induced cell death for essential NTRs (**Figure I**, **Table S4** for colony PCR primers). For colony PCR, a 20 µl pipette tip was used to pick a small amount of colony cells and dipped directly into PCR tube containing LongAmp taq 2x master mix, primers

and water. The cells were mixed vigorously until well homogenized in PCR master mix solution. Subsequently, an expression plasmid containing the coding sequence for xβ-catenin (665-782)-GFP under the control of the *ADH1* promoter was transformed into the Anchor Away line. These lines were treated with 1 mg/ml of rapamycin (5-15 minutes of incubation) or vehicle alone (DMSO) before imaging.

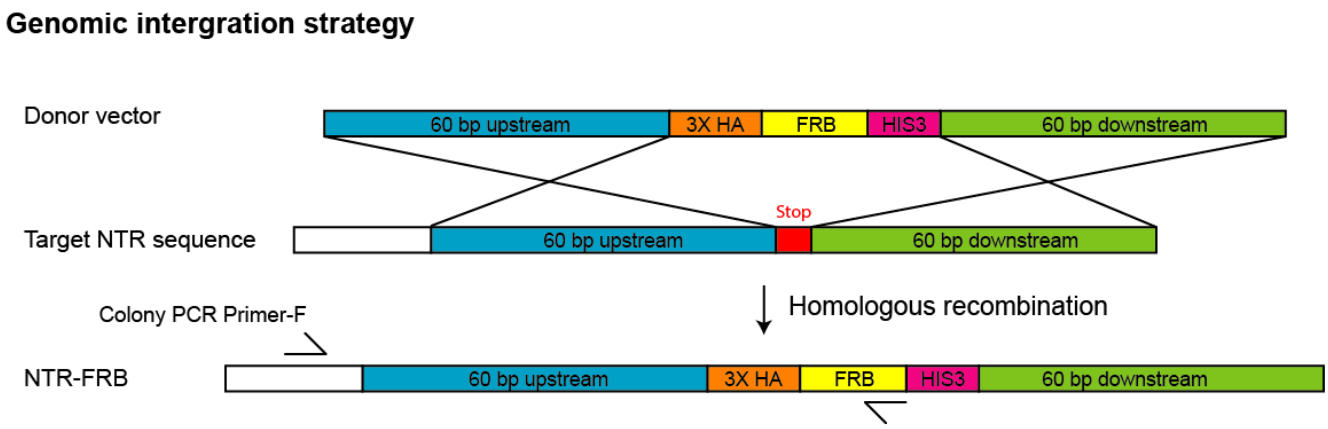

Figure H. Anchor Away cloning strategy in *S. cerevisiae.* Schematic diagram of FRB tagging to individual endogenous NTRs by homologous recombination

Table S3. Anchor away primers

Gene	Primers	Sequence 5'-3'
Kap95	Kap95+F2_F2	CAAGCCACAAAAGATACAGCAAGATGGGCTAGAGAGCAACAGAAG CGTCAATTATCCTTACGGATCCCCGGGTTAATTAA
	Kap95+R1_R	CAGCTAAGATGTTTGCAAGCAAGAATTAACAGATAAGCCGCTTCGC TAGTAACGCAACTCGAATTCGAGCTCGTTTAAAC
Kap104	Kap104+F2_F	CAAATTTCTGCAATAAATTTCACGCCCGATGAAATCTCCTTCTTACA ACAGTTCACCAGCCGGATCCCCGGGTTAATTAA
	Kap104+R1_R	CATGTCTGGCTGCATTATGTATATGCTGCACCATGGATATGCTATTC TAAGAGAACCCGCGAATTCGAGCTCGTTTAAAC
Kap108/ Sxm1	Kap108+F2_F	TATCTGGATGAATCTAAGAGAGATTCCTTGCAGGTAATTCTGGAATT TGTTTCTCAACACCGGATCCCCGGGTTAATTAA
	Kap108+R1_R	TGTTTAGACAGTCAAGGTCCAGATTACACCACAATAGTGTATCTGAT CCGGTTAAGTCGGGAATTCGAGCTCGTTTAAAC
Kap111/ Mtr10	Kap111+F2_F	GAAGGAATTAGGGCGTTTGTTGGATGGTATTCAAGAAAGAATATCA ATTCGAGGTTTGAACGGATCCCCGGGTTAATTAA
	Kap111+R1_R	TCTAAGGTTTACCTCGCCTCAATACAATTCGAACGGCGCTTACAACG GCGCCCTAATGGCGAATTCGAGCTCGTTTAAAC
Kap114	Kap114+F2_F	CATTGTATTTACGAGACTCTATCCGACAGTGAACGTAAAGTTCTTTC AGAAGCCCTTTTGCGGATCCCCGGGTTAATTAA
	Kap114+R1_R	GCTCTGAGGGTGCTAAATGGTCCAAGACTTTGTTTATTCCAATCGGG TCCATTATCTGACGAATTCGAGCTCGTTTAAAC
Kap119/ Nmd5	Kap119+F2_F	GGAATCTTGAGACATCTGACCCCGGCTGATCAAGAACTATTCATGG GAATTATGAATGCCCGGATCCCCGGGTTAATTAA
	Kap119+R1_R	ACTCCCTGACAAAGCTTGTGAATATTATTATAGGAGATGTACATTCT CTCATTTTCGGCCGAATTCGAGCTCGTTTAAAC
Kap120	Kap120+F2_F	CCTAGTTTACTAGAGAACTTACAAATGTTTTTATCCATCCAGCCTCA AGAGGCTCGTCCACGGATCCCCGGGTTAATTAA
	Kap120+R1_R	TTACCTGTGGGAGACAATCTATGTAATGGCGAACTCATCCTTTCCTG TGCTCTATAGTGCGAATTCGAGCTCGTTTAAAC
Kap121/ Pse1	Kap121+F2_F	ATGGCAATTTTCAATAGATATCCAGCTGATATTATGGAGAAAGTAC ATAAATGGTTTGCACGGATCCCCGGGTTAATTAA
	Kap121+R1_R	TAACTTAGCACAAGTGGTCTTTACCTCCATCATTTCCTTATCCATTGC CGCTGGTGTCGGGAATTCGAGCTCGTTTAAAC
Kap122/ Pdr6	Kap122+F2_F	GCTGGAAATGTTATTTTGCAGTGGTGGTTGGATTGTACCACACTTCC AAATTACCAAGGACGGATCCCCGGGTTAATTAA
	Kap122+R1_R	CACTCCATGGAAGACACGATACGTCCATTAAATTACGCAGATATCG AGACCAGCGGGCCCGAATTCGAGCTCGTTTAAAC
Kap123	Kap123+F2_F	CTAAACACTACTTACAACGGAATTGTTGCTCAAAATCCGGTTTTAGC TGCCGTCATTGCTCGGATCCCCGGGTTAATTAA
	Kap123+R1_R	CTCAGGACACATACATACAAGATTGGCAAAAGTGAAGGCAGGTGCC TAAGATTGGGTGGGGAATTCGAGCTCGTTTAAAC

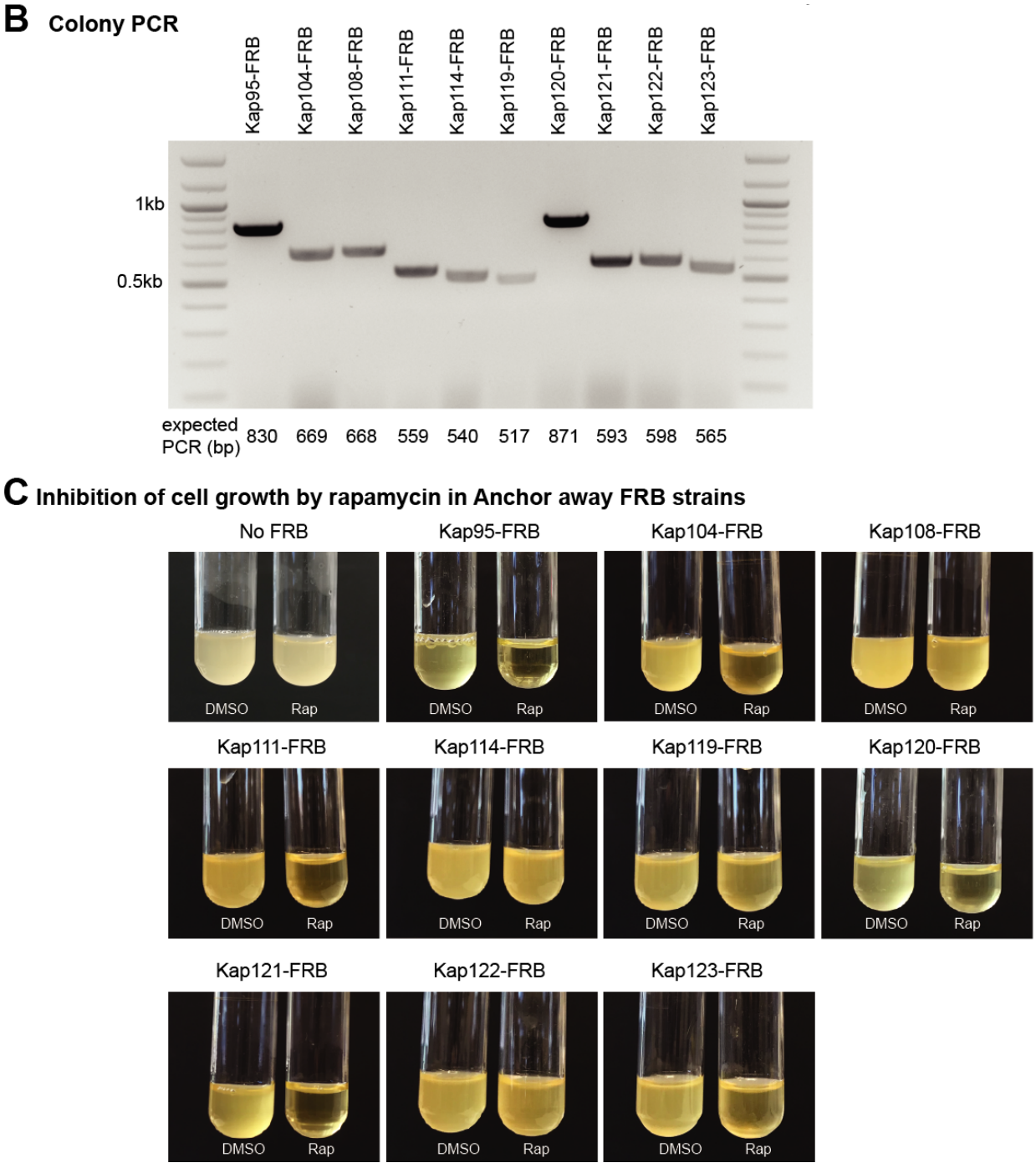

Figure I. Validation of Anchor Away strains in *S. cerevisiae.* (B) Screening of NTR-FRB strains by colony PCR. Primers are listed in Table S3. **(C)** Positive NTR-FRB strains from the colony PCR in **(B)** were further tested for cell growth as some NTRs are essential for survival. No FRB and DMSO were used negative controls.

Table S4. Anchor away colony PCR

Gene	Primers	Sequence 5'-3'	Colony PCR size
Kap 95	Kap95_F1	ACATCATGGCGTTGTGTGTT	830bp
Kap 104	Kap104_F1	TCCGTTAACGCATTGGAC	669bp
Kap 108	Kap108_F1	ACCGTGATGCTGTTACCG	668bp
Kap 111	Kap111_F1	TGGCCAAGTAACCCTTAATG	559bp
Kap 114	Kap114_F1	GAATCTGTTGTTCAGCTACTGG	540bp
Kap 119	Kap119_F1	GTCCATTGCGAACTTACAAC	517bp
Kap 120	Kap120_F2	CAAGCTTTTAACCGGATGGA	800bp
Kap 121	Kap121_F1	CCGCTGTAGTTGATTCAGTC	593bp
Kap 122	Kap122_F1	GGTAGCCAAGTTTCCAATTG	598bp
Kap 123	Kap123_F1	GTCTACTCTAGGTAGGGAAGAG	565bp
	FRB_R1 (reverse primer)	TTGGAGGAGGTCCTTGAC	

2.7 TCF/LEF Luciferase Assay

The engineered 3T3 mouse fibroblast cell line that has a stable integration of the luciferase reporter gene under the Wnt responsive TCF/LEF promoters were used for this assay (Enzo life sciences). Cells were maintained with DMEM medium + Cell Growth Medium Concentrate (Enzo life sciences). Prior to the transfection, cells were seeded on a 24 well plate in media containing DMEM + Cell Assay Medium Concentrate (Enzo life sciences). Subsequently, cells were transfected with siRNA (25 pmol) first, then GFP or human β-catenin-GFP DNA (0.5 µg) for 48 hours and 24 hours, respectively using JetPRIME per the manufacturer's instructions. Luciferase was quantified using the Luciferase Assay System (Promega) and the Promega Glomax luminometer according to the manufacturer's instructions. For the M9M peptide experiment, cells were transfected with an M9M or M9M-A peptide dose ranging from 0.635 µg to 0.5 µg using ProteoJuice Protein transfection following the manufacturer's instructions for 20 hours and Wnt signaling was activated either by Wnt3a ligand (50 ng/ml) or human β-catenin-GFP DNA (0.5 µg) for 16-24 hours.

2.8 *In vivo* TCF/LEF GFP *in situ* hybridization

Heterozygous *Xenopus tropicalis Tg(pbin7Lef-dGFP)* were crossed with wild-type *X. tropicalis*. Fertilized embryos were injected with sgRNAs targeting *tnpo1* and *tnpo2* and Cas9 protein at one-cell stage and collected at stage 10 for *in situ* hybridization as previously described (Khokha et al., 2002). Digoxigenin-labeled anti-sense GFP probe was used to detect GFP transcript expression. Progeny that did not carry the transgene were used as a negative control.

2.9 Western blotting

3T3 mouse fibroblast cells were lysed in RIPA buffer to harvest protein samples. Protein levels are normalized and immunoblots were carried out in Bolt 4%-12% Bis-Tris plus gels following standard protocols. Antibodies used in this study are listed in Key Resources Table.

2.10 *In vitro* binding experiment

pGEX-6P1, pGEX-human β-catenin or pGEX-human transportin 1 were transformed into the BL21 *E. coli* strain and cultured in LB with antibiotics to mid-log phase (OD_{600} 0.6-0.8). To induce expression of the recombinant proteins (GST alone, GST-hβ-catenin and GST-hTNPO1), IPTG was added at a final concentration of 1 mM for 3 hours . All cultures were harvested in 50 mL batches and stored at -20°C until further use. Glutathione Sepharose (GT) beads (Millipore Sigma) were washed and equilibrated in lysis buffer (50 mM Tris pH 7.4, 150 mM NaCl, 2 mM $MgCl_2$, 10% glycerol, 0.05% NP-40, 1 mM DTT and protease inhibitor cocktail mix (Millipore Sigma)). Bacterial pellets were resuspended with the ice cold lysis buffer, sonicated and spun down at 4°C at 30,000 x g for 20 minutes. The supernatant was collected into a new 50 ml conical tube and incubated with 200 µl of GT bead slurry for 1 hour at 4°C. Subsequently, the GST-GT bead slurry was collected and washed with lysis buffer (excluding the protease cocktail mix). The GST tag was removed from hTNPO1 using proTEV Plus Protease (Promega), and the protease enzyme was further removed from hTNPO1 protein by Ni-NTA Magnetic Beads (NEB) per the manufacturer's instructions. To pulldown His6-RanQ69L, bacterial pellets were resuspended with ice cold lysis buffer 2 (50mM Tris pH 7.4, 500 mM NaCl, 2mM MgCl2, 20mM Imidazole, 10% glycerol, 0.05% NP-40, and protease inhibitor cocktail mix), sonicated, and spun down at 4°C at 30,000 x g for 20 minutes. The supernatant was collected into a new 50

ml conical tube and incubated with 200 µl of equilibrated Ni NTA bead slurry for 1 hour at 4°C. The His-Ni bead slurry was collected and washed with lysis buffer 2. His6-RanQ69L was eluted from Ni beads by adding the elution buffer (50mM pH Tris 7.4, 500mM NaCl, 2mM MgCl2, 500mM Imidazole, 10% glycerol, 0.05% NP-40, and protease inhibitor cocktail mix) and rotating at 4°C for 1 hour. The supernatant containing His-RanQ69L was collected by centrifugation at 500 x g for 3 minutes and dialyzed in the buffer (50mM pH Tris 7.4, 150mM NaCl, 2mM MgCl2, 10% Glycerol, and 1mM PMSF) at 4°C overnight. Subsequently, RanQ69L was incubated in GTP buffer (400uM GTP in 5mM EDTA) 4°C for 1 hour. hNTPO1 protein was incubated with GT beads preloaded with GST fusion protein (GST alone or GST-hβ-catenin) for 1 hour at 4°C. The beads were washed with the lysis buffer and eluted with SDS-PAGE sample buffer. Protein samples were separated by SDS-PAGE and detected with Coomassie (BioRad).

2.11 Quantification and Statistical Analysis

Statistical significance was defined as $p<0.05$ (*), 0.002 (**), 0.0002 (***), and 0.0001 (****). The double axis assay and *in situ* data were analyzed by Fisher's exact tests. Otherwise, unpaired two-tailed Student's t tests or a one-way ANOVA test was used to determine significance of mean ratio of nuclear to cytosolic fluorescence intensity in GraphPad Prism 8.4.3.

Chapter 3: Results

3.1 **β-catenin requires a functional Ran GTPase to localize in the nucleus of *S. cerevisiae***

Investigating the β-catenin nuclear import mechanism in yeast relies on the premise that a minimal, conserved β-catenin transport machinery exists in this organism. Therefore, we first tested whether β-catenin accumulates in the yeast nucleus. Specifically, we assessed the localization of a *Xenopus* β-catenin-GFP (xβ-catenin-GFP) in a wildtype yeast strain expressing an endogenously tagged nuclear envelope membrane protein, Heh2-mCherry, to help visualize the nuclear boundary. Indeed, xβ-catenin-GFP was enriched in the nucleus compared to GFP alone (**Figure 1A**). To quantify this steady state distribution, we measured the nuclear enrichment of xβ-catenin-GFP by relating the mean GFP fluorescence in the nucleus (N) and cytoplasm (C) (**Figure 1A**, plot at right). The xβ-catenin-GFP had a mean N:C ratio of ~1.6, which was significantly higher than GFP alone (1.1). As xβ-catenin-GFP is 119 kD, it would be unable to easily pass through the NPC diffusion barrier suggesting that xβ-catenin-GFP can access a facilitated nuclear transport mechanism through the NPC (Popken, Ghavami, Onck, Poolman, & Veenhoff, 2015; Timney et al., 2016; Weis, 2003).

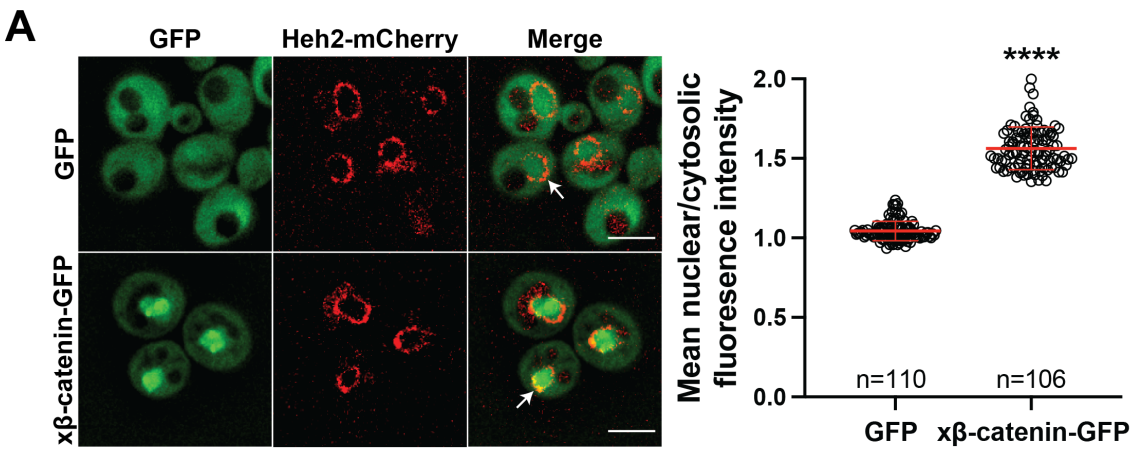

Figure 1A. β-catenin localizes in the nucleus of *S. cerevisiae.* Representative deconvolved fluorescence image of xβ-catenin-GFP in a wild-type yeast strain that expresses Heh2-mCherry to label the nucleus (left). White arrows indicate the nuclear compartment. Plot showing the quantification of mean nuclear to cytosolic fluorescence intensity from three independent replicates (right). Scale bar is 5µm. Red bar indicates the mean value with the standard deviation (SD). *p*-values are from unpaired two-tailed t-test where ns is $p>0.05$, and ****$p<0.0001$.

In principle, three mechanisms of xβ-catenin nuclear import are possible: 1) xβ-catenin-GFP is imported by an NTR, 2) xβ-catenin-GFP piggybacks on an unknown binding partner that is itself imported by an NTR or 3) xβ-catenin-GFP has an intrinsic ability to cross the NPC free of NTRs. To rule out the latter possibility, we tested whether xβ-catenin-GFP nuclear accumulation was dependent on a functional Ran gradient, which would specifically impact NTR-mediated transport (Schmidt & Gorlich, 2016; Weis, 2003; Wente & Rout, 2010). We therefore assessed β-catenin-GFP localization in the *mtr1-1* mutant strain, which is a temperature sensitive, loss of function allele in the gene encoding the yeast Ran-GEF (*SRM1*/*MTR1/PRP20*) (Kadowaki, Zhao, & Tartakoff, 1992). As Ran-GEF exchanges GDP for GTP on Ran in the nucleus, it is essential for the functioning of the nuclear transport system (Weis, 2003). At room temperature, xβ-catenin-GFP is localized in the nucleus with a N:C ratio similar to the wild type strain (~1.6) (**Figure 1B**). In striking contrast, growth at 37ºC, which is non-permissive for mtr1-1p function, resulted in the re-distribution of xβ-catenin-GFP such that it was evenly distributed between the nucleus and cytoplasm with N:C ratios identical to GFP alone (1.1) (**Figure 1B**). Importantly, xβ-catenin-GFP localization was not affected by the elevated temperature as wild-type cells showed N:C ratios of ~1.6 even at 37ºC. Thus, nuclear accumulation of xβ-catenin-GFP is dependent on a functioning Ran GTPase system raising the possibility that it requires a NTR-mediated pathway to accumulate in the nucleus.

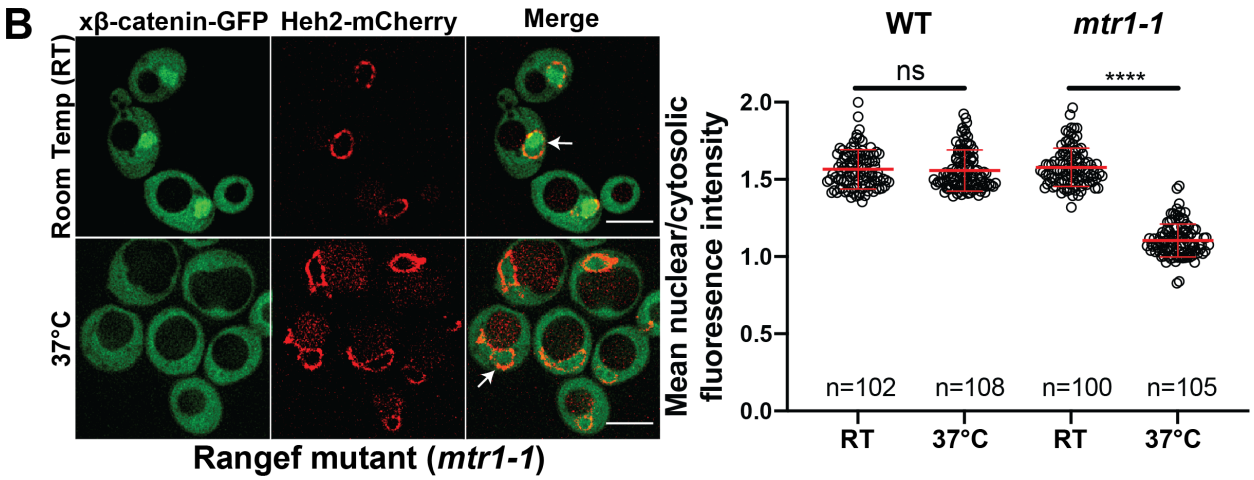

Figure 1B. β-catenin requires a functional Ran GTPase to localize in the nucleus of *S. cerevisiae.* Representative deconvolved fluorescence image of xβ-catenin-GFP in the RanGEF mutant (*mtr1-1*) strain at room temperature or 37°C that co-expresses Heh2-mCherry as a nuclear envelope marker (left). The ratio of mean nuclear to cytosolic fluorescence intensity was measured in the wild-type or *mtr1-1* strain from three independent replicates (right). Scale bar is 5µm. Red bar indicates the mean value with the standard deviation (SD). *p*-values are from unpaired two-tailed t-test where ns is $p>0.05$, and ****$p<0.0001$.

3.2 **The C-terminus of β-catenin contains a NLS**

Having established that β-catenin import requires a functional Ran pathway, we next sought to map the sequence elements of β-catenin that confer nuclear localization. β-catenin can be divided into three domains: a central region rich in armadillo (ARM) repeats sandwiched between two unstructured domains (**Figure 2A**). We generated constructs where each of these domains was individually deleted and examined their localization in yeast. Removal of the C-terminus significantly reduced nuclear enrichment of xβ-catenin-(1-664)-GFP (mean N:C values of 1.4) compared to constructs lacking either the N [xβ-catenin-(141-782)-GFP] or ARM (Δ141-664) domains, which accumulated in the nucleus at levels similar to the full length protein (mean N:C of 1.6) (**Figures 2A-C**). These data suggested that the C-terminus contains sequence elements required for nuclear accumulation. Consistent with this idea, the C-terminus of β-catenin [xβ-catenin-(665-782)-GFP] was sufficient to confer nuclear accumulation of GFP to levels comparable to the full length protein (mean N:C 1.6) (**Figures 2A, 2B, and 2D**). Of note, both the ARM repeats [xβ-catenin-(141-664)-GFP]) and the N-terminus of β-catenin [xβ-catenin-(1-141)-GFP] could confer some nuclear localization of GFP but to a considerably lesser extent than the C-terminus (mean N:C of ~1.3) (**Figures 2A, 2B, and 2D**). Additionally, the ARM repeats had some affinity for the nuclear periphery (Figures 2D, xβ-catenin-(141-664)-GFP, white arrows). Of future interest, even the weaker nuclear accumulation driven by the N-terminal and ARM repeat sequences is dependent on a functional Ran pathway as xβ-catenin-1-664 does not accumulate in the nucleus in the *mtr1-1* strain at the non-permissive temperature (**Figure 2F)**. Thus, when taken together, there are several elements of xβ-catenin that, in isolation, can target to the nucleus in a Ran pathway dependent fashion but the C-terminus contains a sequence that was both necessary and sufficient for nuclear accumulation at levels

comparable to the full length protein. Consistent with previous work (Koike et al., 2004; Mis et al., 2020), these data suggested that the C-terminus of xβ-catenin contains the dominant NLS in β-catenin, which we further mapped to amino acids 665-745 (**Figures 2A, 2B, and 2E**).

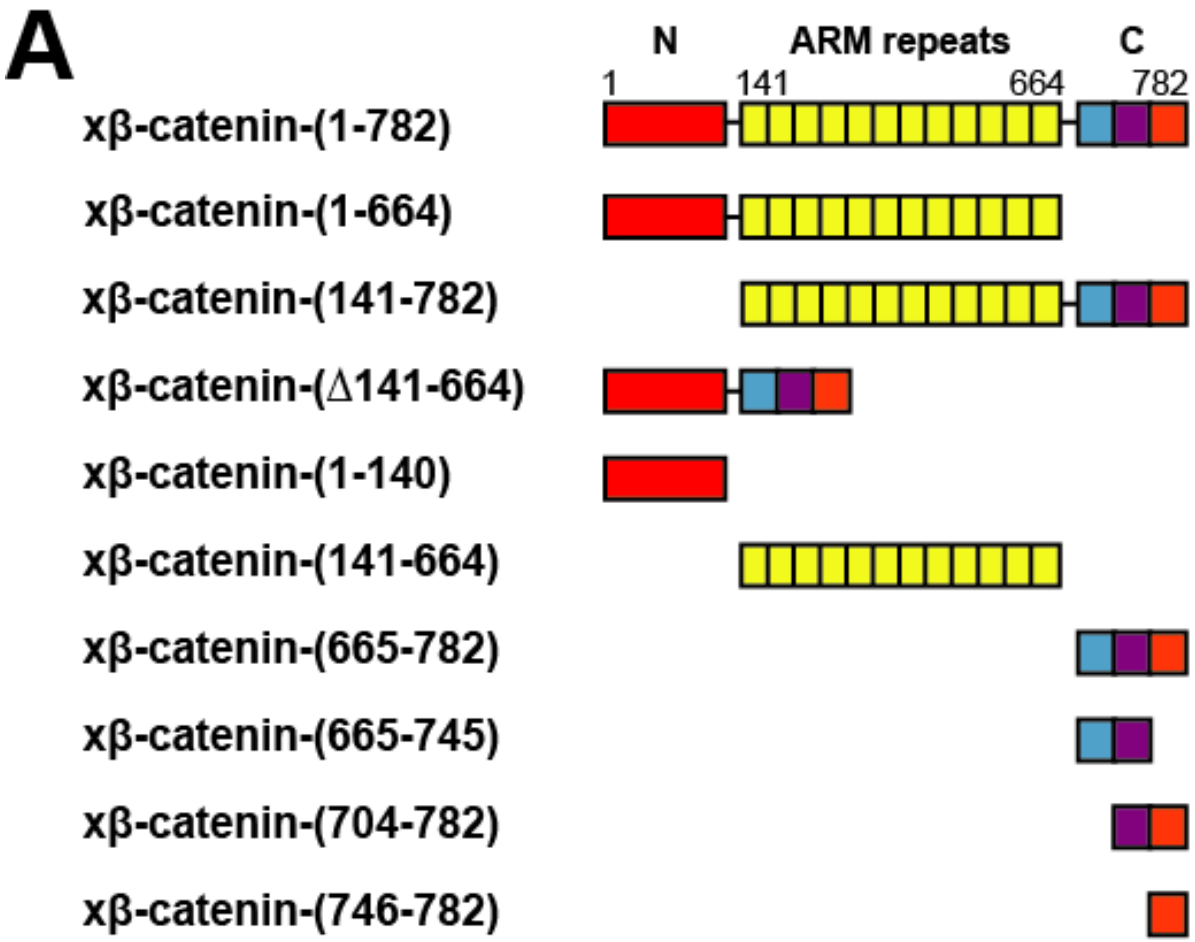

Figure 2A. Schematic diagram of *Xenopus* β-catenin truncation constructs tested in this study.

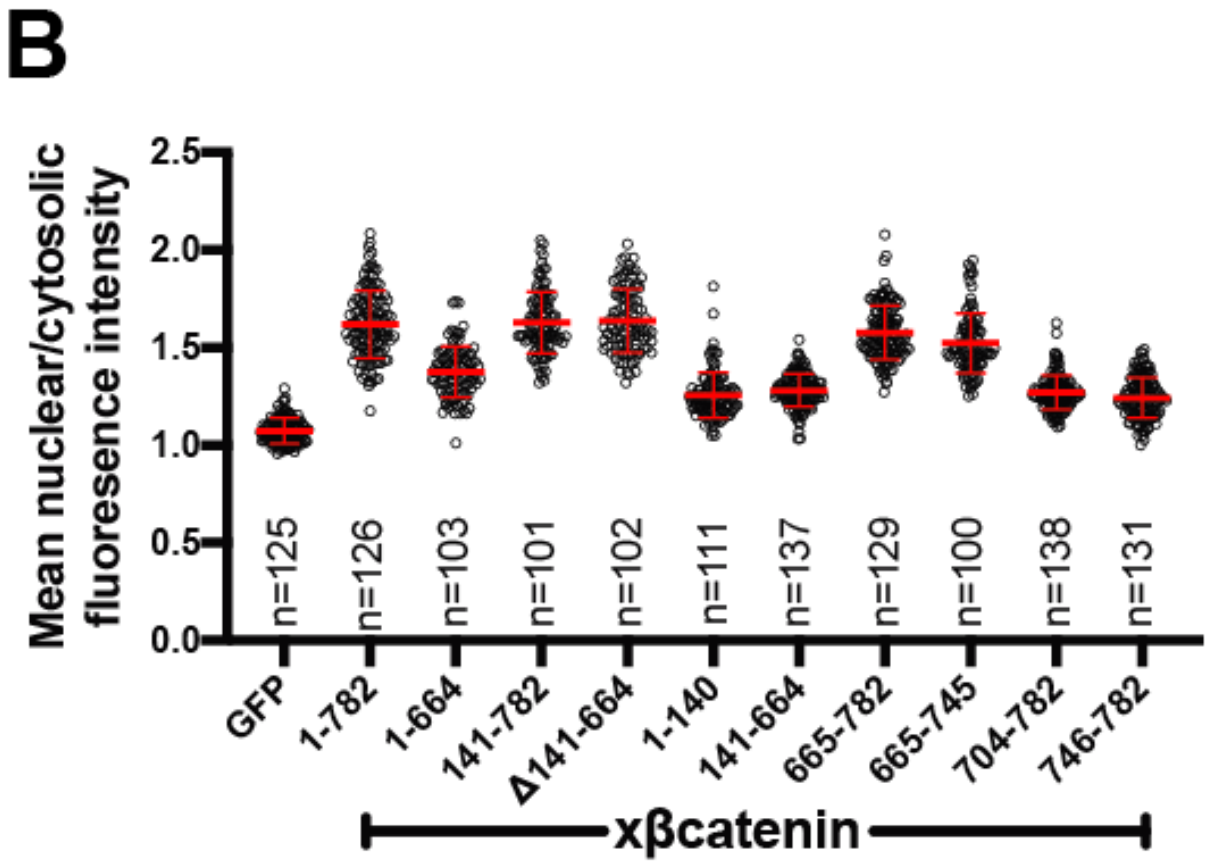

Figure 2B. The C-terminus of β-catenin contains a NLS. Plot of the ratio of mean nuclear to cytosolic fluorescence intensity of *Xenopus* β-catenin GFP truncation constructs tested in a wild-type yeast strain from three independent replicates. Red bar indicates the mean value with the SD.

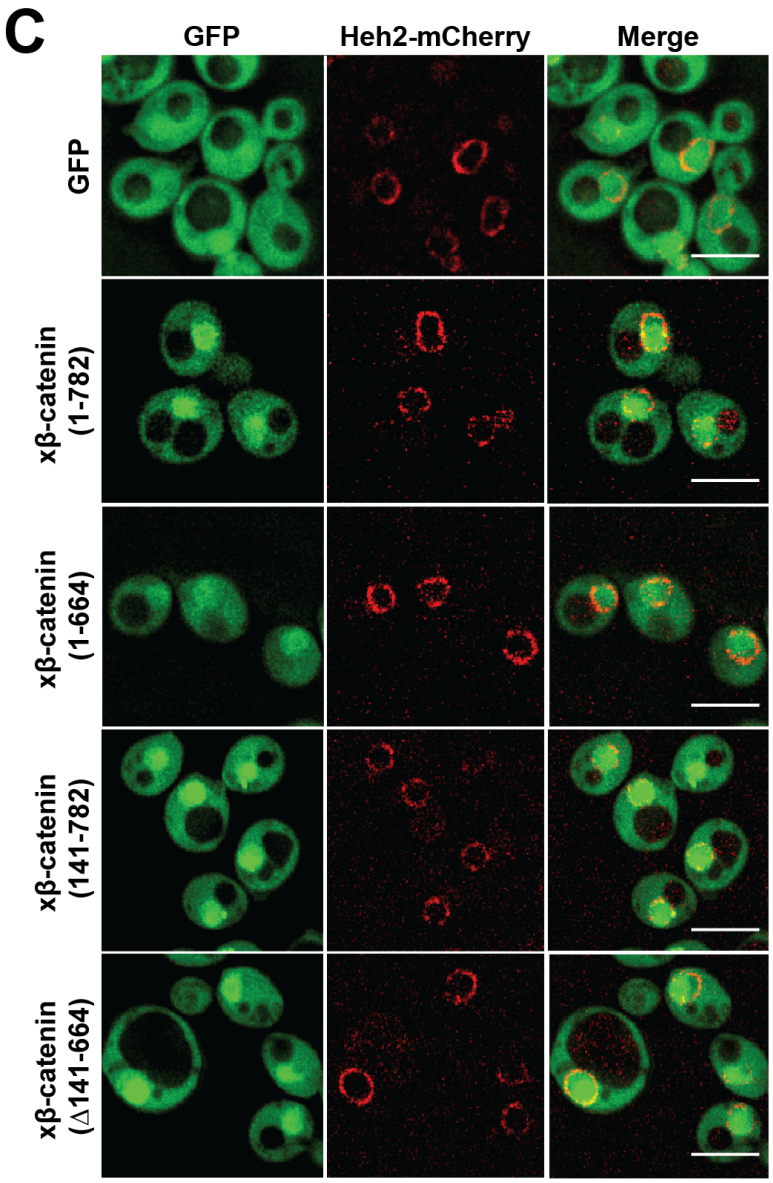

Figure 2C. Deconvolved fluorescence image of *Xenopus* β-catenin truncation constructs in *S. cerevisiae* Part 1. Representative images of the N-terminal deletion (141-782), ARM-repeats deletion (Δ141-664) or C-terminal deletion (1-664) of *Xenopus* β-catenin GFP in the wild-type strain. GFP and full-length *Xenopus* β-catenin-GFP were used as controls. Heh2-mCherry was co-expressed to label the nuclear membrane Scale bar is 5µm.

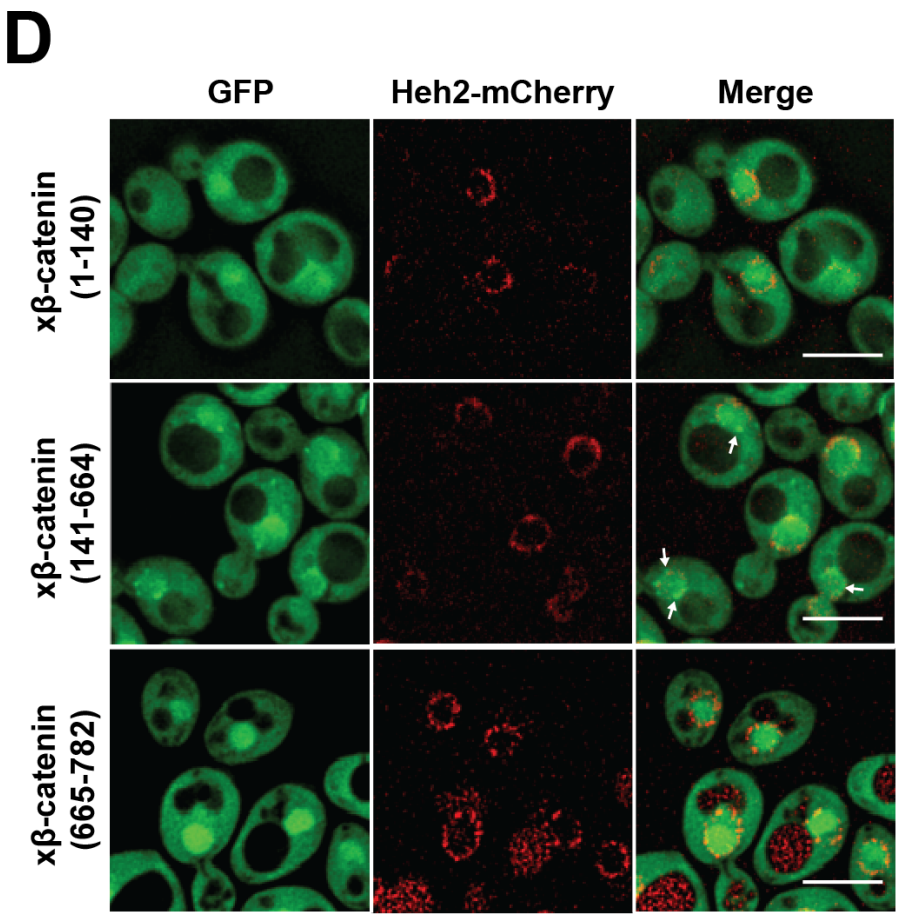

Figure 2D. Deconvolved fluorescence image of *Xenopus* β-catenin truncation constructs in *S. cerevisiae* Part 2. Representative images of the indicated fragments of *Xenopus* β-catenin GFP in the wild-type strain. White arrows indicate nuclear rim localization. Heh2-mCherry was co-expressed to label the nuclear membrane. Scale bar is 5μm.

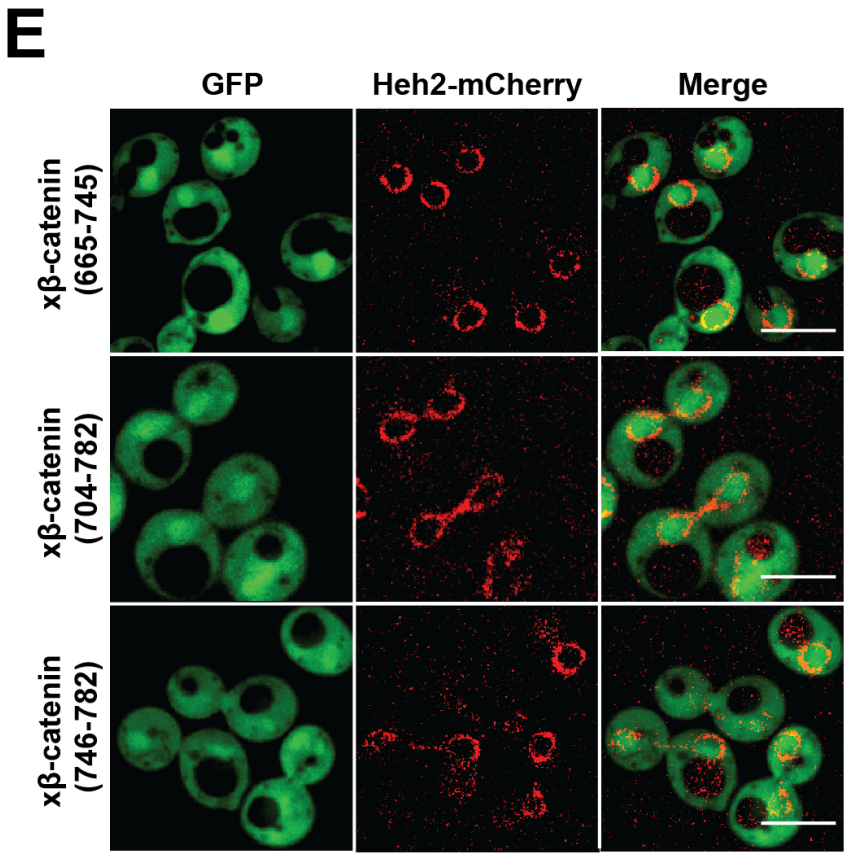

Figure 2E. Deconvolved fluorescence image of *Xenopus* β-catenin truncation constructs in *S. cerevisiae* Part 3. Representative images of indicated C-terminus fragments of *Xenopus* β-catenin GFP in the wild-type strain. Heh2-mCherry was co-expressed to label the nuclear membrane. Scale bar is 5μm.

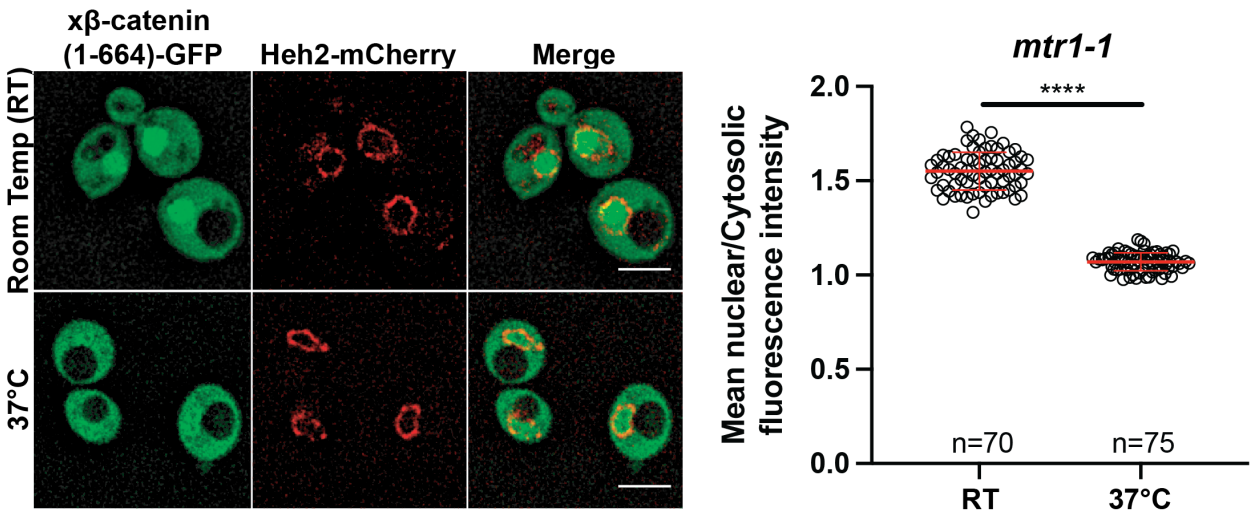

Figure 2F. β-catenin (1-664) localizes to the nucleus in a RanGTPase dependent manner in *S. cerevisiae.* Representative deconvolved fluorescence image of xβ-catenin (1-664)-GFP in the RanGEF mutant (*mtr1-1*) strain at room temperature or 37°C that co-expresses Heh2-mCherry as a nuclear envelope marker (left). The ratio of mean nuclear to cytosolic fluorescence intensity was measured in the *mtr1-1* strain from three independent replicates (right). Red bar indicates the mean value with the standard deviation (SD). *p*-values are from unpaired two-tailed t-test where ns is $p>0.05$ and **** is $p<0.0001$. Scale bar is 5μm. The data is uploaded as source data 1.

We confirmed that nuclear accumulation of xβ-catenin-(665-745)-GFP was dependent on the Ran pathway using the *mtr1-1* strain (**Figure 2G**). To ensure that this sequence did not confer binding to a yeast-specific factor, we also tested localization of xβ-catenin-(665-745)-GFP in HEK293T cells, a human embryonic kidney cell line. In line with the yeast results, xβ-catenin-(665-745)-GFP showed higher levels of nuclear accumulation compared to GFP alone (**Figure 2H**). Furthermore, to test if this NLS is required for β-catenin localization in human cells, we also examined human β-catenin that lacks aa 665-745 in HEK293T cells. Indeed, deletion of aa 665-745 [hβ-catenin-(Δ665-745)-GFP] led to a significant reduction in nuclear to cytoplasmic ratio compared to the full-length hβ-catenin localization (**Figure 2I**).

Next, we investigated the function of the β-catenin NLS in the context of Wnt signaling using the secondary axis assay in *Xenopus*(McMahon & Moon, 1989; Smith & Harland, 1991; Sokol et al., 1991). Overexpression of Wnt effectors including β-catenin induces a secondary axis in *Xenopus* embryos. By injecting a moderate dose (200 pg) of xβ-catenin mRNA, secondary axes develop in roughly half of the embryos (**Figure 2J-K**) compared to none in the uninjected controls (UIC). If we delete the coding sequence for the NLS [xβ-catenin-(Δ665-745)-GFP], then the number of embryos with secondary axes is significantly reduced (**Figure 2J-K**). To ensure that this loss of function is due to the inhibition of β-catenin nuclear import, we added the classical NLS of the SV40 Large T-antigen (cNLS), which is imported by Kap-α/β1, to the N-terminus of β-catenin [cNLS-xβ-catenin-(Δ665-745)-GFP]. cNLS-xβ-catenin-(Δ665-745)-GFP could induce secondary axes similarly to the full length β-catenin (**Figure 2K**), consistent with the conclusion that xβ-catenin-(Δ665-745)-GFP was still functional for Wnt signaling but lacked the nuclear localization element. Supporting this supposition, we imaged xβ-catenin-GFP in these *Xenopus* embryos and found that while xβ-catenin-GFP localizes to the cell membrane

and nucleus, xβ-catenin-(Δ665-745)-GFP shows a reduction in nuclear accumulation, which is rescued by the addition of the cNLS (**Figure 2L**).

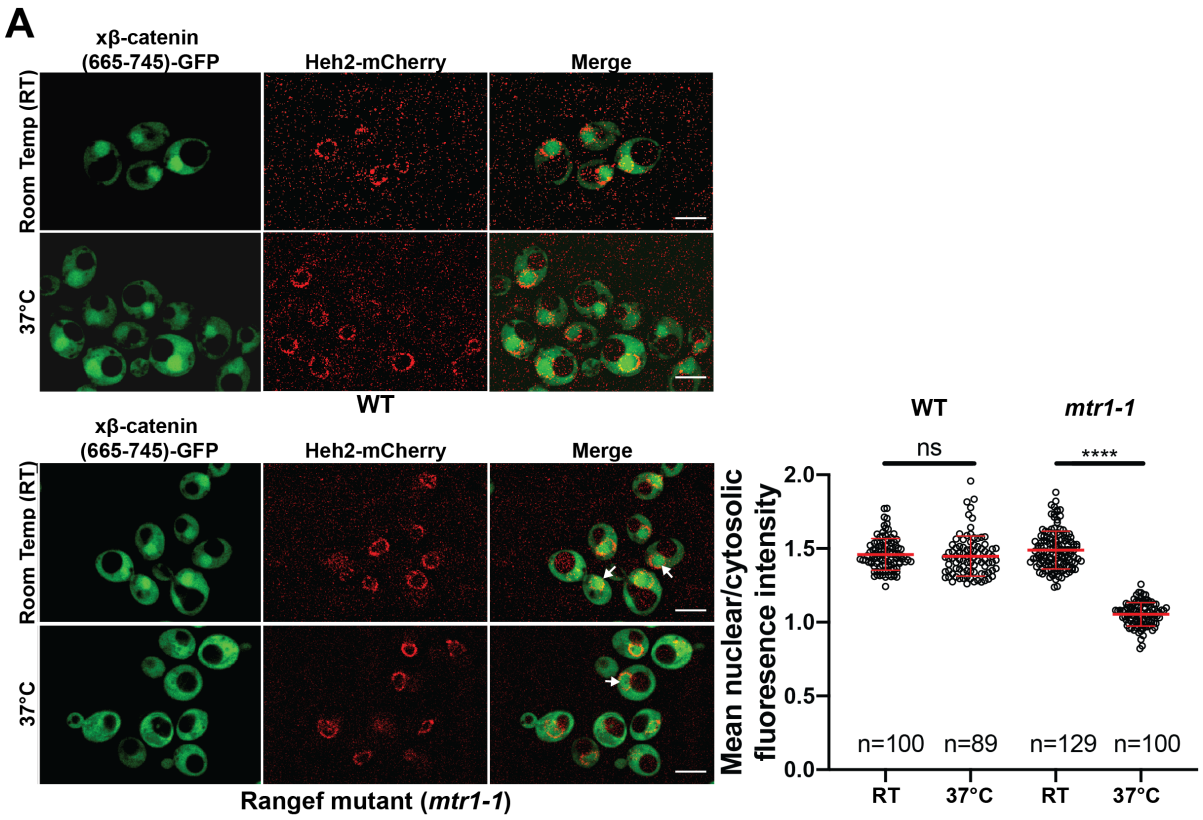

Figure 2G. Sub-cellular localization of *Xenopus* β-catenin (665-745)-GFP in the *S. cerevisiae* *mtr1-1* strain. Deconvolved fluorescence image of *Xenopus* β-catenin-(665-745)-GFP in the wild-type (top left) and RanGEF mutant (*mtr1-1*) (bottom left) strain at room temperature (RT) or 37°C that co-expresses Heh2-mCherry as a nuclear envelope marker. White arrows indicate the nuclear compartment. Scale bar is 5µm. The ratio of mean nuclear to cytosolic fluorescence intensity from a single experiment (right). *p*-values are from unpaired two-tailed t-test where ns is p>0.05, and ****p<0.0001.

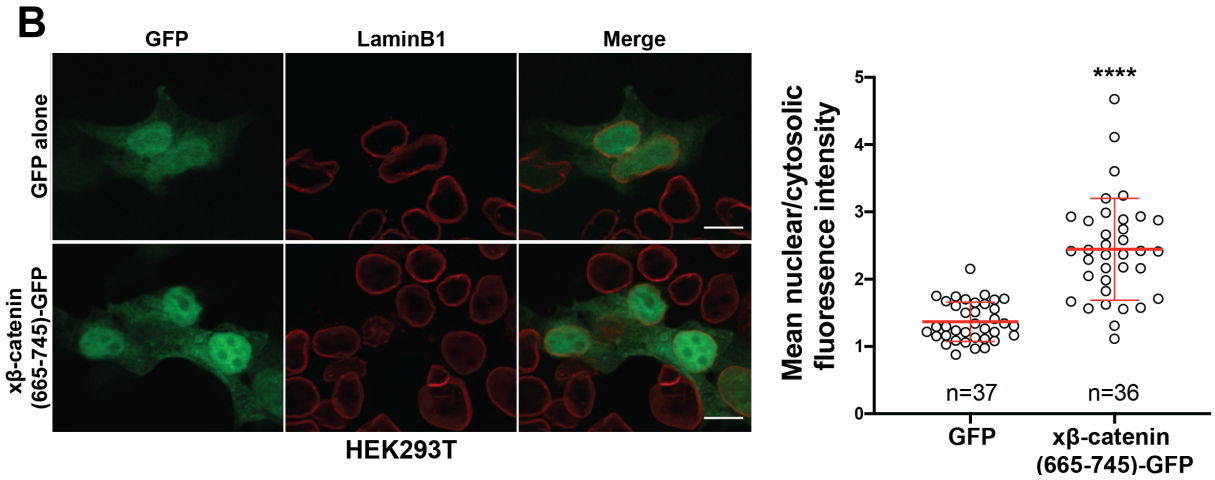

Figure 2H. Sub-cellular localization of *Xenopus* β-catenin (665-745)-GFP in HEK293T cells. Representative image of HEK293T cells expressing *Xenopus* β-catenin (665-745)-GFP. LaminB1 was labeled to locate the nuclear envelope. GFP was used as a control. Scale bar is 10μm. Ratio of nuclear to cytoplasmic intensities from two independent replicates (right). *p*-values are from unpaired two-tailed t-test where ns is $p>0.05$, and ****$p<0.0001$.

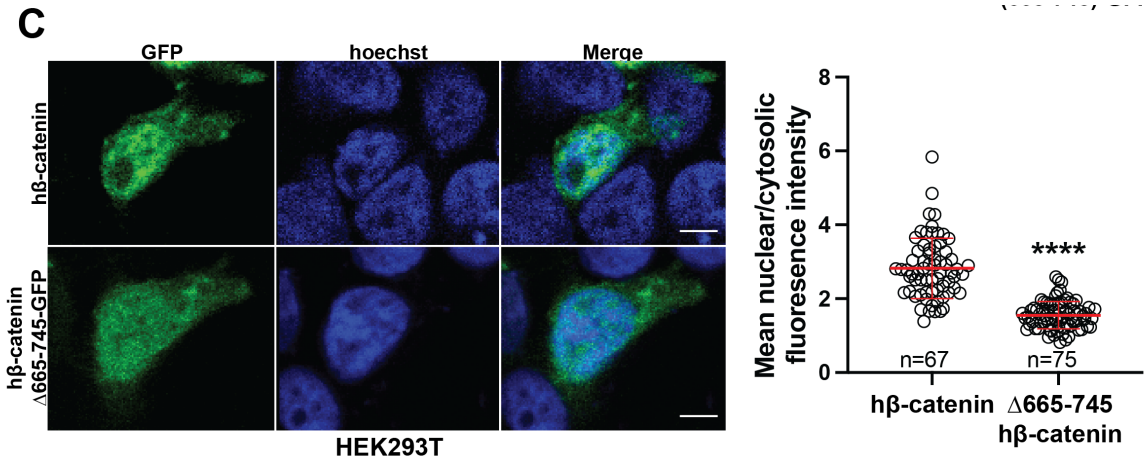

Figure 2I. Sub-cellular localization of human β-catenin (Δ665-745)-GFP in HEK293T cells. Representative image of HEK293T expressing full length human β-catenin GFP and human β-catenin (Δ665-745)-GFP. Ratio of nuclear to cytoplasmic intensities from three independent replicates (right). Hoechst was labeled to locate the nuclear compartment. Scale bar is 6µm. *P*-values are from unpaired two-tailed t-test where ns is $p>0.05$, and ****$p<0.0001$.

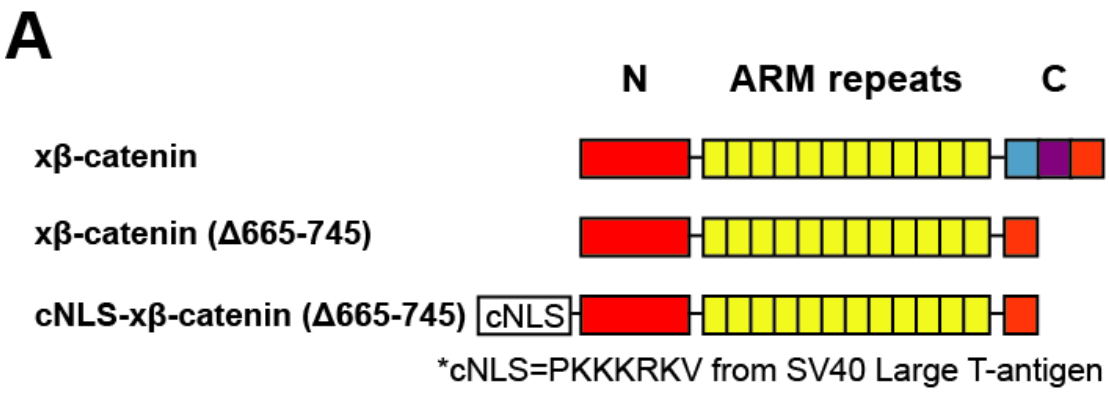

Figure 2J. Schematic diagram of *Xenopus* β-catenin constructs

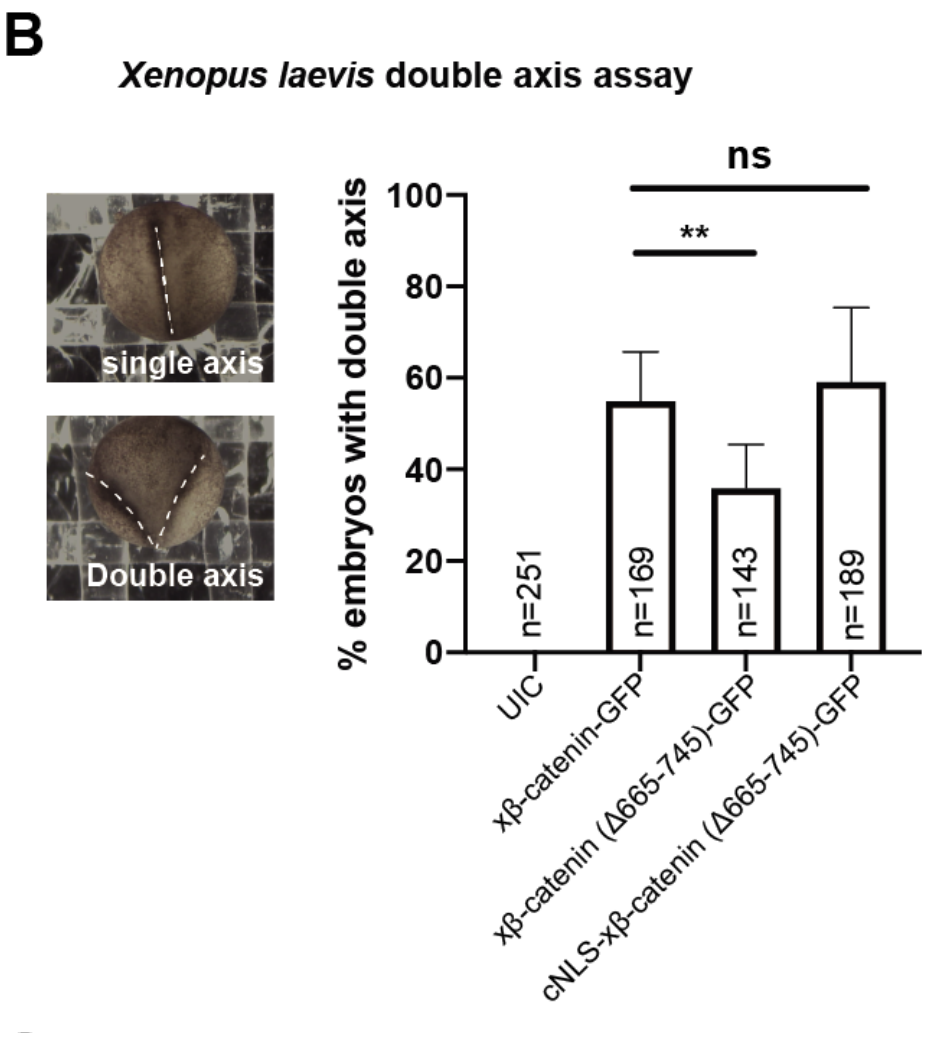

Figure 2K. Residues 665-745 of β-catenin are required to induce secondary axes in *Xenopus laevis.* Double axes were scored in st 19 embryos viewed dorsally with anterior to the top (left). Data from three independent replicates depicted in histogram (right). *p*-values are from Fisher's exact test where ns is $p>0.05$, $p<0.05$ (*), and 0.0021 (**).

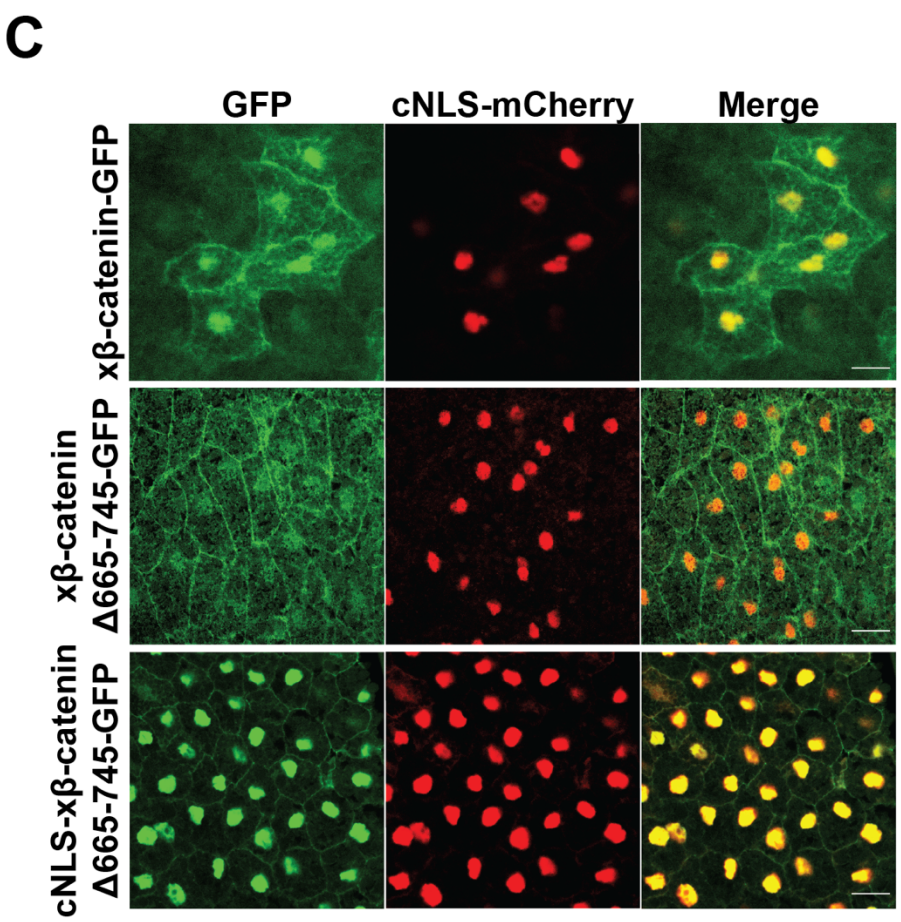

Figure 2L. Subcellular localization of GFP tagged *Xenopus* β-catenin constructs. Representative images of *x*β-catenin-GFP, *x*β-catenin (Δ665-745)-GFP or cNLS-*x*β-catenin (Δ665-745)-GFP in the dorsal blastopore lip of stage 10 *Xenopus laevis* embryos. cNLS-mCherry mRNA was co-injected to mark the nucleus. Scale bar is 30µm.

3.3 **Kap 104 is specifically required for β-catenin nuclear localization in *S. cerevisiae***

Next, to define the NTR responsible for xβ-catenin-GFP nuclear import, we used the Anchor-Away approach (Haruki et al., 2008) to systematically inhibit 10 budding yeast NTRs, all of which have orthologues in human cells (**Table 1**). This strategy takes advantage of the rapamycin-induced dimerization of a FK506 binding protein (FKBP12) with the FKBP-rapamycin binding (FRB) domain (**Figure 3A**). In this system, NTR-FRB fusions are expressed in a strain harboring FKBP12 fused to a highly abundant plasma membrane protein (Pma1) (**Figure 3A**). The addition of rapamycin leads to the rapid (~15 min) trapping of the NTRs at the plasma membrane (Haruki et al., 2008). We systematically tested whether the addition of rapamycin (or the DMSO carrier alone) impacted the nuclear accumulation of xβ-catenin-(665-782)-GFP in each of the 10 NTR-FRB strains. Consistent with prior data (Fagotto et al., 1998), plasma membrane trapping of the Kapβ1 orthologue, Kap95-FRB, did not impact nuclear localization of xβ-catenin-(665-782)-GFP (**Figure 3B**). Indeed, trapping 9 of the 10 NTRs, including the Imp-11 orthologue, Kap120, had no overt influence on xβ-catenin-(665-782)-GFP nuclear localization (**Figure 3B, 3C, and Figure 3– figure supplement 1**). In contrast, we observed a remarkable inhibition of nuclear accumulation specifically when Kap104-FRB [orthologue of Kapβ2/Transportin-1(TNPO1)] was anchored away (Figure 3B and 3C). These data support a model in which Kap104 specifically mediates the nuclear import of xβ-catenin-(665-782)-GFP in the yeast system.

Human NTR	Yeast Orthologs
Kap β1	Kap95
Kap α	Kap60/Srp1
Transportin 1	Kap104
Importin-5/Kap β3	Kap121/Pse1
Importin-4/RanBP5	Kap123
Importin-7/RanBP7	Kap119/Nmd5
Importin-8/RanBP8	Kap108/Sxm1
Importin-9	Kap114
Importin-11	Kap120
Transportin-SR/TNPO3	Kap111/Mtr10
Importin-13	Kap122/Pdr6
CRM1/Exportin-1	Xpo1
Exportin-t	Los1
Exportin-5	Kap142/Msn5
CAS	Cse1

Table 1. List of human NTR and Yeast orthologs

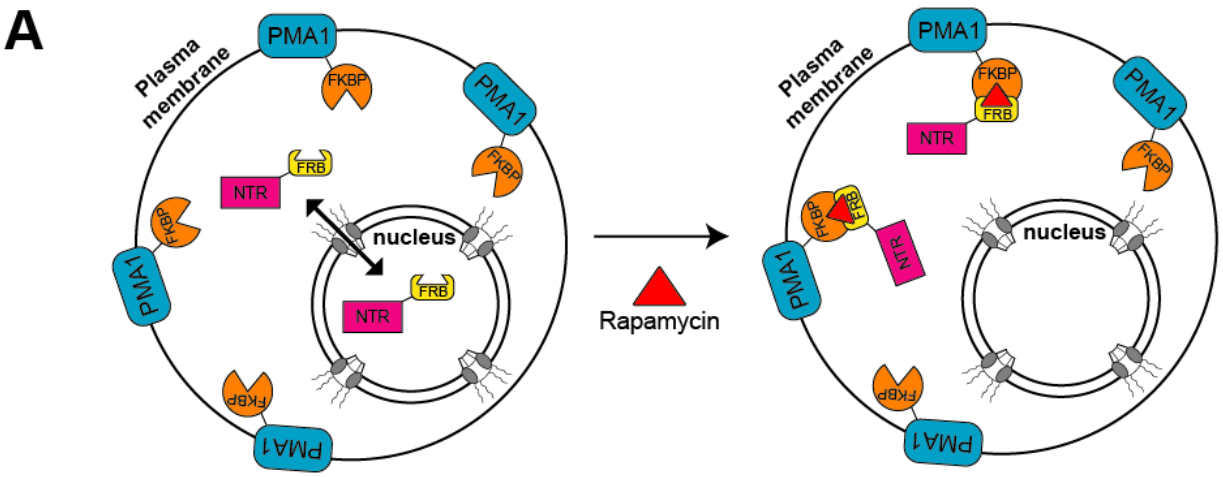

Figure 3A. Schematic of the Anchor Away assay. A target NTR is anchored to the plasma membrane by the rapamycin induced dimerization of NTR-FRB and Pma1-FKBP12. Pma1 is a plasma membrane ATPase.

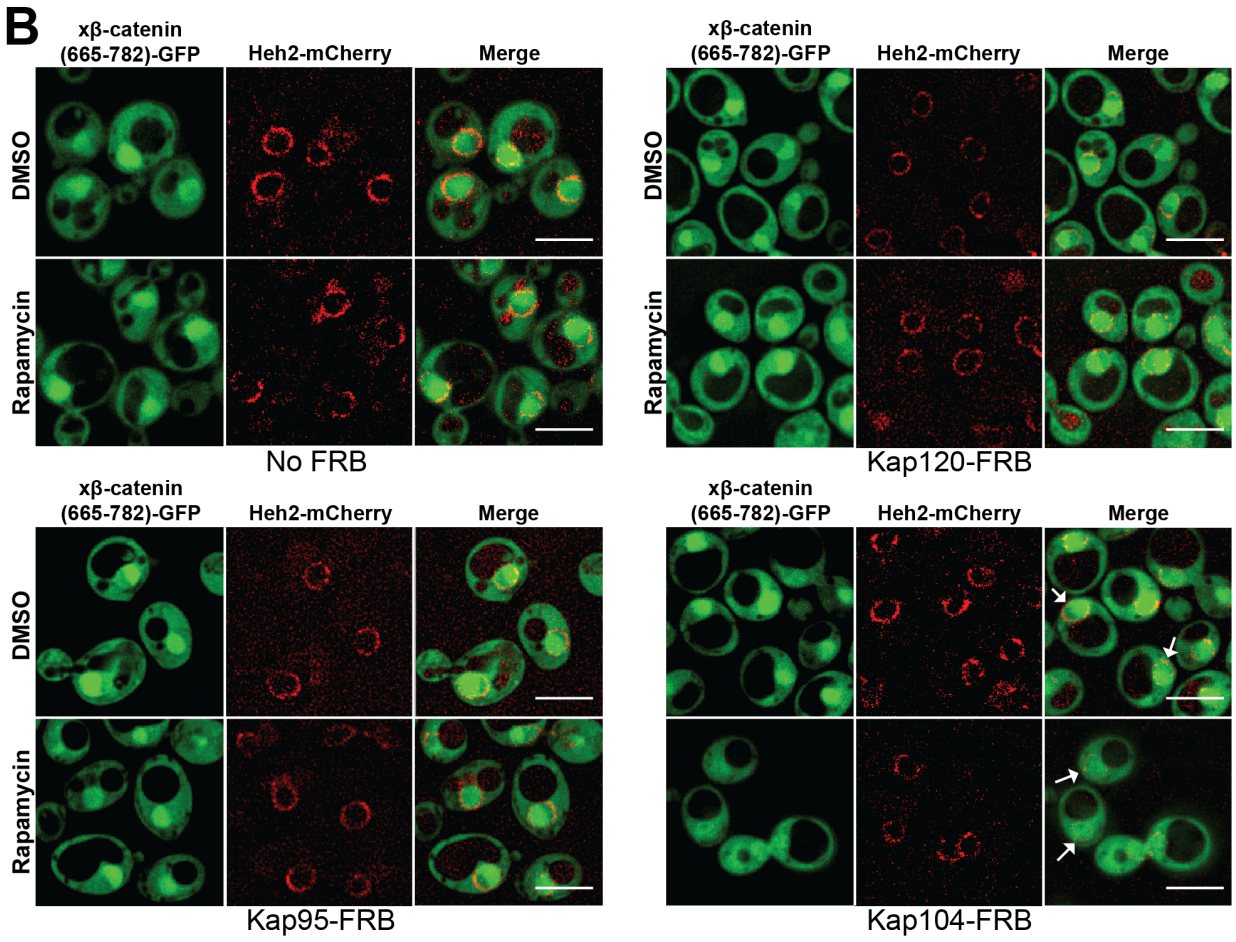

Figure 3B. Kap104 is specifically required for β-catenin nuclear localization in *S. cerevisiae* (Image). Deconvolved fluorescence image of Xenopus β-catenin (665-782)-GFP treated with DMSO (vehicle) or rapamycin for 15 min in the no FRB, Kap95 (Karyopherin β1 in human)-FRB, Kap120 (importin 11 in human) and Kap104 (Kapβ2/Transportin 1 in human)-FRB. Heh2-mCherry was used as a nuclear envelope marker. White arrows indicate the nuclear compartment. Scale bar is 5μm.

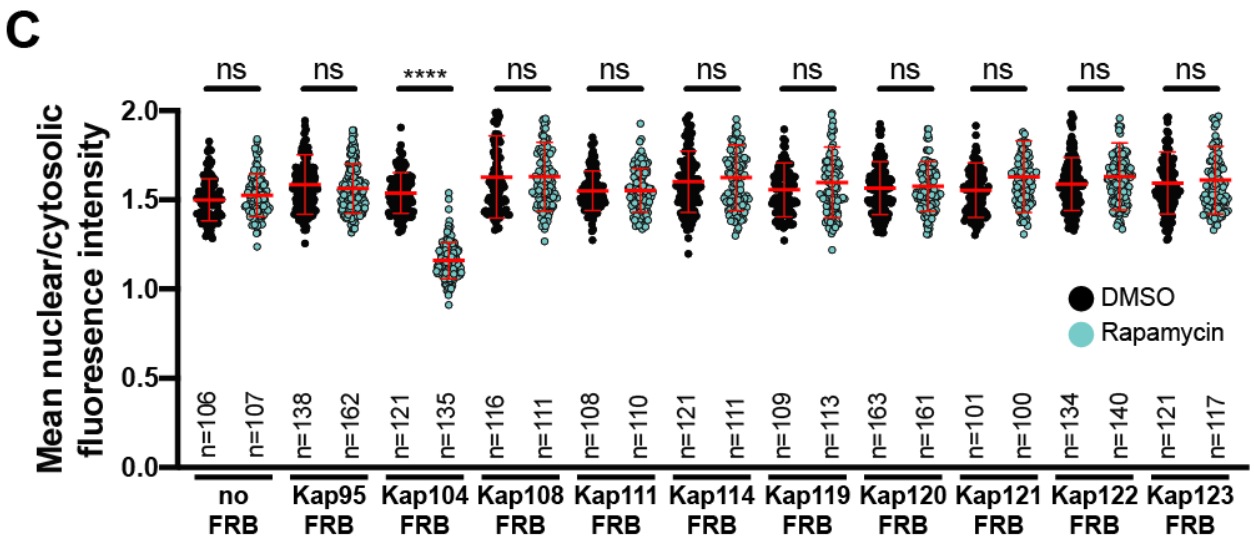

Figure 3C. Kap104 is specifically required for β-catenin nuclear localization in *S. cerevisiae* (Quantification). Plot showing the ratio of mean nuclear to cytosolic fluorescence intensity of Xenopus β-catenin (665-782)-GFP in the 10 NTR-FRB strains treated with DMSO or rapamycin. Red bar indicates the mean value with the SD. Experiments were performed three times. p-values are from unpaired two-tailed t-test where ns is $p>0.05$, and ****$p<0.0001$.

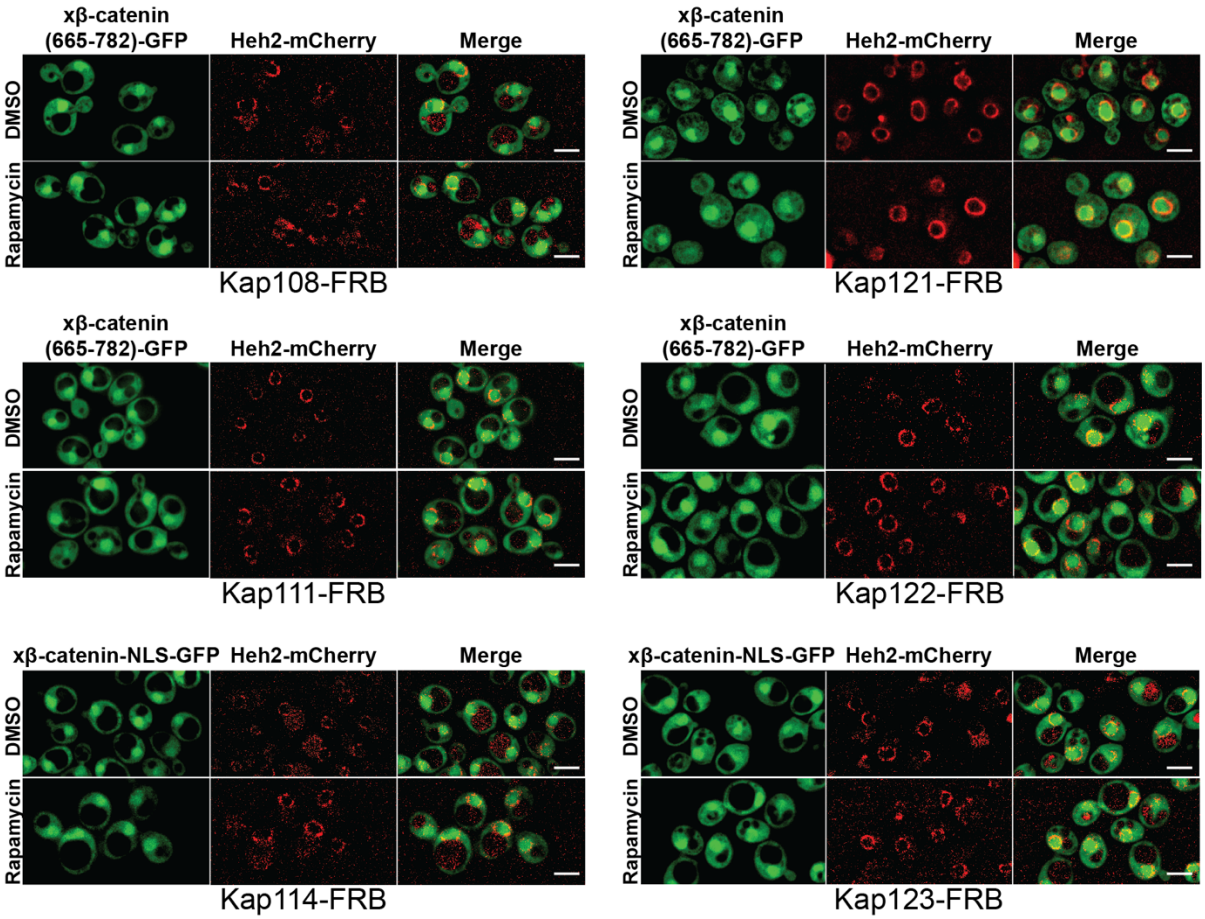

Figure 3– figure supplement 1. Sub-cellular localization of *Xenopus* β-catenin (665-782)-GFP in Anchor Away strains in *S. cerevisiae.* Representative deconvolved fluorescence image of *x*β-catenin (665-782)-GFP treated with DMSO (carrier) or rapamycin in the indicated NTR-FRB strain. Heh2-mCherry was used as a nuclear membrane marker. Scale bar is 5μm.

3.4 **β-catenin contains a PY-like NLS that is required for nuclear import**

Having established that Kap104 mediates β-catenin nuclear transport in yeast, we compared the xβ-catenin-(665-782) protein sequence to an established TNPO1 NLS (eg. PY-NLS) (B. J. Lee et al., 2006; Soniat & Chook, 2015; Soniat et al., 2013). By close inspection, the xβ-catenin amino acid sequence (665-703) does conform to the loose PY-NLS consensus with a hydrophobic methionine (M) in place of a tyrosine (Y; **Figure 4A**) (Soniat & Chook, 2015); this NLS is conserved across vertebrate species (**Figure 4A**). We therefore mutated the PM motif in β-catenin by substituting the proline (P) and methionine (M) residues for tandem alanine (A) amino acids. We tested whether these changes impacted the ability of the xβ-catenin-(665-703) to import a GFP fusion to 3 maltose binding proteins. MBP(x3)-GFP is constitutively excluded from the nucleus due to its large molecular weight (149 kDa) (**Figure 4B**) (Popken et al., 2015). Fusion of the xβ-catenin-(665-703) can confer nuclear localization of this large fusion protein. Further, this localization is dependent on the PM motif as substitution of PM with AA abolishes nuclear localization (**Figure 4B**). These amino acids were also critical for human (h)β-catenin-(665-782)-GFP nuclear accumulation in human cell lines (HeLa) as the PM to AA substitution reduced the mean N:C ratios of this construct from 2.5 to 1.5 (**Figure 4C**). Thus, the PM sequence in the β-catenin PY-NLS is required for nuclear import in yeast and human cells.

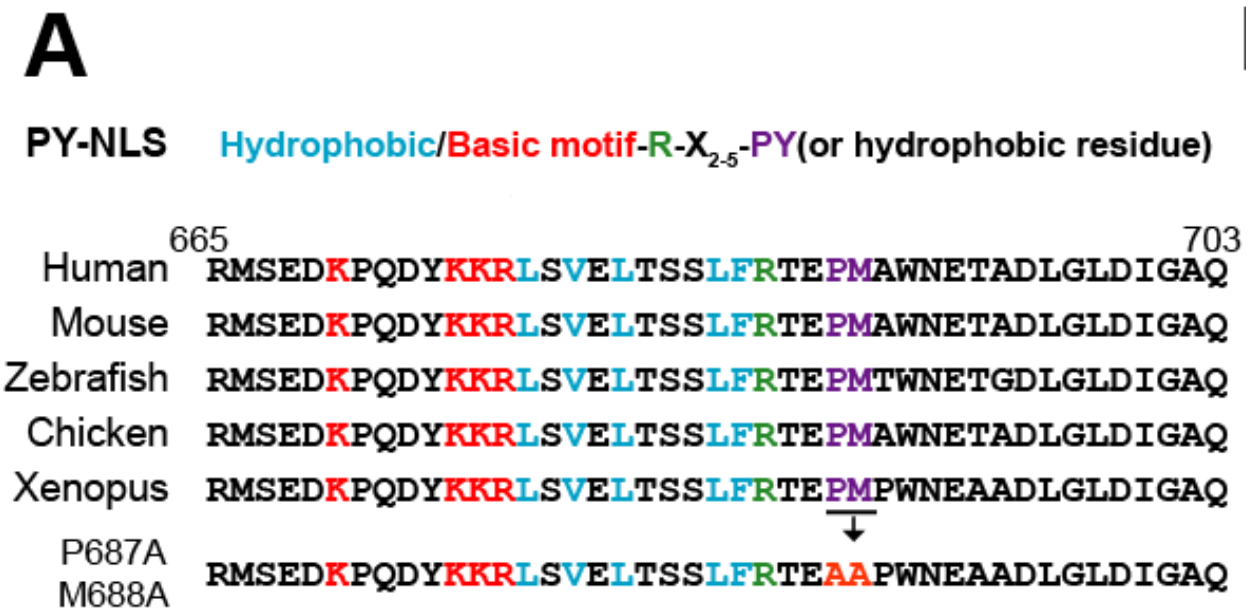

Figure 4A. Conservation of amino acid sequences that conform to the PY-NLS consensus in the C-terminus of β-catenin.

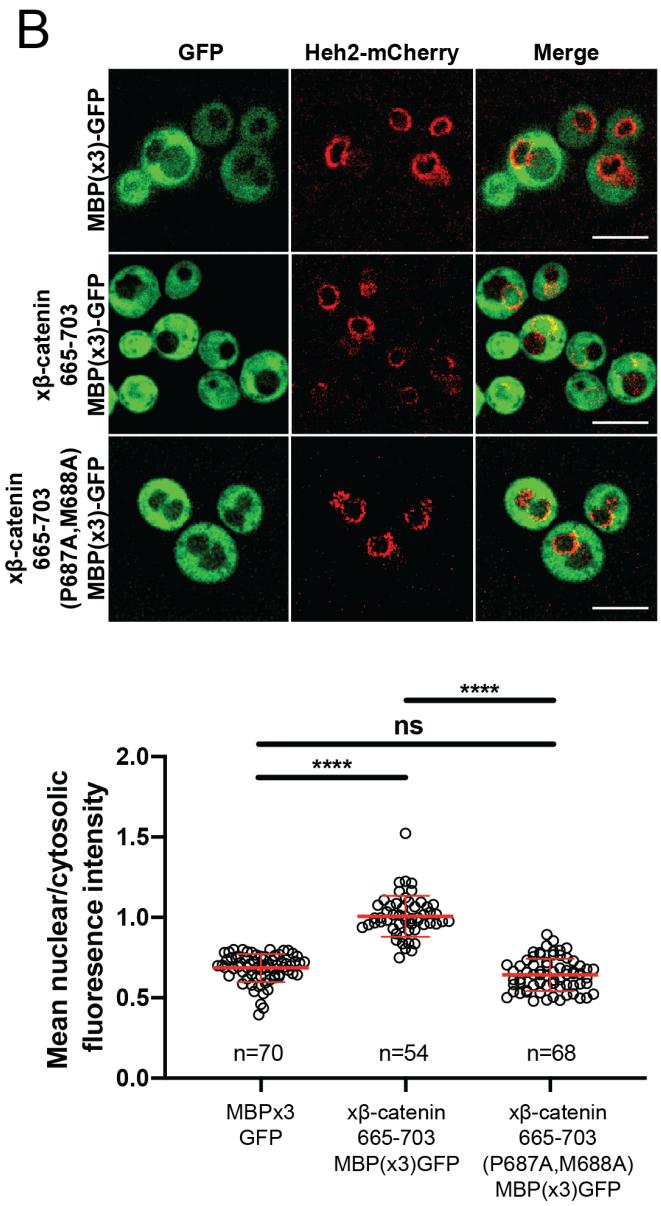

Figure 4B. β-catenin PY-like NLS is sufficient and required to drive a large inert MBP(x3) GFP protein to the nucleus in *S. cerevisiae*. Deconvolved fluorescence images of wildtype yeast cells expressing MBP(x3)-GFP tagged with the Xenopus β-catenin NLS (665-703) and also an NLS that contains the PM to AA mutation (top). Untagged MBP(x3)-GFP was used as a control. Plot of the ratio of mean nuclear to cytoplasmic fluorescence intensity from a single experiment (bottom). Scale bar is 5 μm. p-values are from unpaired two-tailed t-test where ns is $p>0.05$, and ****$p<0.0001$.

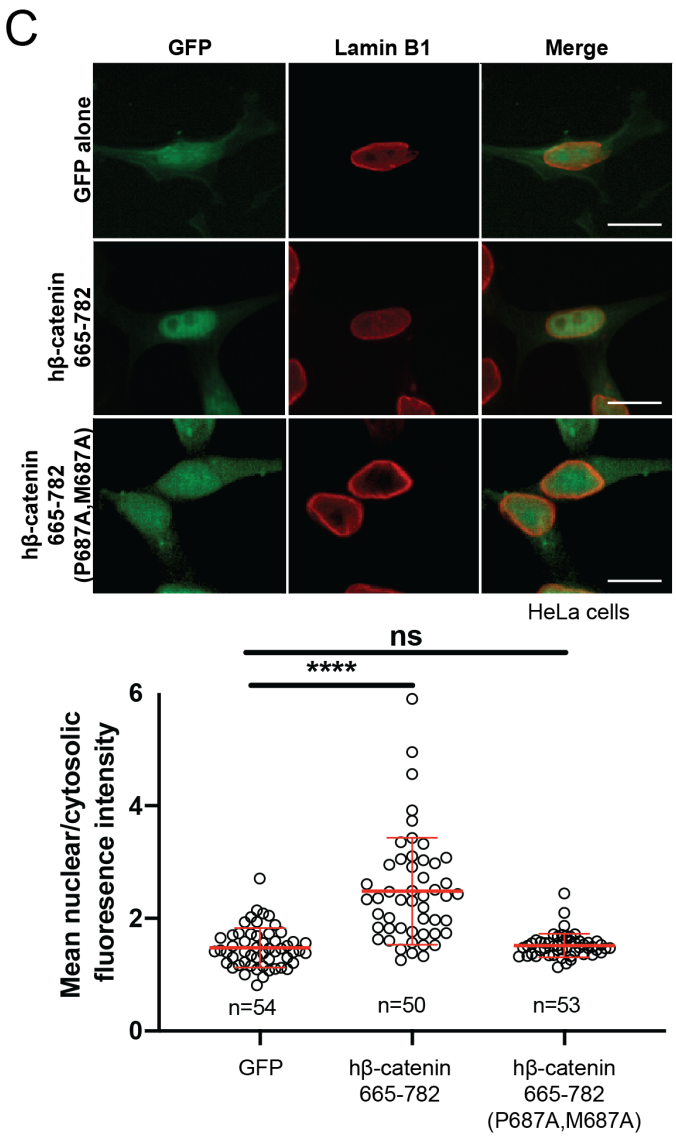

Figure 4C. PM to AA substitution impedes β-catenin nuclear enrichment in HeLa cells. Representative fluorescence image of HeLa cells expressing human β-catenin (665-782) or the PM to AA mutant version (top). LaminB1 was labeled to locate the nuclear envelope. GFP alone was used as a control. Plot of the ratio of mean nuclear to cytoplasmic fluorescence intensity from three experiments (bottom). Scale bar is 15 μm. p-values are from unpaired two-tailed t-test where ns is $p>0.05$, and ****$p<0.0001$.

3.5 **Direct binding of β-catenin and TNPO1 is destabilized by Ran-GTP**

To test that the β-catenin-NLS is directly recognized by TNPO1, we generated recombinant TNPO1 and GST fusions of human β-catenin (GST-hβ-catenin) and human β-catenin containing the PM-AA mutations (GST-hβ-catenin P687A,M688A). We immobilized these GST fusions (and GST alone) on GT Sepharose beads and tested binding to purified TNPO1. We observed specific binding of TNPO1 to the GST-hβ-catenin (**Figure 5A**), which was disrupted by the PM to AA mutations in the NLS. Furthermore, as NTR-NLS interactions are disrupted by the binding of Ran-GTP to the NTR in the nucleus, we tested the Ran-GTP sensitivity of the TNPO1:β-catenin complex. We generated recombinant RanQ69L, which cannot hydrolyze GTP, and confirmed that RanQ69L-GTP specifically interacted with TPNO1 and not to β-catenin (**Figure 5-figure supplement 1B**). Next, we assessed the formation of the TNPO1:β-catenin complex in the presence or absence of RanQ69L-GTP. Adding RanQ69L-GTP specifically disrupted β-catenin binding to TPNO1 indicating that the TNPO1:β-catenin complex reflects the formation of a canonical NTR-NLS import complex (**Figure 5B**). When taken together, these data establish a model in which TNPO1 imports β-catenin through a direct interaction with its PY-NLS that is modulated by TPNO1-binding to Ran-GTP.

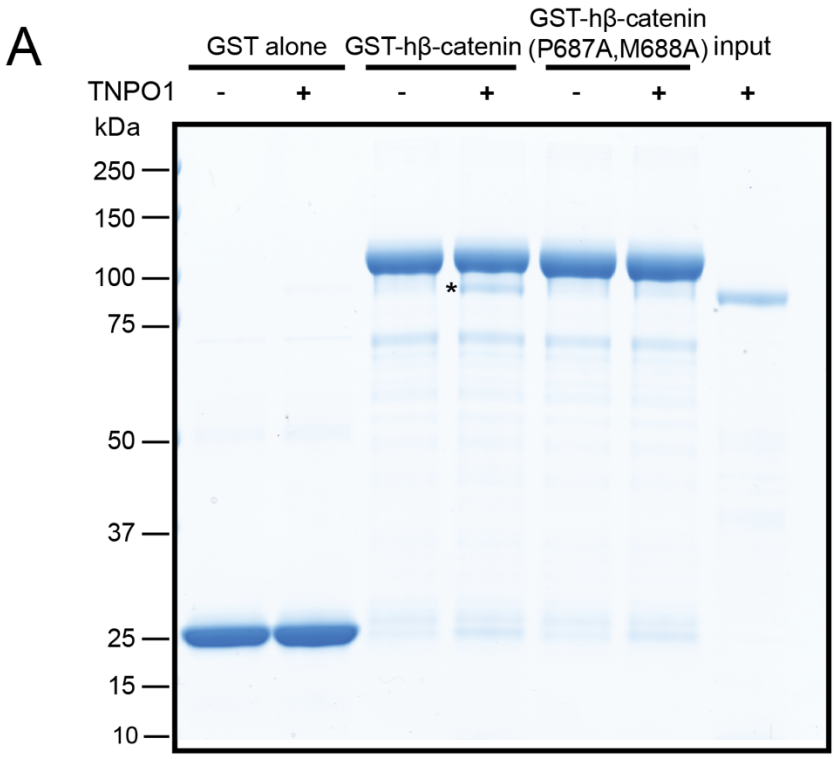

Figure 5A. Direct binding of β-catenin and TNPO1 is destabilized by PM to AA mutation. *In vitro* binding assay of purified recombinant TNPO1 and GST fusions of human β-catenin and human β-catenin containing the PM to AA mutations. GST alone was used as a negative control. Proteins were separated by SDS-PAGE and stained with Coomassie Blue. * indicates TNPO1 bound to GST-hβ-catenin.

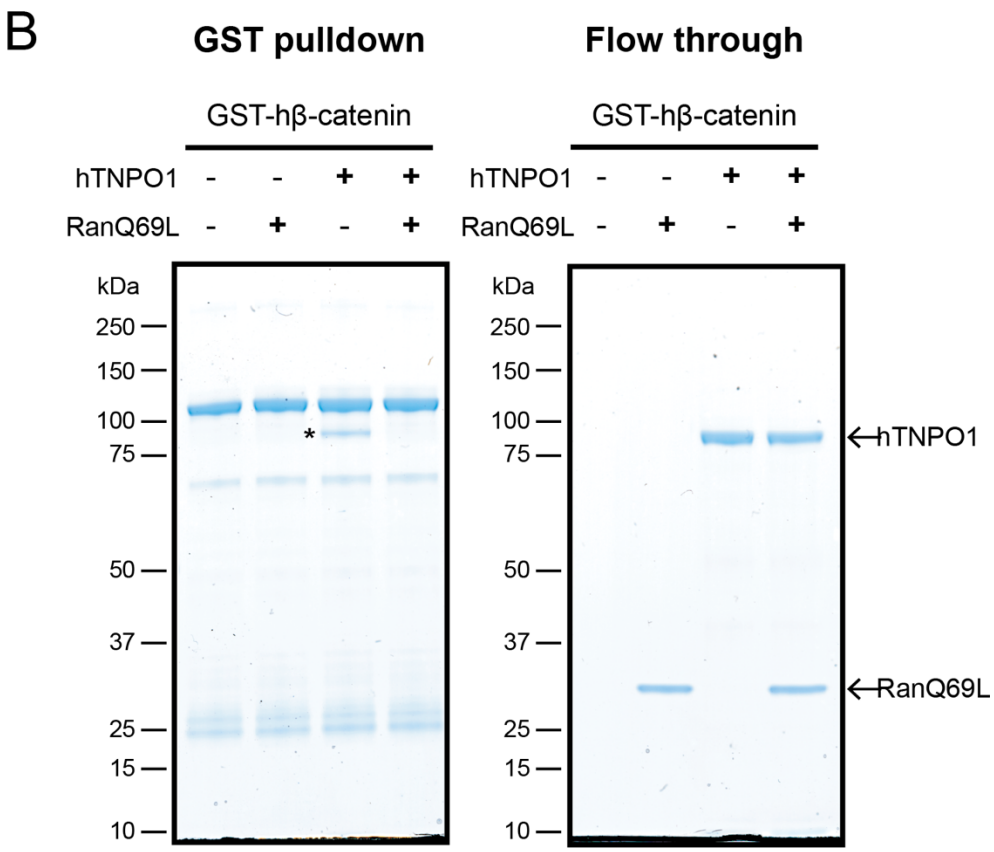

Figure 5B. Direct binding of β-catenin and TNPO1 is destabilized by Ran-GTP. *In vitro* binding assay of purified recombinant TNPO1 to GST fusions of human β-catenin in the presence of GTP hydrolysis deficient Ran mutant loaded with GTP (RanQ69L). Proteins were separated by SDS-PAGE and stained with Coomassie Blue. * indicates TNPO1 bound to GST-hβ-catenin.

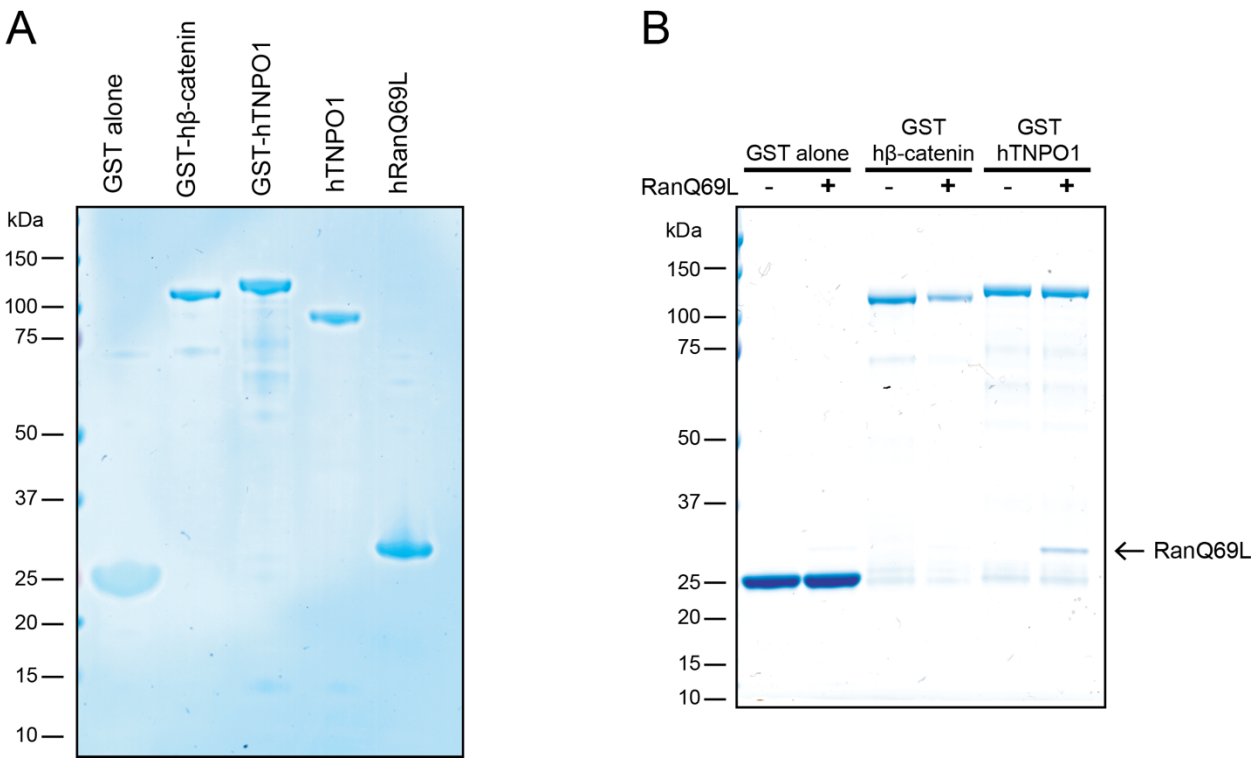

Figure 5-figure supplement 1. TNPO1 selectively binds to RanGTP *in vitro*. (A) generation of recombinant GST fusions of human β-catenin and TNPO1 and RanQ69L *in vitro* **(B)** *in vitro* binding assay of purified recombinant RanQ69L to GST fusions of human TNPO1. GST fusions of human β-catenin and RanQ69L buffer were used as a control. Proteins were separated by SDS-PAGE and stained with Coomassie Blue in **(A) and (B)**.

3.6 **TNPO1/2 and the β-catenin NLS are required for Wnt signaling *in vivo***

To explore the function of TNPO1-mediated import of β-catenin in vertebrates, we applied two different Wnt signaling assays: 1) a TCF/LEF reporter and 2) *Xenopus* secondary axis development. First, once β-catenin enters the nucleus, it binds to the TCF/LEF complex to activate transcription of Wnt responsive genes (Molenaar et al., 1996; van de Wetering et al., 1997; van de Wetering, Oosterwegel, Dooijes, & Clevers, 1991). A well-established reporter assay (commonly known as TOPFLASH) places the TCF/LEF DNA binding element upstream of a reporter such as GFP or luciferase (Molenaar et al., 1996; van de Wetering et al., 1991). In *X. tropicalis*, the *Tg(pbin7Lef-dGFP)* line has seven tandem TCF/LEF DNA binding sites upstream of GFP and is an effective reporter of Wnt signaling(Borday et al., 2018; Denayer, Tran, & Vleminckx, 2008). We crossed heterozygous transgenic animals with a wildtype animal such that half of the resultant progeny had the transgene. In vertebrates, the *tnpo1* gene is duplicated (*tnpo1* and *tnpo2*), and both paralogs have nearly identical sequence and function (**Figure 6- figure supplement 1**) (Dormann et al., 2010; Rebane, Aab, & Steitz, 2004; Twyffels, Gueydan, & Kruys, 2014). Therefore, we injected sgRNAs targeting both *tnpo1* and *tnpo2* with Cas9 protein at the one cell stage and raised embryos to st10 before fixing them. Because GFP fluorescence is undetectable at these early stages, we used whole mount *in situ* hybridization (WMISH) to visualize GFP transcripts as an assay for Wnt reporter activation and used sibling embryos without the transgene as a WMISH negative control. When we depleted both *tnpo1* and *tnpo2* using F0 CRISPR, significantly more embryos had weak expression of the GFP transgene compared to uninjected control embryos (**Figure 6A**, see images of embryos stained for GFP transcripts as key to histogram). This result was specific as a second set of non-overlapping sgRNAs gave comparable results (**Figure 6A**, *tnpo1*/2 sgRNAs#2). Importantly, we detected

deleterious gene modification at the appropriate targeted sites using Inference of CRISPR Edits (ICE) analysis (**Figure 6- figure supplement 2**).

We next tested the function of mouse Tnpo1/2 in a stable transgenic mouse fibroblast cell line in which luciferase is expressed under the control of TCF/LEF DNA binding elements. To activate Wnt signaling, we transfected a full length human β-catenin-GFP that increased luciferase signal 7.7 fold over transfection of GFP alone (**Figure 6B**). Then we measured luciferase activity in transgenic fibroblasts transfected with hβ-catenin-GFP in which we depleted transcripts of TNPO1 or TNPO2 (alone or simultaneously) using specific siRNAs. Compared to control siRNA, depletion of either TNPO1 or TNPO2 led to a 34% reduction in luciferase signal (**Figure 6B**). By targeting both transcripts, the luciferase signals was reduced by 64% (**Figure 5B**). By Western blot, we observed the production of hβ-catenin-GFP and the specific reduction of TNPO1/2 (**Figure 6- figure supplement 3**). We next examined the dependence of β-catenin nuclear localization on TNPO1/2 in colorectal cancer cell lines, HCT-116 and DLD-1, which harbor an activating Ser45 β-catenin mutation and a deactivating frameshift mutation in APC, respectively. Similar to the TCF/LEF mouse fibroblast cell line, TNPO1/2 depletion by siRNA reduced β-catenin levels specifically in nuclear fractions compared to control siRNA condition (**Figure 6- figure supplement 4**). Taken together, TNPO1/2 are required for β-catenin nuclear localization across a wide range of species: *Xenopus*, mouse, and human cancer cell lines.

Having established the importance of TNPO1/2 for β-catenin nuclear localization in vertebrates, we next evaluated the specific impact of inhibiting β-catenin nuclear import by testing the function of the PY-AA mutant in the *Xenopus* secondary axis assay. We compared the number of secondary axes induced by the wildtype hβ-catenin mRNA to a PM to AA mutated

version (P687A, M688A). We noted a significant reduction in the number of secondary axes induced by the PM-AA mutant β-catenin (**Figure 6C**). If we add the cNLS to the N-terminus of the PM-AA mutant, then induction of secondary axes is rescued suggesting that the PM-AA mutant fails to enter the nucleus to activate Wnt signaling (**Figure 6C**).

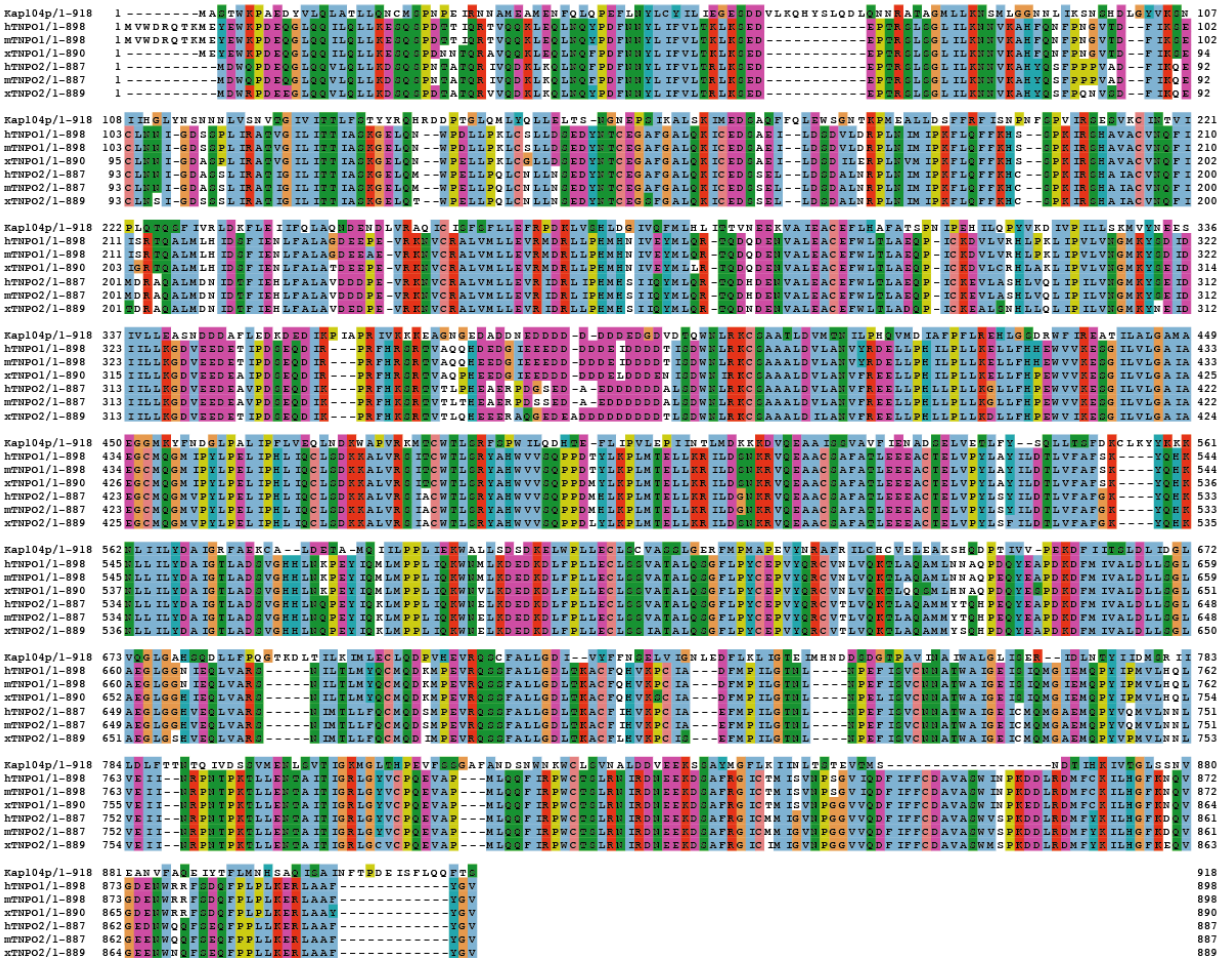

Figure 6- figure supplement 1. Sequence alignment of Tnpo1 and Tnpo2 across species. Amino acid sequences of transportin 1 and transportin 2 were compared across four different species (*S. cerevisiae*, human, mouse and *Xenopus tropicalis).* Each residue in the alignment is colored using Jalview software (Waterhouse, Procter, Martin, Clamp, & Barton, 2009).

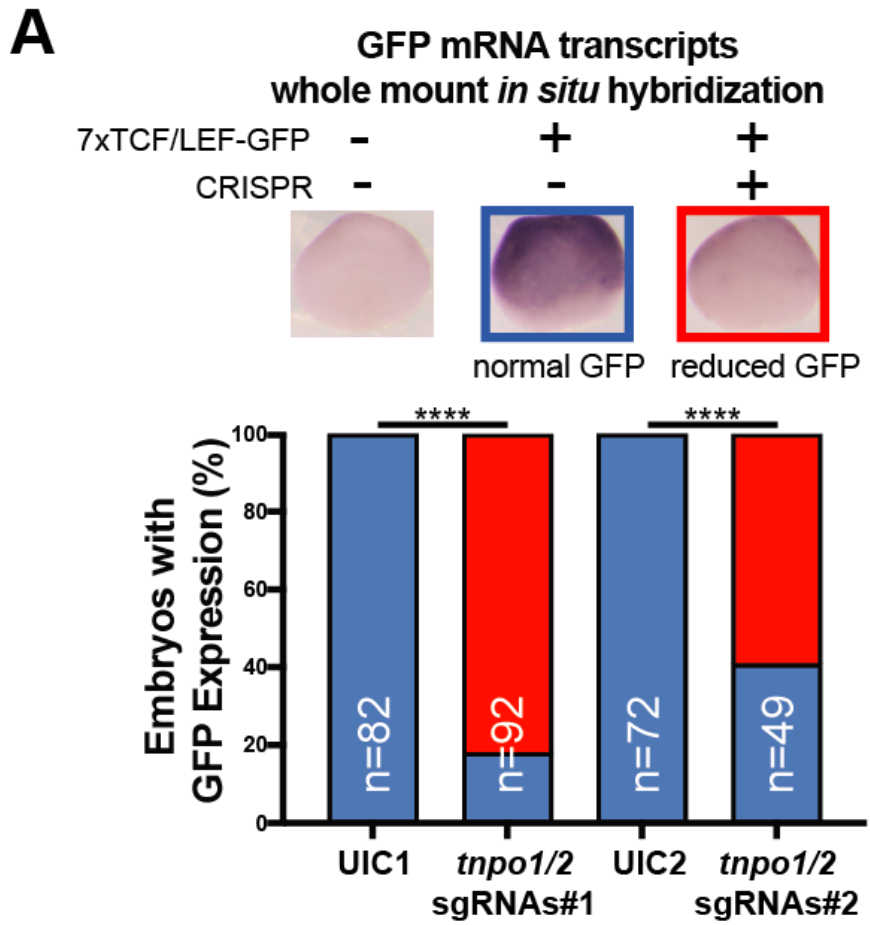

Figure 6A. TNPO1/2 is required for Wnt signaling *in vivo*. Depletion of tnpo1 and tnpo2 using two different pairs of non-overlapping sgRNAs represses gfp expression in X. tropicalis Tg(pbin7Lef-dGFP) embryos at stage 10. Key used to quantify embryos with WMISH signal (blue – normal gfp signal, red – reduced gfp signal). Uninjected (UIC) embryos were used as a negative control. p-values are from Fisher's exact test where ns is $p>0.05$, $p<0.05$ (*), 0.0021 (**), 0,0002 (***) and $p<0.0001$ (****).

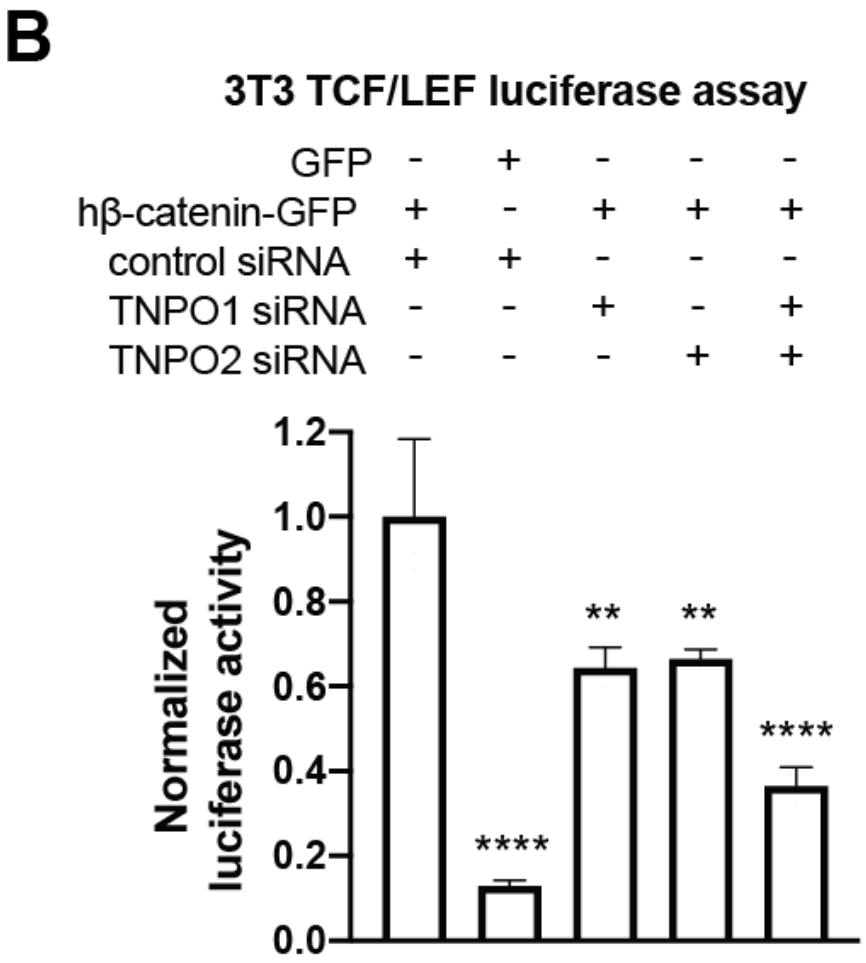

Figure 6B. TNPO1/2 knockdown reduces Wnt activity in Wnt reporter mouse embryonic fibroblast cells. siRNA mediated TNPO1 and/or TNPO2 knockdown reduces luciferase activity in mouse embryonic fibroblasts that harbor a stable integration of luciferase under the control of TCF/LEF promoters. Wnt signaling was activated by human β-catenin-GFP overexpression. Control siRNA and GFP were used as negative controls. Experiments were performed in triplicate. p-values are unpaired two-tailed t-test where ns is $p>0.05$, $p<0.05$ (*), 0.0021 (**), 0,0002 (***) and $p<0.0001$ (****).

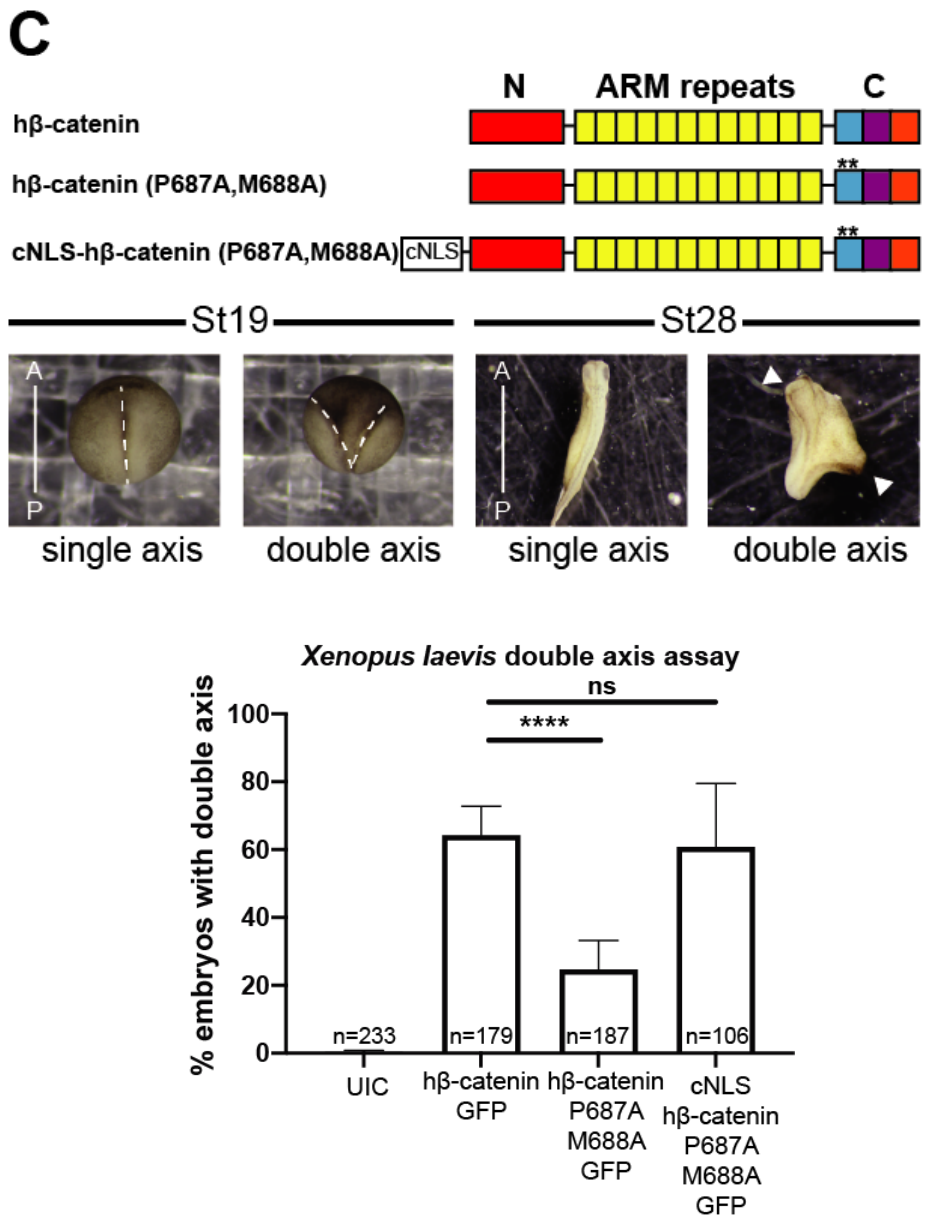

Figure 6C. β-catenin PY-NLS is required for Wnt signaling *in vivo*. Schematic diagram of three β-catenin constructs used in the double axis assay in Xenopus laevis. ** indicates P687A, M688A substitutions (top left). Dorsal views of X. laevis embryos with anterior to the top (bottom left). Dotted lines indicate the embryonic axis and the white arrows indicate the head. Histogram of the percent of embryos with secondary axes from three independent replicates. p-values are from Fisher's exact test where ns is $p>0.05$, $p<0.05$ (*), 0.0021 (**), 0,0002 (***) and $p<0.0001$ (****).

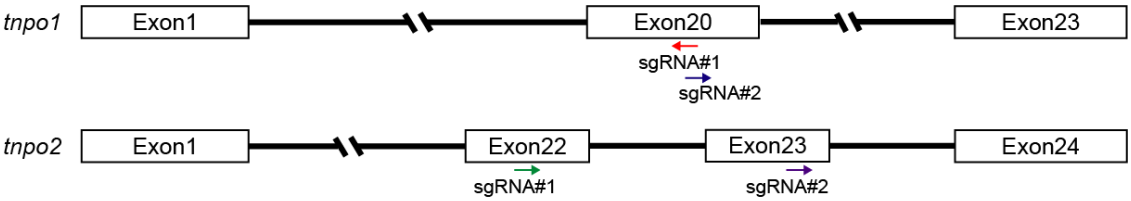

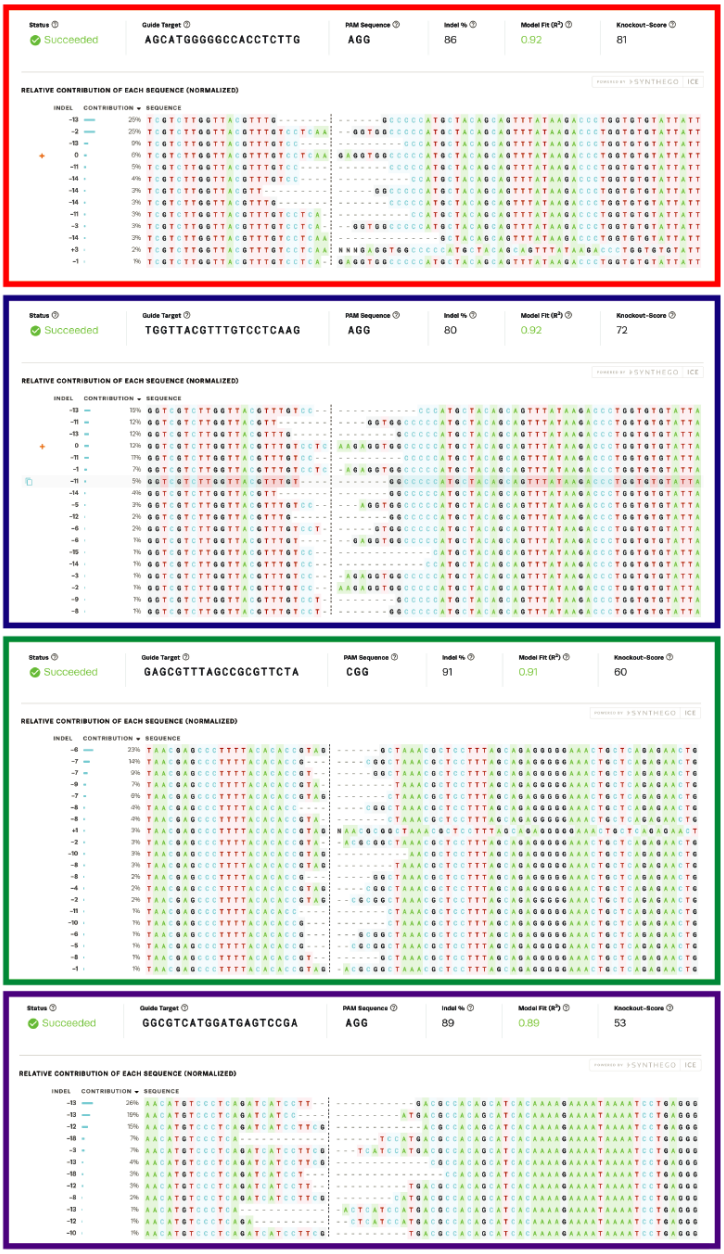

Figure 6- figure supplement 2. ***X. tropicalis tnpo1*** **and** ***tnpo2*** **gene depletion by CRISPR/Cas9.** Schematic diagram of *tnpo1* and *tnpo2* sgRNA target sites (top). ICE analysis of indel mutations at predicted target sites (bottom).

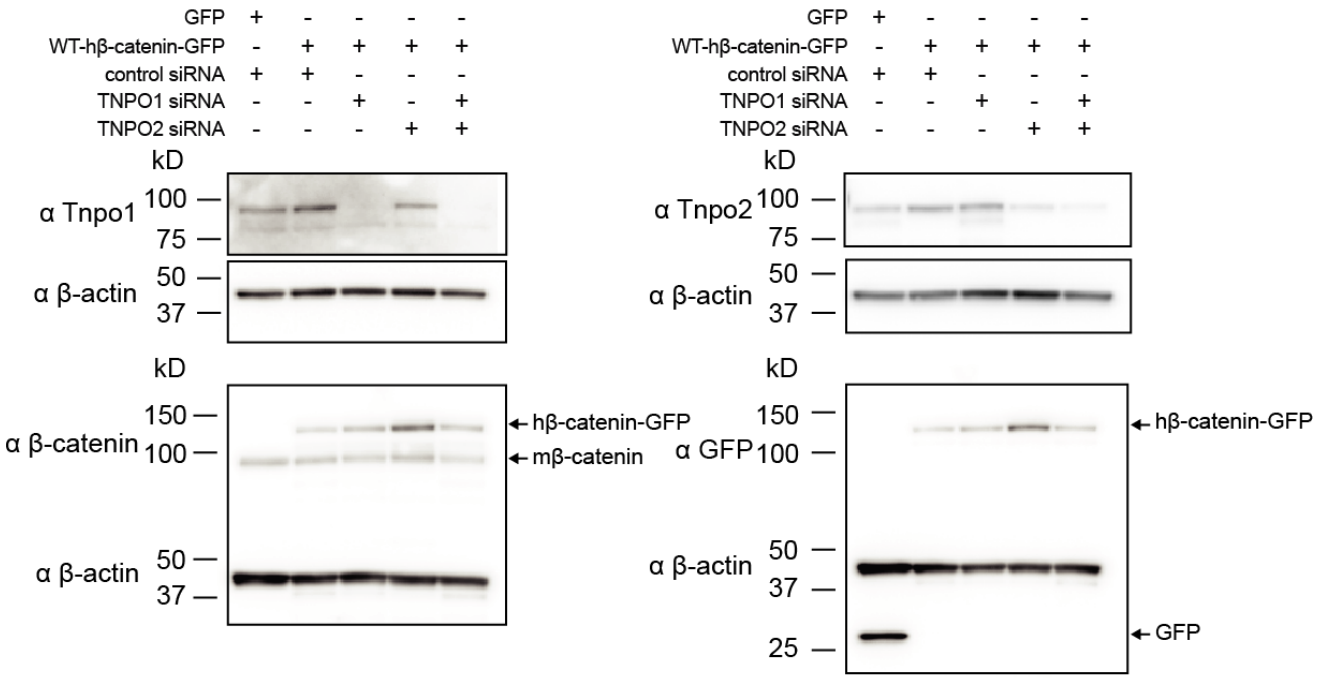

Figure 6- figure supplement 3. Western blots of Tnpo1/2 and β-catenin from 3T3 TCF/LEF luciferase assays. Western blot demonstrating the efficacy of siRNA mediated Tnpo1 and Tnpo2 depletion in mouse embryonic fibroblast Wnt reporter cell lines.

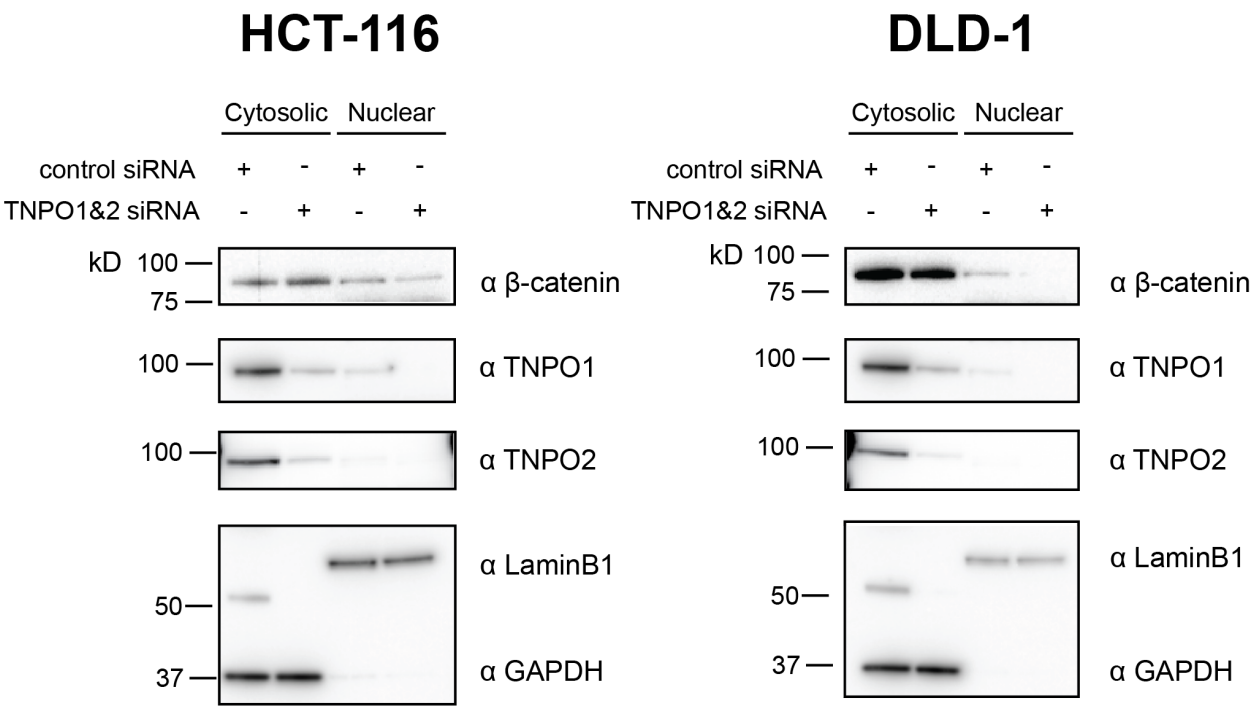

Figure 6- figure supplement 4. TNPO1/2 regulates nuclear β-catenin levels in colorectal cancer cells. Western blot demonstrating the efficacy of siRNA mediated Tnpo1 and Tnpo2 depletion on β-catenin nuclear and cytoplasmic levels in two colorectal cancer cell lines, HCT-116 and DLD-1.

3.7 **The M9M peptide inhibits TCF/LEF luciferase activity**

Having established that TNPO1 binds directly to a PY-like NLS and imports β-catenin into the nucleus, we wondered whether direct perturbation of the β-catenin-TNPO1 interaction could, in principle, be a viable therapeutic strategy. We therefore took advantage of the prior design of a potent TNPO1 peptide inhibitor, M9M, that binds with high affinity to the TNPO1 NLS binding site (Cansizoglu, Lee, Zhang, Fontoura, & Chook, 2007). We tested whether this peptide could inhibit Wnt signaling in the mouse fibroblast TCF/LEF luciferase reporter cell line (Cansizoglu et al., 2007). Excitingly, transfection of the M9M peptide reduced luciferase activity in a dose dependent manner, regardless of whether activation was induced with a Wnt ligand (Wnt3a) or by co-transfection with human β-catenin (**Figure 7A**, **Figure 7- figure supplement 1A-B**).

The M9M peptide is a chimera of the NLSs of hnRNP M and A1(Cansizoglu et al., 2007). To test specificity, we leveraged the understanding of the key amino acids that confer binding to TNPO1 in each individual NLS to design a control M9M-A peptide. M9M-A contains 7 amino acid substitutions that would be expected to abrogate binding to TNPO1 (**Figure 7-figure supplement 1C**). The M9M-A peptide only reduced luciferase activity by 24% (compared to 45% by M9M at the similar dosage; **Figure 7B**).

As the M9M peptide inhibits the nuclear import of a multitude of TNPO1/2 cargos (Cansizoglu et al., 2007), we sought to ensure that the M9M-mediated inhibition of Wnt signaling was specifically due to the reduced nuclear import of β-catenin. We therefore transfected a human β-catenin with a cNLS, which would be imported by Kap-α/Kap-β1 and thus be insensitive to M9M inhibition. The cNLS-human β-catenin could drive the luciferase reporter to levels comparable to human β-catenin but the M9M peptide only reduced this signal

by ~15% (**Figure 7B**). Thus, these data support the conclusion that the M9M peptide's impact on Wnt signaling is due, at least in part, to the inhibition of β-catenin nuclear transport via TNPO1/2. Together, Wnt signaling can be inhibited by blocking TNPO1 mediated import of β-catenin either by mutating the β-catenin NLS or competitive inhibition with the M9M peptide.

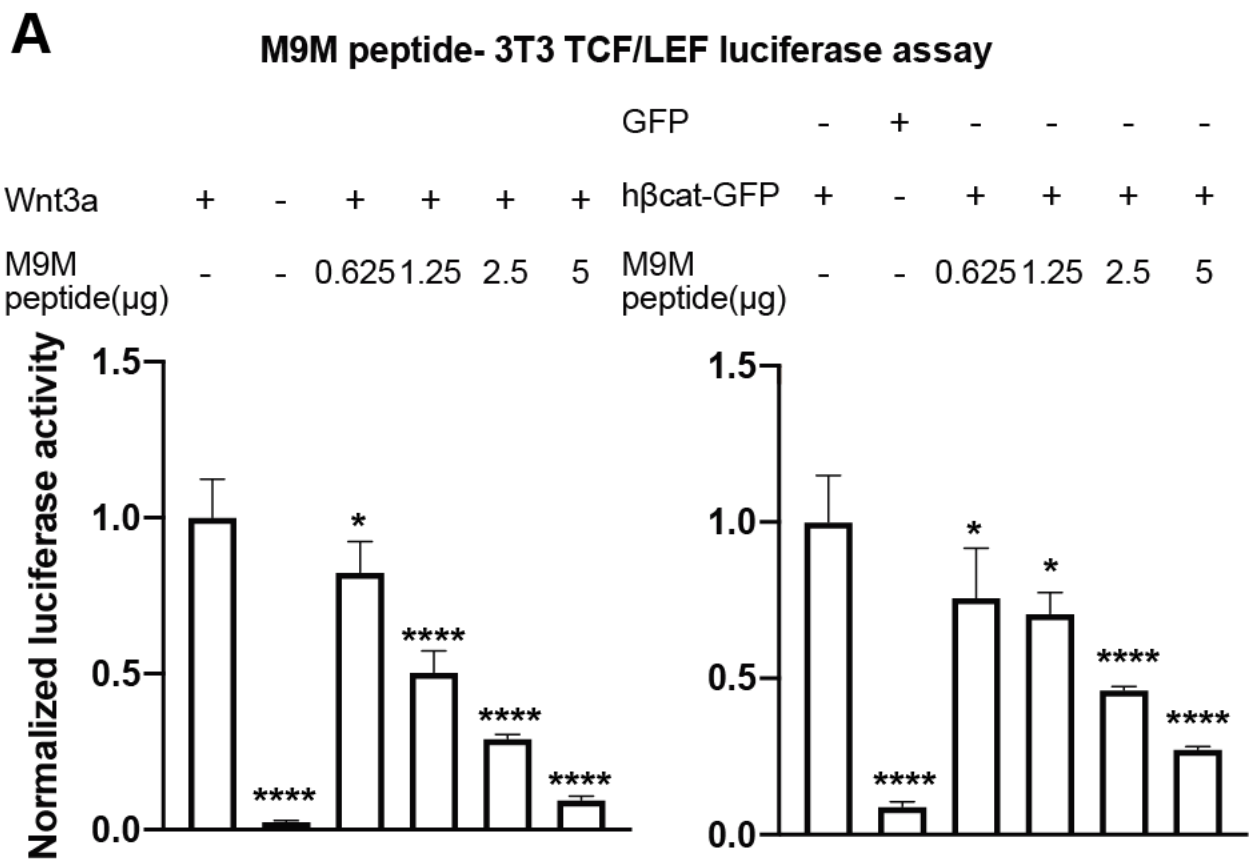

Figure 7A. The M9M peptide inhibits Wnt signaling

Wnt signaling was activated by Wnt3a (A, left) or human β-catenin-GFP overexpression (A, Right). No Wnt3a or GFP overexpression were used as negative controls. Experiments were performed in triplicate. **(**p-values are from unpaired two-tailed t-test where ns is $p>0.05$, $p<0.05$ (*), 0.0021 (**), 0.0002 (***) and $p<0.0001$ (****).

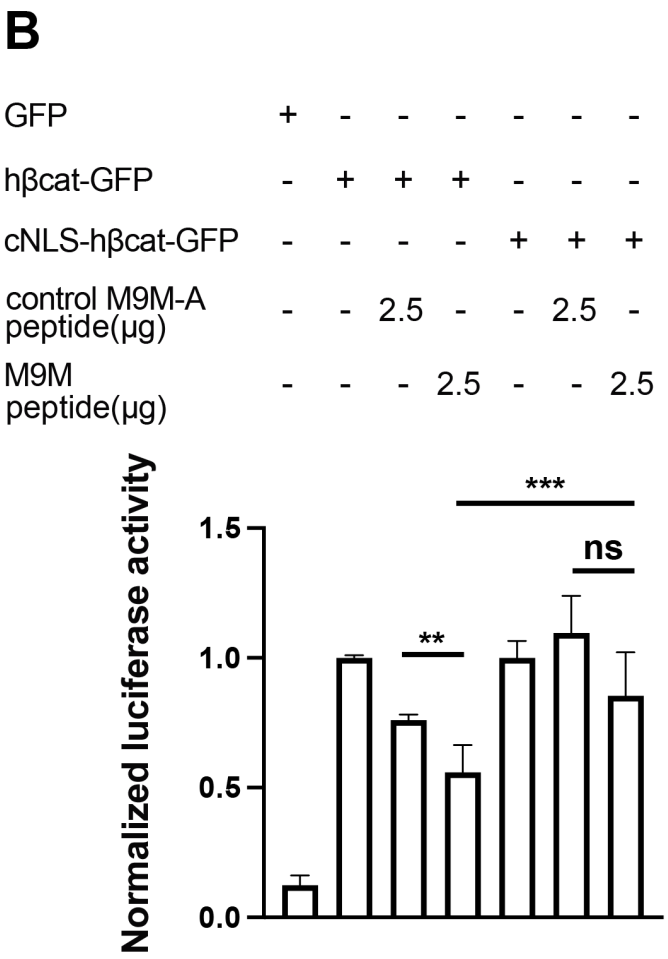

Figure 7B. cNLS-β-catenin is insensitive to M9M mediated Wnt inhibition. Wnt signaling was activated by human β-catenin-GFP overexpression or cNLS-human β-catenin-GFP. No Wnt3a or GFP overexpression were used as negative controls. Quantification from two independent experiments. **(**p-values are from unpaired two-tailed t-test where ns is $p>0.05$, $p<0.05$ (*), 0.0021 (**), 0.0002 (***) and $p<0.0001$ (****).

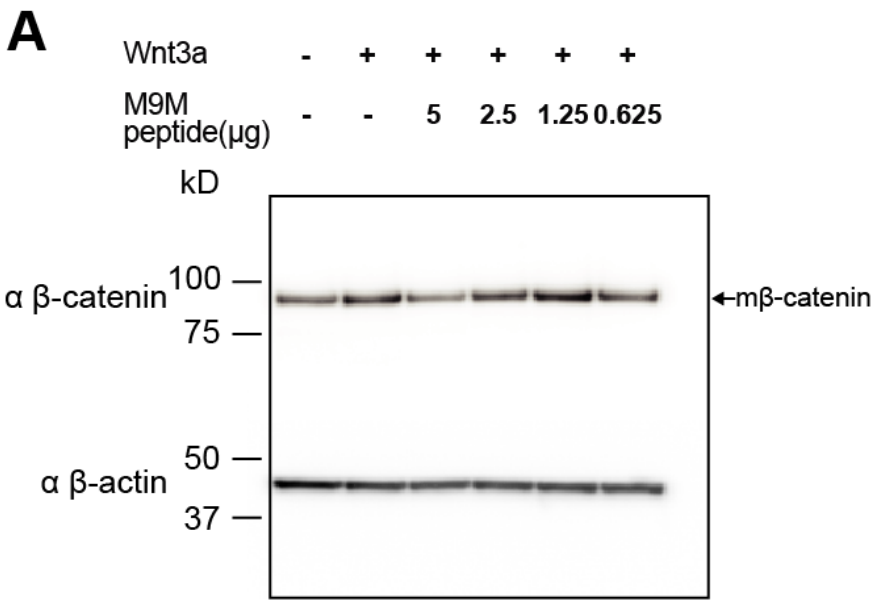

Figure 7- figure supplement 1A. Western blots of β-catenin from 3T3 TCF/LEF luciferase assays with M9M peptide treatment. Western blot data for M9M peptide treatment in mouse embryonic fibroblast Wnt reporter cell lines. Wnt signaling is activated by Wnt3a.

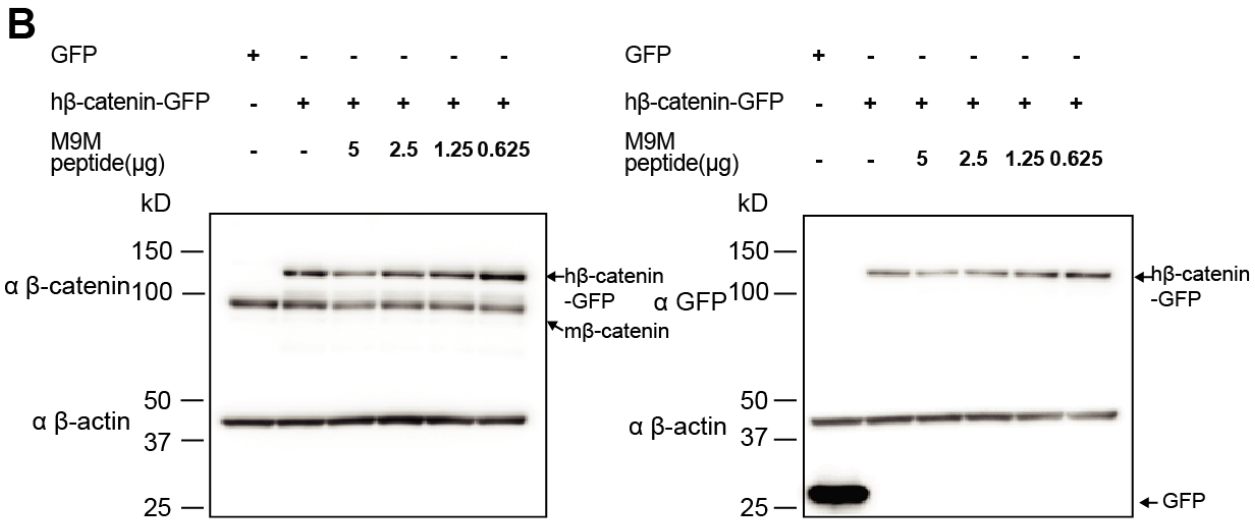

Figure 7- figure supplement 1B. Western blots of β-catenin from 3T3 TCF/LEF luciferase assays with M9M peptide treatment. Western blot data for M9M peptide treatment in mouse embryonic fibroblast Wnt reporter cell lines. Wnt signaling is activated by human β-catenin.

Figure 7- figure supplement 1C. PY-NLS residues (blue) in M9M peptide were mutated to alanine (red) to create M9M-A peptide.

Chapter 4: Discussion

One of challenges using mammalian organisms for studying Wnt signaling is the versatile nature of β-catenin; β-catenin can be dynamically present at several cellular compartments, including the plasma membrane, the cytosol, and the nucleus where different modulators directly interact with β-catenin for sub-cellular localization. Such a multiplex relationship with numerous regulatory proteins makes it difficult to investigate the nuclear transport step alone. To circumvent confounding variables and solely interrogate β-catenin nuclear transport mechanism, we utilized a simple organism *Saccharomyces cerevisiae* as a screening model (**Figure 8**). Since Wnt evolved with the onset of multicellularity, Wnt related degradation complex and cell-adhesion proteins were not found in yeast but maintain the conserved nuclear transport system. Indeed, another group has shown that yeast can be a powerful system to study canonical Wnt pathway (M. S. Lee, D'Amour, & Papkoff, 2002). Taking advantage of a Wnt free environment in yeast, this study examined minimal components necessary to reconstitute a functional destruction complex and transcription complex (M. S. Lee et al., 2002). However, no one has investigated the β-catenin nuclear import mechanism in yeast to date. Thus we have applied the budding yeast to explore β-catenin nuclear import machinery in an unbiased manner by systematic deletion of β-catenin coding sequences and all of known 10 import NTRs (**Table 1 & Figure 3**). Our study demonstrates that β-catenin indeed can enrich in the yeast nucleus which can be impaired by the loss of nuclear RanGTP and/or Kap104p. And we also validated both the physiological and functional relevance of the PY-NLS and transportin 1 and/or 2 in multiple species including *Xenopus laevis*, *Xenopus tropicalis,* mouse and human cells (**Figure 8**). We further have mapped the PY-NLS in the C-terminal domain of β-catenin and confirmed the importance of the NLS for direct binding to transportin 1 by PM to AA mutation analysis.

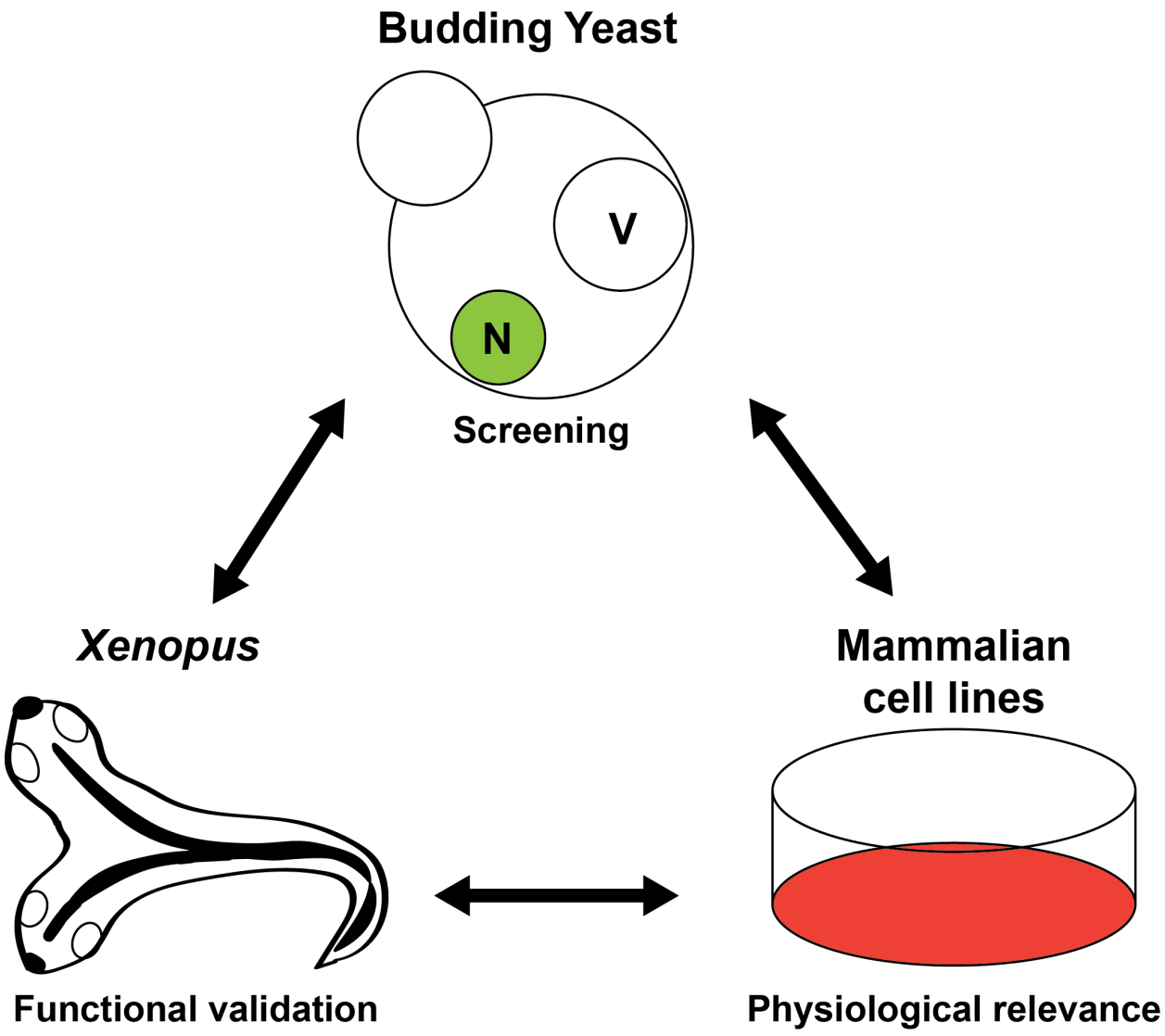

Figure 8. Research strategy. Three model systems (*Saccharomyces cerevisiae*, *Xenopus*, and mammalian cell lines) to screen and validate components of β-catenin nuclear import.

Our lack of understanding of the mechanism of β-catenin nuclear transport has been a major stumbling block for opening up new avenues of Wnt-targeted anti-cancer therapies. Numerous transport models have been proposed including piggybacking on TCF/LEF (Behrens et al., 1996; O. Huber et al., 1996; Molenaar et al., 1996) or APC (Henderson, 2000; Neufeld, Zhang, Cullen, & White, 2000; Rosin-Arbesfeld, Townsley, & Bienz, 2000) although neither factor was ultimately found to be required for import (Eleftheriou, Yoshida, & Henderson, 2001; Orsulic & Peifer, 1996; Prieve & Waterman, 1999). There is also a model in which β-catenin directly binds to the FG-nups and translocates through the NPC in a NTR-like (yet Ran independent) mechanism (Fagotto, 2013; Xu & Massague, 2004). Indeed, while some of our data suggests that there are additional nuclear localization elements in the ARM repeats or N-terminus (**Figure 2- figure supplement 1**) that might also confer an affinity for the NPC (**Figure 2D, white arrows**), they are dependent on a functional Ran cycle. Thus, we disfavor the idea that there is a Ran-independent pathway for β-catenin nuclear import while acknowledging that there is still more to be learned.

Overall, the most parsimonious mechanism of β-catenin nuclear import is also the most straightforward - it is a Kap-β2/TNPO1 cargo. This conclusion is based on 1) The identification of a PY NLS in the C-terminus of β-catenin, 2) The direct binding between TNPO1 and this NLS *in vitro* and 3) The essential role for this NLS sequence and TNPO1/2 in mediating TCF/LEF binding activation and secondary axis formation of β-catenin in multiple model systems (**Figure 9**). It would be worthwhile to test if either TNPO 1/2 depletion or manipulation of the PY-NLS domain in β-catenin affects Wnt signaling in primary colon cancer cells.

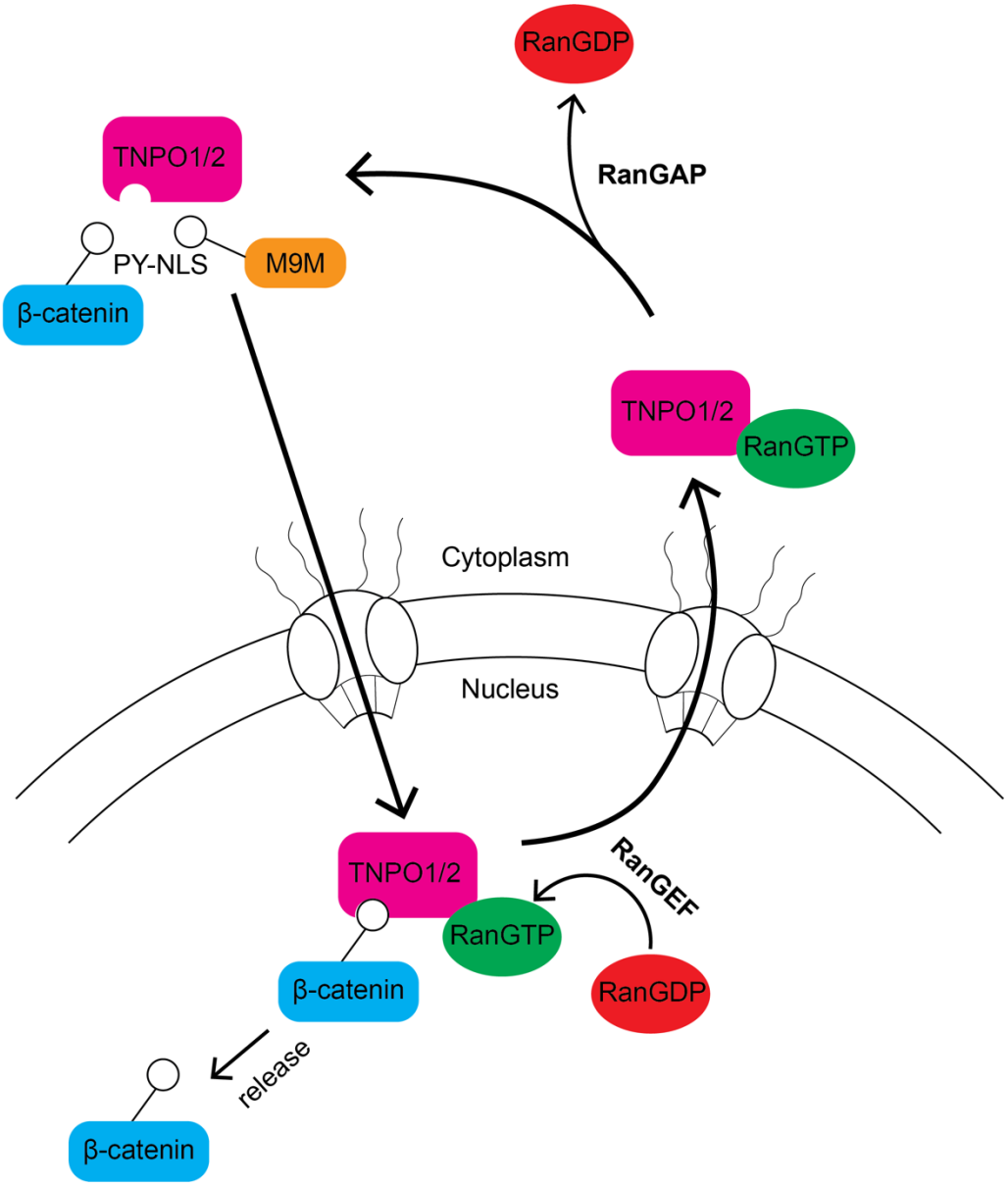

Figure 9. Summary of β-catenin nuclear transport mechanism

By far the major determinant of β-catenin's nuclear accumulation is the PY-NLS in its C-terminus. This NLS functions in yeast, *Xenopus* and human cells supporting that it can be recognized by TPNO1 orthologues across eukaryotes. It turns out, however, that although the β-catenin NLS can be imported in yeast, Kap104 (the yeast TPNO1 orthologue) does not recognize the same spectrum of NLSs as its human counterpart (Suel, Gu, & Chook, 2008). Indeed, Kap104 only recognizes PY-NLSs with an N-terminal basic motif whereas human TPNO1 can bind to PY-NLSs with both a basic or a hydrophobic N-terminal motif (Soniat & Chook, 2016; Suel et al., 2008). Thus, we were fortunate that β-catenin's PY-NLS could be recognized by Kap104, enabling our yeast screen and the ultimate identification of the dominant NLS in β-catenin.

This work must also be reconciled with a recent study that implicated Importin 11 as an important factor for β-catenin nuclear transport in a subset of cancer cells (Mis et al., 2020). The latter work also identified the C-terminus as essential for β-catenin nuclear transport, and our study adds further resolution to a specific PY-like NLS. However, we did not determine any requirement for Importin 11 (Kap120) in β-catenin import, at least in the yeast system. Although it remains possible that Importin 11 might ultimately have a role in β-catenin nuclear transport in some vertebrate cells, the current evidence suggests that it plays a critical role only in a subset of colon cancer cells (Mis et al., 2020). In contrast, our work establishes that TNPO1 imports β-catenin in yeast, amphibian, mouse and human cells, providing confidence that there is a TNPO1-specific mechanism at play. How importin 11 specifically contributes to β-catenin nuclear import in the context of specific cancer cell lines remains to be fully established.

For the purposes of rational drug design, we fortuitously identified the β-catenin NTR as TNPO1, as it is one of the few NTRs where the NLS-NTR interaction is resolved to the atomic

level (Cansizoglu et al., 2007; Soniat et al., 2013). This knowledgebase has established a consensus amino acid sequence (PY-NLS) that helped us identify the β-catenin NLS and the key PM residues required for TNPO1 binding. Further, it has led to the generation of the high affinity M9M peptide (Cansizoglu et al., 2007) that, as shown here, can be used to inhibit Wnt signaling in TCF/LEF luciferase mouse fibroblast cell lines, demonstrating proof of principle that inhibiting TNPO1 could be a viable therapeutic strategy. Nonetheless, such a strategy might benefit from future crystallographic studies of the TNPO1-β-catenin complex as the overall binding of different NLSs can vary depending on the contribution of individual amino acids. It may be possible, for example, to identify small molecules that specifically block the β-catenin-TNPO1 interaction without more broadly impacting other TNPO1 cargos. Our findings will therefore form the basis for future work to identify small molecules that could specifically target and ameliorate the multitude of Wnt related diseases including cancers.

References

Aberle, H., Bauer, A., Stappert, J., Kispert, A., & Kemler, R. (1997). beta-catenin is a target for the ubiquitin-proteasome pathway. *EMBO J, 16*(13), 3797-3804. doi:10.1093/emboj/16.13.3797

Amberg, D. C. B., D. J.; Strathern, J. N. (2005). Methods in Yeast Genetics: A Cold Spring Harbor Laboratory Course Manual. *CSHL Press*.

Andrade, M. A., Petosa, C., O'Donoghue, S. I., Muller, C. W., & Bork, P. (2001). Comparison of ARM and HEAT protein repeats. *J Mol Biol, 309*(1), 1-18. doi:10.1006/jmbi.2001.4624

Barker, N. (2014). Adult intestinal stem cells: critical drivers of epithelial homeostasis and regeneration. *Nat Rev Mol Cell Biol, 15*(1), 19-33. doi:10.1038/nrm3721

Behrens, J., von Kries, J. P., Kuhl, M., Bruhn, L., Wedlich, D., Grosschedl, R., & Birchmeier, W. (1996). Functional interaction of beta-catenin with the transcription factor LEF-1. *Nature, 382*(6592), 638-642. doi:10.1038/382638a0

Bhattacharya, D., Marfo, C. A., Li, D., Lane, M., & Khokha, M. K. (2015). CRISPR/Cas9: An inexpensive, efficient loss of function tool to screen human disease genes in Xenopus. *Dev Biol, 408*(2), 196-204. doi:10.1016/j.ydbio.2015.11.003

Bischoff, F. R., & Ponstingl, H. (1991). Catalysis of guanine nucleotide exchange on Ran by the mitotic regulator RCC1. *Nature, 354*(6348), 80-82. doi:10.1038/354080a0

Borday, C., Parain, K., Thi Tran, H., Vleminckx, K., Perron, M., & Monsoro-Burq, A. H. (2018). An atlas of Wnt activity during embryogenesis in Xenopus tropicalis. *PLoS One, 13*(4), e0193606. doi:10.1371/journal.pone.0193606

Brunner, E., Peter, O., Schweizer, L., & Basler, K. (1997). pangolin encodes a Lef-1 homologue that acts downstream of Armadillo to transduce the Wingless signal in Drosophila. *Nature, 385*(6619), 829-833. doi:10.1038/385829a0

Cancer Genome Atlas, N. (2012). Comprehensive molecular characterization of human colon and rectal cancer. *Nature, 487*(7407), 330-337. doi:10.1038/nature11252

Cansizoglu, A. E., Lee, B. J., Zhang, Z. C., Fontoura, B. M., & Chook, Y. M. (2007). Structure-based design of a pathway-specific nuclear import inhibitor. *Nat Struct Mol Biol, 14*(5), 452-454. doi:10.1038/nsmb1229

Cautain, B., Hill, R., de Pedro, N., & Link, W. (2015). Components and regulation of nuclear transport processes. *FEBS J, 282*(3), 445-462. doi:10.1111/febs.13163

Cavazza, T., & Vernos, I. (2015). The RanGTP Pathway: From Nucleo-Cytoplasmic Transport to Spindle Assembly and Beyond. *Front Cell Dev Biol, 3*, 82. doi:10.3389/fcell.2015.00082

Clevers, H., & Nusse, R. (2012). Wnt/beta-catenin signaling and disease. *Cell, 149*(6), 1192-1205. doi:10.1016/j.cell.2012.05.012

Conti, E., & Kuriyan, J. (2000). Crystallographic analysis of the specific yet versatile recognition of distinct nuclear localization signals by karyopherin alpha. *Structure, 8*(3), 329-338. doi:10.1016/s0969-2126(00)00107-6

Croner, R. S., Brueckl, W. M., Reingruber, B., Hohenberger, W., & Guenther, K. (2005). Age and manifestation related symptoms in familial adenomatous polyposis. *BMC Cancer, 5*, 24. doi:10.1186/1471-2407-5-24

De Robertis, E. M., Larrain, J., Oelgeschlager, M., & Wessely, O. (2000). The establishment of Spemann's organizer and patterning of the vertebrate embryo. *Nat Rev Genet, 1*(3), 171-181. doi:10.1038/35042039

del Viso, F., & Khokha, M. (2012). Generating diploid embryos from Xenopus tropicalis. *Methods Mol Biol, 917*, 33-41. doi:10.1007/978-1-61779-992-1_3

Denayer, T., Tran, H. T., & Vleminckx, K. (2008). Transgenic reporter tools tracing endogenous canonical Wnt signaling in Xenopus. *Methods Mol Biol, 469*, 381-400. doi:10.1007/978-1-60327-469-2_24

Dormann, D., Rodde, R., Edbauer, D., Bentmann, E., Fischer, I., Hruscha, A., . . . Haass, C. (2010). ALS-associated fused in sarcoma (FUS) mutations disrupt Transportin-mediated nuclear import. *EMBO J, 29*(16), 2841-2857. doi:10.1038/emboj.2010.143

Eleftheriou, A., Yoshida, M., & Henderson, B. R. (2001). Nuclear export of human beta-catenin can occur independent of CRM1 and the adenomatous polyposis coli tumor suppressor. *J Biol Chem, 276*(28), 25883-25888. doi:10.1074/jbc.M102656200

Fagotto, F. (2013). Looking beyond the Wnt pathway for the deep nature of beta-catenin. *EMBO Rep, 14*(5), 422-433. doi:10.1038/embor.2013.45

Fagotto, F., Gluck, U., & Gumbiner, B. M. (1998). Nuclear localization signal-independent and importin/karyopherin-independent nuclear import of beta-catenin. *Curr Biol, 8*(4), 181-190. doi:10.1016/s0960-9822(98)70082-x

Fahrenkrog, B., & Aebi, U. (2003). The nuclear pore complex: nucleocytoplasmic transport and beyond. *Nat Rev Mol Cell Biol, 4*(10), 757-766. doi:10.1038/nrm1230

Fontes, M. R., Teh, T., & Kobe, B. (2000). Structural basis of recognition of monopartite and bipartite nuclear localization sequences by mammalian importin-alpha. *J Mol Biol, 297*(5), 1183-1194. doi:10.1006/jmbi.2000.3642

Gorlich, D., Pante, N., Kutay, U., Aebi, U., & Bischoff, F. R. (1996). Identification of different roles for RanGDP and RanGTP in nuclear protein import. *EMBO J, 15*(20), 5584-5594. Retrieved from https://www.ncbi.nlm.nih.gov/pubmed/8896452

Goto, T., Sato, A., Adachi, S., Iemura, S., Natsume, T., & Shibuya, H. (2013). IQGAP1 protein regulates nuclear localization of beta-catenin via importin-beta5 protein in Wnt signaling. *J Biol Chem, 288*(51), 36351-36360. doi:10.1074/jbc.M113.520528

Griffin, J. N., Del Viso, F., Duncan, A. R., Robson, A., Hwang, W., Kulkarni, S., . . . Khokha, M. K. (2018). RAPGEF5 Regulates Nuclear Translocation of beta-Catenin. *Dev Cell, 44*(2), 248-260 e244. doi:10.1016/j.devcel.2017.12.001

Groden, J., Thliveris, A., Samowitz, W., Carlson, M., Gelbert, L., Albertsen, H., . . . et al. (1991). Identification and characterization of the familial adenomatous polyposis coli gene. *Cell, 66*(3), 589-600. doi:10.1016/0092-8674(81)90021-0

Harel, A., & Forbes, D. J. (2004). Importin beta: conducting a much larger cellular symphony. *Mol Cell, 16*(3), 319-330. doi:10.1016/j.molcel.2004.10.026

Harland, R., & Gerhart, J. (1997). Formation and function of Spemann's organizer. *Annu Rev Cell Dev Biol, 13*, 611-667. doi:10.1146/annurev.cellbio.13.1.611

Haruki, H., Nishikawa, J., & Laemmli, U. K. (2008). The anchor-away technique: rapid, conditional establishment of yeast mutant phenotypes. *Mol Cell, 31*(6), 925-932. doi:10.1016/j.molcel.2008.07.020

Heasman, J., Crawford, A., Goldstone, K., Garner-Hamrick, P., Gumbiner, B., McCrea, P., . . . Wylie, C. (1994). Overexpression of cadherins and underexpression of beta-catenin inhibit dorsal mesoderm induction in early Xenopus embryos. *Cell, 79*(5), 791-803. doi:10.1016/0092-8674(94)90069-8

Heasman, J., Kofron, M., & Wylie, C. (2000). Beta-catenin signaling activity dissected in the early Xenopus embryo: a novel antisense approach. *Dev Biol, 222*(1), 124-134. doi:10.1006/dbio.2000.9720

Henderson, B. R. (2000). Nuclear-cytoplasmic shuttling of APC regulates beta-catenin subcellular localization and turnover. *Nat Cell Biol, 2*(9), 653-660. doi:10.1038/35023605

Holstein, T. W. (2012). The evolution of the Wnt pathway. *Cold Spring Harb Perspect Biol, 4*(7), a007922. doi:10.1101/cshperspect.a007922

Huber, A. H., Nelson, W. J., & Weis, W. I. (1997). Three-dimensional structure of the armadillo repeat region of beta-catenin. *Cell, 90*(5), 871-882. doi:10.1016/s0092-8674(00)80352-9

Huber, O., Korn, R., McLaughlin, J., Ohsugi, M., Herrmann, B. G., & Kemler, R. (1996). Nuclear localization of beta-catenin by interaction with transcription factor LEF-1. *Mech Dev, 59*(1), 3-10. doi:10.1016/0925-4773(96)00597-7

Izaurralde, E., Kutay, U., von Kobbe, C., Mattaj, I. W., & Gorlich, D. (1997). The asymmetric distribution of the constituents of the Ran system is essential for transport into and out of the nucleus. *EMBO J, 16*(21), 6535-6547. doi:10.1093/emboj/16.21.6535

Jans, D. A., Xiao, C. Y., & Lam, M. H. (2000). Nuclear targeting signal recognition: a key control point in nuclear transport? *Bioessays, 22*(6), 532-544. doi:10.1002/(SICI)1521-1878(200006)22:6<532::AID-BIES6>3.0.CO;2-O

Jung, Y. S., & Park, J. I. (2020). Wnt signaling in cancer: therapeutic targeting of Wnt signaling beyond beta-catenin and the destruction complex. *Exp Mol Med, 52*(2), 183-191. doi:10.1038/s12276-020-0380-6

Kadowaki, T., Zhao, Y., & Tartakoff, A. M. (1992). A conditional yeast mutant deficient in mRNA transport from nucleus to cytoplasm. *Proc Natl Acad Sci U S A, 89*(6), 2312-2316. doi:10.1073/pnas.89.6.2312

Khokha, M. K., Chung, C., Bustamante, E. L., Gaw, L. W., Trott, K. A., Yeh, J., . . . Grammer, T. C. (2002). Techniques and probes for the study of Xenopus tropicalis development. *Dev Dyn, 225*(4), 499-510. doi:10.1002/dvdy.10184

Khokha, M. K., Yeh, J., Grammer, T. C., & Harland, R. M. (2005). Depletion of three BMP antagonists from Spemann's organizer leads to a catastrophic loss of dorsal structures. *Dev Cell, 8*(3), 401-411. doi:10.1016/j.devcel.2005.01.013

Koike, M., Kose, S., Furuta, M., Taniguchi, N., Yokoya, F., Yoneda, Y., & Imamoto, N. (2004). beta-Catenin shows an overlapping sequence requirement but distinct molecular interactions for its bidirectional passage through nuclear pores. *J Biol Chem, 279*(32), 34038-34047. doi:10.1074/jbc.M405821200

Komiya, Y., Mandrekar, N., Sato, A., Dawid, I. B., & Habas, R. (2014). Custos controls beta-catenin to regulate head development during vertebrate embryogenesis. *Proc Natl Acad Sci U S A, 111*(36), 13099-13104. doi:10.1073/pnas.1414437111

Kosugi, S., Hasebe, M., Tomita, M., & Yanagawa, H. (2008). Nuclear export signal consensus sequences defined using a localization-based yeast selection system. *Traffic, 9*(12), 2053-2062. doi:10.1111/j.1600-0854.2008.00825.x

Lange, A., Mills, R. E., Devine, S. E., & Corbett, A. H. (2008). A PY-NLS nuclear targeting signal is required for nuclear localization and function of the Saccharomyces cerevisiae mRNA-binding protein Hrp1. *J Biol Chem, 283*(19), 12926-12934. doi:10.1074/jbc.M800898200

Lee, B. J., Cansizoglu, A. E., Suel, K. E., Louis, T. H., Zhang, Z., & Chook, Y. M. (2006). Rules for nuclear localization sequence recognition by karyopherin beta 2. *Cell, 126*(3), 543-558. doi:10.1016/j.cell.2006.05.049

Lee, M. S., D'Amour, K. A., & Papkoff, J. (2002). A yeast model system for functional analysis of beta-catenin signaling. *J Cell Biol, 158*(6), 1067-1078. doi:10.1083/jcb.200204063

Liu, C., Kato, Y., Zhang, Z., Do, V. M., Yankner, B. A., & He, X. (1999). beta-Trcp couples beta-catenin phosphorylation-degradation and regulates Xenopus axis formation. *Proc Natl Acad Sci U S A, 96*(11), 6273-6278. doi:10.1073/pnas.96.11.6273

Longtine, M. S., McKenzie, A., 3rd, Demarini, D. J., Shah, N. G., Wach, A., Brachat, A., . . . Pringle, J. R. (1998). Additional modules for versatile and economical PCR-based gene deletion and modification in Saccharomyces cerevisiae. *Yeast, 14*(10), 953-961. doi:10.1002/(SICI)1097-0061(199807)14:10<953::AID-YEA293>3.0.CO;2-U

MacDonald, B. T., Tamai, K., & He, X. (2009). Wnt/beta-catenin signaling: components, mechanisms, and diseases. *Dev Cell, 17*(1), 9-26. doi:10.1016/j.devcel.2009.06.016

Malik, H. S., Eickbush, T. H., & Goldfarb, D. S. (1997). Evolutionary specialization of the nuclear targeting apparatus. *Proc Natl Acad Sci U S A, 94*(25), 13738-13742. doi:10.1073/pnas.94.25.13738

Marlow, F. L. (2010). In *Maternal Control of Development in Vertebrates: My Mother Made Me Do It!* San Rafael (CA).

McMahon, A. P., & Moon, R. T. (1989). Ectopic expression of the proto-oncogene int-1 in Xenopus embryos leads to duplication of the embryonic axis. *Cell, 58*(6), 1075-1084. doi:10.1016/0092-8674(89)90506-0

Mis, M., O'Brien, S., Steinhart, Z., Lin, S., Hart, T., Moffat, J., & Angers, S. (2020). IPO11 mediates betacatenin nuclear import in a subset of colorectal cancers. *J Cell Biol, 219*(2). doi:10.1083/jcb.201903017

Molenaar, M., van de Wetering, M., Oosterwegel, M., Peterson-Maduro, J., Godsave, S., Korinek, V., . . . Clevers, H. (1996). XTcf-3 transcription factor mediates beta-catenin-induced axis formation in Xenopus embryos. *Cell, 86*(3), 391-399. doi:10.1016/s0092-8674(00)80112-9

Moon, R. T., Brown, J. D., & Torres, M. (1997). WNTs modulate cell fate and behavior during vertebrate development. *Trends Genet, 13*(4), 157-162. doi:10.1016/s0168-9525(97)01093-7

Moon, R. T., Kohn, A. D., De Ferrari, G. V., & Kaykas, A. (2004). WNT and beta-catenin signalling: diseases and therapies. *Nat Rev Genet, 5*(9), 691-701. doi:10.1038/nrg1427

Moreno-Mateos, M. A., Vejnar, C. E., Beaudoin, J. D., Fernandez, J. P., Mis, E. K., Khokha, M. K., & Giraldez, A. J. (2015). CRISPRscan: designing highly efficient sgRNAs for CRISPR-Cas9 targeting in vivo. *Nat Methods, 12*(10), 982-988. doi:10.1038/nmeth.3543

Morin, P. J., Sparks, A. B., Korinek, V., Barker, N., Clevers, H., Vogelstein, B., & Kinzler, K. W. (1997). Activation of beta-catenin-Tcf signaling in colon cancer by mutations in beta-catenin or APC. *Science, 275*(5307), 1787-1790. doi:10.1126/science.275.5307.1787

Neufeld, K. L., Zhang, F., Cullen, B. R., & White, R. L. (2000). APC-mediated downregulation of beta-catenin activity involves nuclear sequestration and nuclear export. *EMBO Rep, 1*(6), 519-523. doi:10.1093/embo-reports/kvd117

Niehrs, C. (2012). The complex world of WNT receptor signalling. *Nat Rev Mol Cell Biol, 13*(12), 767-779. doi:10.1038/nrm3470

Nishisho, I., Nakamura, Y., Miyoshi, Y., Miki, Y., Ando, H., Horii, A., . . . Hedge, P. (1991). Mutations of chromosome 5q21 genes in FAP and colorectal cancer patients. *Science, 253*(5020), 665-669. doi:10.1126/science.1651563

Nusse, R., & Clevers, H. (2017). Wnt/beta-Catenin Signaling, Disease, and Emerging Therapeutic Modalities. *Cell, 169*(6), 985-999. doi:10.1016/j.cell.2017.05.016

Nusse, R., & Varmus, H. E. (1982). Many tumors induced by the mouse mammary tumor virus contain a provirus integrated in the same region of the host genome. *Cell, 31*(1), 99-109. doi:10.1016/0092-8674(82)90409-3

Nusslein-Volhard, C., & Wieschaus, E. (1980). Mutations affecting segment number and polarity in Drosophila. *Nature, 287*(5785), 795-801. doi:10.1038/287795a0

Orsulic, S., & Peifer, M. (1996). An in vivo structure-function study of armadillo, the beta-catenin homologue, reveals both separate and overlapping regions of the protein required for cell adhesion and for wingless signaling. *J Cell Biol, 134*(5), 1283-1300. doi:10.1083/jcb.134.5.1283

Ozawa, M., Baribault, H., & Kemler, R. (1989). The cytoplasmic domain of the cell adhesion molecule uvomorulin associates with three independent proteins structurally related in different species. *EMBO J, 8*(6), 1711-1717. Retrieved from https://www.ncbi.nlm.nih.gov/pubmed/2788574

Petersen, C. P., & Reddien, P. W. (2009). Wnt signaling and the polarity of the primary body axis. *Cell, 139*(6), 1056-1068. doi:10.1016/j.cell.2009.11.035

Polakis, P. (2012). Wnt signaling in cancer. *Cold Spring Harb Perspect Biol, 4*(5). doi:10.1101/cshperspect.a008052

Popken, P., Ghavami, A., Onck, P. R., Poolman, B., & Veenhoff, L. M. (2015). Size-dependent leak of soluble and membrane proteins through the yeast nuclear pore complex. *Mol Biol Cell, 26*(7), 1386-1394. doi:10.1091/mbc.E14-07-1175

Prieve, M. G., & Waterman, M. L. (1999). Nuclear localization and formation of beta-catenin-lymphoid enhancer factor 1 complexes are not sufficient for activation of gene expression. *Mol Cell Biol, 19*(6), 4503-4515. doi:10.1128/mcb.19.6.4503

Rebane, A., Aab, A., & Steitz, J. A. (2004). Transportins 1 and 2 are redundant nuclear import factors for hnRNP A1 and HuR. *RNA, 10*(4), 590-599. doi:10.1261/rna.5224304

Riggleman, B., Schedl, P., & Wieschaus, E. (1990). Spatial expression of the Drosophila segment polarity gene armadillo is posttranscriptionally regulated by wingless. *Cell, 63*(3), 549-560. doi:10.1016/0092-8674(90)90451-j

Rijsewijk, F., Schuermann, M., Wagenaar, E., Parren, P., Weigel, D., & Nusse, R. (1987). The Drosophila homolog of the mouse mammary oncogene int-1 is identical to the segment polarity gene wingless. *Cell, 50*(4), 649-657. doi:10.1016/0092-8674(87)90038-9

Rosin-Arbesfeld, R., Townsley, F., & Bienz, M. (2000). The APC tumour suppressor has a nuclear export function. *Nature, 406*(6799), 1009-1012. doi:10.1038/35023016

Ruiz-Trillo, I., Roger, A. J., Burger, G., Gray, M. W., & Lang, B. F. (2008). A phylogenomic investigation into the origin of metazoa. *Mol Biol Evol, 25*(4), 664-672. doi:10.1093/molbev/msn006

Schepers, A., & Clevers, H. (2012). Wnt signaling, stem cells, and cancer of the gastrointestinal tract. *Cold Spring Harb Perspect Biol, 4*(4), a007989. doi:10.1101/cshperspect.a007989

Schier, A. F., & Talbot, W. S. (2005). Molecular genetics of axis formation in zebrafish. *Annu Rev Genet, 39*, 561-613. doi:10.1146/annurev.genet.37.110801.143752

Schierwater, B., Eitel, M., Jakob, W., Osigus, H. J., Hadrys, H., Dellaporta, S. L., . . . Desalle, R. (2009). Concatenated analysis sheds light on early metazoan evolution and fuels a modern "urmetazoon" hypothesis. *PLoS Biol, 7*(1), e20. doi:10.1371/journal.pbio.1000020

Schmidt, H. B., & Gorlich, D. (2016). Transport Selectivity of Nuclear Pores, Phase Separation, and Membraneless Organelles. *Trends Biochem Sci, 41*(1), 46-61. doi:10.1016/j.tibs.2015.11.001

Schneider, S., Steinbeisser, H., Warga, R. M., & Hausen, P. (1996). Beta-catenin translocation into nuclei demarcates the dorsalizing centers in frog and fish embryos. *Mech Dev, 57*(2), 191-198. doi:10.1016/0925-4773(96)00546-1

Schohl, A., & Fagotto, F. (2002). Beta-catenin, MAPK and Smad signaling during early Xenopus development. *Development, 129*(1), 37-52. Retrieved from https://www.ncbi.nlm.nih.gov/pubmed/11782399

Sempou, E., Lakhani, O. A., Amalraj, S., & Khokha, M. K. (2018). Candidate Heterotaxy Gene FGFR4 Is Essential for Patterning of the Left-Right Organizer in Xenopus. *Front Physiol, 9*, 1705. doi:10.3389/fphys.2018.01705

Sharma, M., Jamieson, C., Lui, C., & Henderson, B. R. (2014). WITHDRAWN: The hydrophobic rich N- and C-terminal tails of beta-catenin facilitate nuclear import of beta-catenin. *J Biol Chem*. doi:10.1074/jbc.M114.603209

Sharma, M., Johnson, M., Brocardo, M., Jamieson, C., & Henderson, B. R. (2014). Wnt signaling proteins associate with the nuclear pore complex: implications for cancer. *Adv Exp Med Biol, 773*, 353-372. doi:10.1007/978-1-4899-8032-8_16

Sive, H. L., Grainger, R. M., & Harland, R. M. (2007). Xenopus laevis In Vitro Fertilization and Natural Mating Methods. *CSH Protoc, 2007*, pdb prot4737. doi:10.1101/pdb.prot4737

Smith, W. C., & Harland, R. M. (1991). Injected Xwnt-8 RNA acts early in Xenopus embryos to promote formation of a vegetal dorsalizing center. *Cell, 67*(4), 753-765. doi:10.1016/0092-8674(91)90070-f

Sokol, S., Christian, J. L., Moon, R. T., & Melton, D. A. (1991). Injected Wnt RNA induces a complete body axis in Xenopus embryos. *Cell, 67*(4), 741-752. doi:10.1016/0092-8674(91)90069-b

Soniat, M., & Chook, Y. M. (2015). Nuclear localization signals for four distinct karyopherin-beta nuclear import systems. *Biochem J, 468*(3), 353-362. doi:10.1042/BJ20150368

Soniat, M., & Chook, Y. M. (2016). Karyopherin-beta2 Recognition of a PY-NLS Variant that Lacks the Proline-Tyrosine Motif. *Structure, 24*(10), 1802-1809. doi:10.1016/j.str.2016.07.018

Soniat, M., Sampathkumar, P., Collett, G., Gizzi, A. S., Banu, R. N., Bhosle, R. C., . . . Almo, S. C. (2013). Crystal structure of human Karyopherin beta2 bound to the PY-NLS of Saccharomyces cerevisiae Nab2. *J Struct Funct Genomics, 14*(2), 31-35. doi:10.1007/s10969-013-9150-1

Soravia, C., Berk, T., Madlensky, L., Mitri, A., Cheng, H., Gallinger, S., . . . Bapat, B. (1998). Genotype-phenotype correlations in attenuated adenomatous polyposis coli. *Am J Hum Genet, 62*(6), 1290-1301. doi:10.1086/301883

Stewart, M. (2007). Molecular mechanism of the nuclear protein import cycle. *Nat Rev Mol Cell Biol, 8*(3), 195-208. doi:10.1038/nrm2114

Suel, K. E., Gu, H., & Chook, Y. M. (2008). Modular organization and combinatorial energetics of proline-tyrosine nuclear localization signals. *PLoS Biol, 6*(6), e137. doi:10.1371/journal.pbio.0060137

Suh, E. K., & Gumbiner, B. M. (2003). Translocation of beta-catenin into the nucleus independent of interactions with FG-rich nucleoporins. *Exp Cell Res, 290*(2), 447-456. doi:10.1016/s0014-4827(03)00370-7

Suntharalingam, M., & Wente, S. R. (2003). Peering through the pore: nuclear pore complex structure, assembly, and function. *Dev Cell, 4*(6), 775-789. doi:10.1016/s1534-5807(03)00162-x

Timney, B. L., Raveh, B., Mironska, R., Trivedi, J. M., Kim, S. J., Russel, D., . . . Rout, M. P. (2016). Simple rules for passive diffusion through the nuclear pore complex. *J Cell Biol, 215*(1), 57-76. doi:10.1083/jcb.201601004

Twyffels, L., Gueydan, C., & Kruys, V. (2014). Transportin-1 and Transportin-2: protein nuclear import and beyond. *FEBS Lett, 588*(10), 1857-1868. doi:10.1016/j.febslet.2014.04.023

van de Wetering, M., Cavallo, R., Dooijes, D., van Beest, M., van Es, J., Loureiro, J., . . . Clevers, H. (1997). Armadillo coactivates transcription driven by the product of the Drosophila segment polarity gene dTCF. *Cell, 88*(6), 789-799. doi:10.1016/s0092-8674(00)81925-x

van de Wetering, M., Oosterwegel, M., Dooijes, D., & Clevers, H. (1991). Identification and cloning of TCF-1, a T lymphocyte-specific transcription factor containing a sequence-specific HMG box. *EMBO J, 10*(1), 123-132. Retrieved from https://www.ncbi.nlm.nih.gov/pubmed/1989880

Waterhouse, A. M., Procter, J. B., Martin, D. M., Clamp, M., & Barton, G. J. (2009). Jalview Version 2--a multiple sequence alignment editor and analysis workbench. *Bioinformatics, 25*(9), 1189-1191. doi:10.1093/bioinformatics/btp033

Weis, K. (2003). Regulating access to the genome: nucleocytoplasmic transport throughout the cell cycle. *Cell, 112*(4), 441-451. doi:10.1016/s0092-8674(03)00082-5

Wente, S. R., & Rout, M. P. (2010). The nuclear pore complex and nuclear transport. *Cold Spring Harb Perspect Biol, 2*(10), a000562. doi:10.1101/cshperspect.a000562

Wieschaus, E., Nusslein-Volhard, C., & Jurgens, G. (1984). Mutations affecting the pattern of the larval cuticle inDrosophila melanogaster : III. Zygotic loci on the X-chromosome and fourth chromosome. *Wilehm Roux Arch Dev Biol, 193*(5), 296-307. doi:10.1007/BF00848158

Wieschaus, E., & Riggleman, R. (1987). Autonomous requirements for the segment polarity gene armadillo during Drosophila embryogenesis. *Cell, 49*(2), 177-184. doi:10.1016/0092-8674(87)90558-7

Wodarz, A., & Nusse, R. (1998). Mechanisms of Wnt signaling in development. *Annu Rev Cell Dev Biol, 14*, 59-88. doi:10.1146/annurev.cellbio.14.1.59

Wood, L. D., Parsons, D. W., Jones, S., Lin, J., Sjoblom, T., Leary, R. J., . . . Vogelstein, B. (2007). The genomic landscapes of human breast and colorectal cancers. *Science, 318*(5853), 1108-1113. doi:10.1126/science.1145720

Wozniak, R. W., Rout, M. P., & Aitchison, J. D. (1998). Karyopherins and kissing cousins. *Trends Cell Biol, 8*(5), 184-188. doi:10.1016/s0962-8924(98)01248-3

Xu, L., & Massague, J. (2004). Nucleocytoplasmic shuttling of signal transducers. *Nat Rev Mol Cell Biol, 5*(3), 209-219. doi:10.1038/nrm1331

Yano, R., Oakes, M. L., Tabb, M. M., & Nomura, M. (1994). Yeast Srp1p has homology to armadillo/plakoglobin/beta-catenin and participates in apparently multiple nuclear functions including the maintenance of the nucleolar structure. *Proc Natl Acad Sci U S A, 91*(15), 6880-6884. doi:10.1073/pnas.91.15.6880

Yokoya, F., Imamoto, N., Tachibana, T., & Yoneda, Y. (1999). beta-catenin can be transported into the nucleus in a Ran-unassisted manner. *Mol Biol Cell, 10*(4), 1119-1131. doi:10.1091/mbc.10.4.1119